AXON MEMBRANE VOLTAGE FLUCTUATIONS

H. E. DERKSEN

AXON MEMBRANE VOLTAGE FLUCTUATIONS

AXON MEMBRANE VOLTAGE FLUCTUATIONS

PROEFSCHRIFT

TER VERKRIJGING VAN DE GRAAD VAN DOCTOR
IN DE WISKUNDE EN NATUURWETENSCHAPPEN
AAN DE RIJKSUNIVERSITEIT TE LEIDEN,
OP GEZAG VAN DE RECTOR MAGNIFICUS DR. J. DANKMEIJER,
HOOGLERAAR IN DE FACULTEIT DER GENEESKUNDE,
TEN OVERSTAAN VAN EEN COMMISSIE UIT DE SENAAT
TE VERDEDIGEN OP WOENSDAG 10 NOVEMBER 1965
TE 16.00 UUR

DOOR

HANS EDI DERKSEN

GEBOREN TE RENKUM IN 1926

1965
NORTH-HOLLAND PUBLISHING COMPANY - AMSTERDAM

Promotor: J. W. DUYFF

Co-promotor: H. B. G. CASIMIR

Aan mijn ouders
Aan mijn vrouw

SAMENVATTING

Het zenuwstelsel van de gewervelde dieren wordt geschetst in termen van rekensystemen. Opname van informatie vindt plaats via transductoren (de receptorcellen) die de binnenkomende signalen omzetten in elektrische impulsen welke door het rekensysteem verder worden verwerkt. Dit systeem is gemengd, d.w.z. het maakt zowel gebruik van continue (analoge) als van discrete (digitale) bewerkingen. De constituerende elementen van het rekensysteem, de neuronen of zenuwcellen, zijn pulsgeneratoren die uniforme pulsen produceren. Deze zijn weer ingangssignalen voor andere neuronen. De neuronen zijn gerangschikt in netwerken gekenmerkt door combinaties van convergente en divergente onderlinge verbindingen. De verwerking van signalen is over het gehele systeem verspreid, geschiedt simultaan doch niet gesynchroniseerd. Het neuron kan werken als sommeerversterker en kan ook een aantal elementaire logische operaties voltrekken.

Neuronen en receptorcellen zijn omgeven door een gelaagd lipoied-eiwit membraan dat selectief ionen en andere substanties doorlaat. In de rusttoestand is de concentratie van kaliumionen binnen de cel het twintigvoudige van de buitenconcentratie; de elektrische spanning over het celmembraan is door deze concentratieverhouding in hoofdzaak bepaald.

De natriumionenconcentratie in de cel wordt door een zgn. actief transport op een laag relatief niveau gehouden. Bij een bepaalde partiële polarizatievermindering treedt een kortdurende extreme vermeerdering van de natriumdoorlaatbaarheid op, hetgeen leidt tot een implosie van natriumionen en een omslaan van de elektrische polariteit; dit verschijnsel plant zich voort naar de naastbijgelegen gebieden van het membraan (voortplanting van het actiepotentiaal), het membraan gedraagt zich hierbij als een gedistribueerde monostabiele pulsgenerator met—voor korte tijd—de negatieve-weerstandskarakteristiek van de tunneldiode.

Aan de uitgangszijde (eindvertakkingen van het axon, presynaptisch einde) resulteert de aankomst van de zenuwimpuls in het uitstoten van doses transmitterstof waardoor, in het geval van een exciterende koppeling, een gedeeltelijke depolarizatie van de ingangszijde (de dendrietvertakkingen) van het volgende element wordt teweeggebracht.

Bij de transductoren (receptoren) veroorzaakt toediening van de vereiste stimuluse en lokale depolarizatie (generatorpotentiaal) welke, ingeval de receptor een axon heeft, kan leiden tot het ontstaan van een voortgeleid actiepotentiaal en bij receptoren zonder axon resulteert in synaptische activiteit.

Het zenuwstelsel werkt niet deterministisch, maar op statistische wijze en wel om de volgende redenen:

1) De door een stimulus van constante sterkte opgewekte generatorpotentiaal fluctueert.

2) De drempelpotentiaal van het zenuwmembraan vertoont fluctuaties die samenhangen met fluctuaties in de rustpotentiaal.
3) Bij een synaps resulteert de aankomst van een actiepotentiaal niet steeds in een postsynaptische depolarizatie, anderzijds kan transmitterstof vrijkomen bij afwezigheid van een presynaptische impuls.
4) In zenuwcellen kan bij sterke fluctuaties van de rustpotentiaal de drempel zo nu en dan worden overschreden, zodat deze neuronen van tijd tot tijd „spontaan" impulsen genereren bij afwezigheid van binnenkomende prikkels.

De gevolgen van deze verschijnselen voor de informatieverwerking door het zenuwstelsel worden besproken.

Een meetmethode werd ontwikkeld om het spectrum te bepalen van de fluctuaties in de membraanspanning van een enkele knoop van Ranvier in de n. ischiadicus van de kikker. Parallelverliezen langs de internodale segmenten werden geëlimineerd door een tweetal compensatieschakelingen volgens Frankenhaeuser. Op deze wijze werden twee ruisbronnen verkregen met de fluctuatiespanning over de centrale knoop van Ranvier als gemeenschappelijke component. Deze spanning werd gemeten d.m.v. kruiscorrelatie.

Een montagebakje voor de zenuwvezel, montagemethoden en methoden om een goede elektrische isolatie tussen de knopen van Ranvier te bereiken moesten worden ontwikkeld om aan de vereisten van de gekozen methodiek te voldoen. Elektrometerversterkers met lage ruisfactor, grote bandbreedte en stabilizering tegen nulpuntsverloop werden eveneens ontwikkeld. De ruisspectra werden gemeten met behulp van actieve filters, geprogrammeerd op een analoog-rekenmachine. Amplitudeverdelingen werden bepaald door middel van een poortschakeling en een pulshoogte-analysator met 128 sorteerkanalen.

In normale ringeroplossing is de ruis-intensiteit omgekeerd evenredig met de frequentie in het interval $1–10^4$ rad·sec^{-1}. Spectra van dit type komen voor in stroomvoerende koolweerstanden en halfgeleider-schakelelementen. Voor frequenties hoger dan 10^4 rad·sec^{-1} wordt de spectrale intensiteit constant en is dan in de orde van het ruisniveau volgens de formule van Nyquist voor een metallische geleider met een weerstand gelijk aan die van het membraan bij de beschouwde frequentie. De amplitudeverdeling van de fluctuaties volgt een gausscurve.

Het $1/f$ spectrum werd niet onmiddellijk beïnvloed door blokkering van het actieve transport van natrium en evenmin door het elimineren van de natriuminflux d.m.v. toevoeging van urethaan in de externe oplossing. Een direct verband tussen natriumtransport en $1/f$ ruis is daarom uitgesloten. Wordt de zenuwvezel echter overgebracht in een isotone KCl oplossing dan verandert het spectrum onmiddellijk in een wit spectrum van veel lagere totale intensiteit. Dit zelfde kan worden bereikt door vergroten van de membraanpolarizatie tot in de buurt van de kalium-evenwichtspotentiaal. Een en ander leidt tot de gevolgtrekking dat de intensiteit van het $1/f$ spectrum wordt bepaald door de grootte van de kaliumstroom door het membraan.

Gesuperponeerd op de hiervoor beschreven fluctuaties zijn onregelmatig voorkomende depolarizerende pulsen van min of meer driehoekige vorm. Ten gevolge hiervan verandert het spectrum zo nu en dan in een $1/f^2$ spectrum in het interval 0.1–10 rad·sec^{-1}. Dit verschijnsel verhindert vaak een doormeten van het $1/f$ spectrum in dit gebied. In betrekkelijk rustige perioden werden aanwijzingen gevonden van een afbuigen van het $1/f$ spectrum naar een horizontaal spectrum bij de laagste frequenties.

Ter verklaring van het $1/f$-ruisspectrum in stroomvoerende koolweerstanden, dunne metaallagen en halfgeleider-schakelelementen zijn verscheidene theorieën opgesteld. Na analyse blijken deze doorgaans te berusten op een hyperbolische verdeling van elementaire relaxatietijden, op een wisselwerking tussen onafhankelijke toevalsprocessen ofwel op een enkel toevalsproces in combinatie met een niet-lineaire betrekking. Het is nog niet mogelijk vast te stellen welk mechanisme tot een $1/f$ spectrum van de fluctuaties in de rustspanning van het axonmembraan leidt. Onderlinge beïnvloeding van de ingaande en uitgaande diffusiestromen van K^+-ionen en een beïnvloeding van deze stromen door geadsorbeerde calciumionen zijn de meestbelovende uitgangspunten voor verder onderzoek.

Acta Physiol. Pharmacol. Neerl. **13** (1965) 373-466

Department of Physiology, University of Leyden

AXON MEMBRANE VOLTAGE FLUCTUATIONS

BY

H. E. DERKSEN

CONTENTS

1. INTRODUCTION

1.1. The nervous system as a computing system

The nervous system can be regarded as a computing system performing logical and mathematical operations on a continuous flow of input data; the system's output commands the action of effector organs.

The data acquisition system consists of transducers (receptors) which transform a variety of input signal modes into electric signals serving as input data for the computing system proper, which is of a hybrid (analog-digital) character. Receptors responsive to a particular input signal mode are, in many cases, arranged in fields or arrays. Receptor systems exhibit adaptation of sensitivity to input signal strength.

Most types of receptors show, in the case of a continuous input signal of constant strength, a decrease in sensitivity which diminishes from its initial value to a constant level (in some cases to zero level) in a time which is different for different receptor types.

The basic elements of the computing system, the neurons, can be likened to pulse generators incorporating their own power supply and delivering uniform output pulses serving as input signals for similar elements. All pulses in all neurons have the same polarity. Pulse duration and pulse height may differ slightly according to the type of neuron.

The neurons in sensory systems are arrayed in a series-parallel arrangement characterized by a combination of convergent and divergent interconnexions. The neurons directly connected to the receptor units, the first-order neurons, form one functional layer; their output, which consists of a pulse train of a frequency which is, within certain limits, a rising function of input signal strength serves as input to the second-order neurons, which again form a functional layer (which may, however, not be a layer in the anatomical sense). In each functional layer computing operations are performed upon its input data, that is on the pulse trains converging upon the individual neurons of which it consists.

Computing is parallel and asynchronous. Peripherally located functional layers serve as preprocessors for those massed in the central nervous system, where the information from all receptor

systems is integrated. The arrival of a pulse or a pulse train at the input stage of a neuron may either trigger it or tend to suppress its firing. In exceptional cases, one input pulse is sufficient for the neuron to deliver a pulse of its own; usually the arrival, along a given afferent pathway, of a train of pulses with an overall frequency exceeding a given minimum is required to cause it to fire in a frequency of its own, its own firing rate increasing, within a given range, with input pulse frequency. The upper frequency of this range is limited by the fact that, after a pulse has been delivered, the neuron is refractory for a brief period. The simultaneous arrival, along a second channel converging upon the neuron, of a pulse train may result either in an increase in output pulse frequency, if it has not yet reached its maximum (excitatory input) or in its decrease, even to zero rate (inhibitory input).

Simultaneous arrival of two excitatory input pulse trains, each of which is, on its own, of a frequency which is too low to trigger the neuron may cause it to fire.

As a result of its own basic properties and of the nature of the connexions between neurons the neuron thus performs some operations not unlike those in a man-made computing system. It can, in a way, sum and subtract input pulse frequencies, thus serving as a kind of summing amplifier. It can signal the coincidence or near-coincidence in time of occurrences in different receptors the outputs of which converge upon it.

It can perform functions not unlike those of gates in digital computers, but characterized by a degree of plasticity. Thus a neuron of order n can signal the arrival, at its input stage, of an excitatory pulse train along either one or another of the $(n-1)^{\text{th}}$ order neurons converging upon it (or-gate), provided pulse frequency is sufficient; alternatively, it can signal the simultaneous arrival, at its input, of two or more trains which by themselves would be insufficient to trigger it (and-gate); it can react to an excitatory input of a given pulse frequency only in the absence of an inhibitory input with a frequency not surpassing an upper limit set by the frequency of the excitatory pulse train (nand-gate); it can serve as an inverter if its firing is suppressed by an incoming inhibitory train. As a result of the successive transformations of the crude input data in the successive functional layers a body of integrated information is obtained which is a main determinant of the firing

pattern of the efferent neurons by means of which the effector organs are connected with the computing system, which pattern determines their activity.

1.2. Basic concepts in classical neurophysiology

In classical neurophysiology, the properties of receptors and of neurons are described in terms of excitability and excitability thresholds. Elements are supposed to show no activity, that is, to have zero output, in the case of zero input. Receptor input signal strength, measured in appropriate units depending on the nature of the input, has to surpass some minimal value, threshold value, for the receptor to produce an output sufficient to cause the first-order neuron to fire.

A subthreshold input has the effect of a brief, local, exponentially decaying increase in excitability (i.e. lowering of the threshold); as a result of this the second, or the third . . . of a series of near-simultaneous subthreshold stimuli may be effective (temporal summation).

This also applies to the simultaneous or near-simultaneous arrival of subthreshold pulses along different pathways converging upon the element.

Within a certain range the frequency of the pulses delivered by the first-order neuron increases with receptor input signal strength. The first-order neuron thus can signal whether receptor input is subliminal (no output pulse); in a range of signal strengths from threshold strength to an upper limit determined by the duration of the refractory period it "measures" input signal strength by translating it into its own firing frequency; it finally can signal that its input equals or surpasses the strength corresponding to its maximum firing rate. Similarly, a n^{th} order element signals whether the weighted sum of its excitatory and inhibitory inputs is zero or negative, measures it over a range of positive values, or indicates that it equals or surpasses a given positive value. Under constant conditions thresholds are constant, as are pulse heights; to a given value of input signal strength corresponds a given overall frequency of near-equidistant ouput pulses.

1.3. Physical basis of neural activity

Cells, including receptor cells and neurons, consist of a polyphasic system in which inorganic and organic ions and non-electrolytes

are dissolved or suspended in water, and which is surrounded by a membrane about 10 nm thick and which consists of a lipoid layer enclosed in a protein envelope. The thickness of the lipoid layer is 2 molecules; they are arranged tail to tail in a parallel array perpendicular to the surface, and with the hydrophilic groups outside (i.e. on the side of the protein envelope). Functionally the membrane primarily has the character of a porous membrane exhibiting selective permeability towards certain ions and non-electrolytes. Whether the sites where these can pass are actual pores or sites of specific enzyme activities is immaterial.

In the resting state, the ionic composition of the inside differs greatly from that of the interstitial fluid in which the cells are bathed. Inside potassium concentration is about 20 times that in the outside fluid; sodium ion concentration is about 9 times higher outside than inside; chloride ion concentration outside is about 13 times that inside, while organic acids, partially neutralizing the inside potassium, are negligible in the outside fluid.

The resting membrane is permeable to K^+, Na^+ and Cl^-, the approximate ratio of the permeabilities being $P_K : P_{Na} : P_{Cl} = 1 : 0.04 : 0.45$. This results in an inside-negative polarization of the membrane. The transmembrane voltage is dominated by the inside/outside potassium concentration ratio. Potassium is not in exact electrochemical equilibrium, however, and an outward potassium current exists. Together with chloride efflux and an inward sodium leak, this results in a zero electric current in the resting state. The low inside concentration of sodium is maintained by virtue of the existence of an active extrusion mechanism acting against an important electrochemical potential gradient. Consequently the cell, in the so-called resting state, is not in thermodynamic equilibrium. The resting state is a steady state.

The necessary energy is thought to be derived from breakdown of the high energy phosphate, ATP. Uphill transport of sodium ions has been demonstrated by means of radioactive tracer experiments. Evidence for active transport of other ions, in particular of K^+, is not fully conclusive. Although an inward potassium flow has been found to exist through the membrane of the squid giant axon (HODGKIN and KEYNES, 1955) this is by itself not sufficient to conclude that Na^+ and K^+ active fluxes are linked through a common mechanism (FINKELSTEIN, 1964).

Partial depolarization of the membrane by application of an outside potential causes a sudden brief increase of membrane conductance to sodium, as soon as the depolarization reaches a critical level. There is a massive inrush of sodium with which a transient reversal of membrane polarity is associated; for a brief instant the membrane potential has to be considered primarily as a sodium potential. The local reversal of polarity serves to depolarize the adjacent membrane region; the process, of short duration because the resting state is quickly restored, thus is self-propagating. It can be described as the passage, along the membrane, of a brief wave of outside negativity, the action potential [1]). The membrane behaves as a monostable device exhibiting a transient tunnel diode characteristic.

A schematic diagram of one common type of neuron is shown in Fig. 1.3.–1. It consists of a nucleated cell body showing a multitude of fine, arborized processes, the dendrites, and one long process or fibre, which branches at its end. The terminal branches of the fibre or axon of an element of order n always connect with the dendrites of elements of order $n+1$. The dendrites thus serve as input stage, the terminal arborization of the axon as output stage of the neuron. Receptor output signals are the input for the first-order neuron dendritic tree.

Some types of receptors possess an axon-like process; in others the receptor cell connects directly with the dendrites of the first-order neuron.

In all types of receptors, application of the stimulus leads to a local increase in ionic permeability. This results in intracellular currents depolarizing the cell membrane.

Depending on whether the receptor has an axon or not, this depolarization either leads to the generation of a propagated action potential or directly to – graded – synaptic activity. In both cases (excitatory) synaptic activity will incite postsynaptic depolarization, which will reach the critical level the sooner as afferent bombardment is stronger.

---

[1]) In medullated vertebrate nerve, the only regions where depolarization actually occurs and an action potential is generated are the Ranvier nodes; a current is set up from one node, through the extracellular fluid and back through the axoplasm. This increases conduction speed and saves energy.

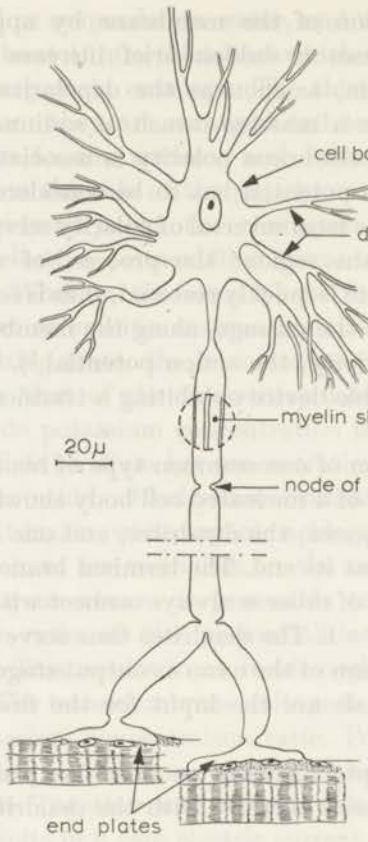

Fig. 1.3.–1.
Schematic representation of neuron.

The terminal ramifications of the axon are separated from the dendritic branches of the element of the next order by a synaptic cleft of a width of about 45–50 nm. In close proximity to the synaptic cleft, the presynaptic terminal contains a multitude of vesicles with a diameter of some 30–50 nm. These vesicles contain a transmitter substance, which is liberated into the synaptic cleft upon arrival of the action potential at the presynaptic terminal. In the case of an excitatory synapse, the transmitter substance induces some degree of depolarization of the postsynaptic membrane. At least for one widely occurring transmitter, the ester acetylcholine, it has been shown that the release is quantal, one action

potential giving rise to liberation of one quantum of transmitter, i.e. the amount contained in one vesicle, which is in the order of two thousand molecules.

The liberated acetylcholine tends to diffuse away from the synaptic cleft; at some small distance from the cleft it is hydrolyzed by the ubiquitous enzyme acetylcholinesterase to the nearly inactive choline and acetic acid; in this way, a concentration gradient from the synaptic cleft to the surrounding enzyme sites is maintained for the active ester, until its concentration in the synaptic cleft has dropped to zero. This allows of repolarization of the membrane, while leakage towards other synapses, which would lead to confusion in signal transmission, is precluded.

1.4. Inadequacy of classical concept

In recent years, evidence has been brought forward showing that the classical concept is, in some respects, inadequate. Those concerned with the technology of communication systems are familiar with the influence, in these systems, of fluctuation phenomena ("noise"). That phenomena of a similar kind are operative in the neuronal computing system, which, as a result, can not be considered as completely deterministic, is evidenced by a variety of phenomena.

Firstly, the dictum according to which output is zero in the case of zero input can, is its generality, no longer be upheld. While it applies to neurons of many types there are classes of neurons exhibiting activity in the absence of an input (so-called neural "noise"). Then it has been shown that the generator potential for a given input signal strength may fluctuate, and that the concept of a resting membrane potential which is constant in time, and of the consequent constancy of the threshold in time is at variance with experimental data: resting membrane voltage exhibits fluctuations (membrane "noise").

Thirdly, the deterministic picture of synaptic transmission needs some revision. This also applies to the transmission of excitation between the efferent fibre and the effector (Fatt and Katz, 1952). In the following, fluctuation phenomena in receptor generator potential, in neuron resting membrane potential, and in synaptic transmission will be considered in the order named, after which

the "spontaneous" neuronal activity in the absence of input will be discussed briefly.

1.4.1. *Fluctuations in generator potential*

Fluctuations in generator potential have been demonstrated for the case of the receptor membrane of the Pacinian corpuscle in the cat's mesentery (LOEWENSTEIN, 1961; ILINSKII and FIKS, 1963). This structure can be likened to a piezoelectric transducer responding to mechanical deformation with the production of a non-propagated generator potential the amplitude of which decreases exponentially with increase of distance from the deformed area. Within a certain range of stimulus strengths, i.e. of sizes of deformed area, the generator potential, which is associated with a non-regenerative charge transfer, increases with stimulus strength at a diminishing rate.

However, if a series of stimuli which are equal to within 0.5 % is applied, generator potential amplitudes show a rather wide fluctuation; the amplitude distribution appears to be unimodal and fairly symmetrical. Over a fairly wide range of stimulus strengths the generator potential variance increases as log stimulus strength, indicating the presence of multiplicative noise. Whether the resting potential of the receptor membrane exhibits fluctuations has not yet been investigated. So far, no direct data on the existence or non-existence of generator potential fluctuations in other receptor types are available because of the inaccessibility and extreme smallness of the structures involved. There is no *a priori* reason, however, why they should be present in one receptor type and not in the other.

1.4.2. *Excitability fluctuations in nerve fibres*

One way of investigating the excitability of the nerve membrane is by inducing local depolarization of the axon membrane by the application of a direct current. An action potential is elicited in the cathodal region when depolarization has exceeded the critical level. This level will be crossed the sooner as current density is higher, so the minimum effective current pulse duration is the greater as current density is less. Threshold measurements can be made either by determining the minimum effective duration for a given

current density, or the minimum effective current density for a set duration.

The action potential travels away from the site of stimulation along the axon and can be detected somewhere along its length by recording electrodes.

Threshold fluctuations of the axon membrane were first described by BLAIR and ERLANGER (1933); they were extensively studied by PECHER (1939) and in particular by VERVEEN (1961, 1962), who studied frog, sepia and crayfish axons. Part of his findings can be summarized as follows:

For current pulses of a given duration there is a stimulus intensity below which an action potential is virtually never elicited; there is a second, higher, level above which an action potential is practically always generated. If a series of identical pulses of an intensity somewhere between these levels is given, care being taken that the interval between pulses is such that the fibre is completely recovered from the effects of one stimulus at the time the next is applied, it is found that the fibre responds to a fraction of the stimuli, the probability of firing increasing from nearly zero to nearly one with increase of stimulus strength.

The relation between probability of response and stimulus intensity can be described by a Gaussian distribution function. The excitability can then be expressed in terms of the distribution, i.e. of the 50 % threshold and its standard deviation. The quotient of the two, called "relative spread", is used as a measure of excitability fluctuation. These fluctuations in excitability can be logically associated with fluctuations of resting membrane potential if it is assumed that the critical depolarization level for initiation of an action potential, the "intrinsic threshold" according to VERVEEN (1961), is constant. It can, then, be expected that, in those cases where an action potential is generated, its "latency", i.e. the interval between the (start of the) pulse and its appearance will also fluctuate. This is indeed found to be the case.

1.4.3. *Fluctuation in synaptic transmission*

For the case of synaptic transmission, including transmission at the neuromuscular junction, the completely deterministic picture has to be revised.

On one hand, the arrival at the synapse of a single impulse sometimes fails to result in the liberation of one quantum of transmitter substance and to evoke a unit postsynaptic potential (KUNO, 1964); on the other hand, a vesicle may discharge its transmitter substance in the absence of a presynaptic impulse (FATT and KATZ, 1952; KATZ and MILEDI, 1963; BLACKMAN *et al.*, 1963; MARTIN and PILAR, 1964; ADOLPH, 1964). These facts put synaptic transmission on a probabilistic basis.

1.4.4. *Neural noise*

In the case of fluctuations in membrane polarization, which are large in relation to the resting level, that is, in the case of a high value of the relative spread of excitability, the critical depolarization level may occasionally be attained in the absence of an input, and the receptor or neuron will fire "spontaneously". This firing will be reflected in the firing pattern of the neurons into whose input stage it feeds; spontaneous activity in one neuron may elicit quasi-spontaneous activity in others, and in neurons arranged in loops, spontaneous firing of one neuron may under certain circumstances result in their prolonged activity ("reverberating network").

In the case of spontaneous activity, the additional effect of an input signal will be a change in interval distribution.

1.4.5. *Consequences*

As a consequence of the facts described above, the original deterministic picture can no longer be upheld. This holds in particular for the view that input signal strength is signalled by the overall frequency of a completely or very nearly periodic pulse train. Equal receptor inputs elicit generator potentials which fluctuate in amplitude, so even if the first order neuron connected with the receptor would have a constant threshold, the periodicity of its discharges would to some degree be disturbed. Its threshold, however, shows fluctuations of its own. Despite this, some first-order neuron pulse trains still are near-periodical at high stimulus intensity. At each synapse, another uncertainty factor enters into the case; also, the picture is further complicated by the admixture

of spontaneous activity. At each successive functional layer, the firing pattern becomes more irregular. Instead of a redundant – and consequently particularly safe – input signal strength coding, there is a signalling system where the lengths of individual interspike intervals, and the sequence in which intervals of different lengths occur, carry information.

1.4.6. *Quantitative data*

To assess the significance of the various types of fluctuations described for neuronal information processing and to try and find out what types of noise are involved, quantitative data are necessary. Quantitative information as to the sensitivity of sensory systems can be obtained in behaviour experiments with animals and in psychophysical experiments on man. Both classes of experiments show that, for many types of receptor systems, sensitivity to the appropriate stimulus mode ("adequate" stimulus) is extraordinarily high. The near-simultaneous impingement of a very few photons upon a small retinal area is sufficient to give rise to a sensation (Bouman, 1961; Pirenne and Marriott, 1959); even in microsmatic man six molecules of mercaptan or less are sufficient to excite one olfactory receptor cell [1]); a subjective sensation is obtained by near-simultaneous excitation of about 40 cells (De Vries and Stuiver, 1961). Similar low values are found for other sense organs. At the absolute hearing threshold the signal power is commensurable with that of Brownian noise at body temperature (Van Gemert, 1955; De Vries, 1956). Behaviour experiments by Lissman and Machin have shown that the tropical fish, *Gymnarchus Niloticus*, detects changes in electric current strength in the order of 3×10^{-15} A through its electroreceptor cells. This is a factor 200 less than the estimated noise current through the receptor cell (Machin, 1962). From behaviour experiments by Bullock and Diecke (1956) it follows that the sensitivity of the pit viper's infrared detector is such that an object of 5 cm radius and of a surface temperature 10° C higher than its own can be detected at a distance of 50 cm. This amounts to a stimulus power of 4×10^{-8} W.

---

[1]) Probably, only one molecule per receptor cell is needed.

1.4.7. *Nature of sensitivity limitation at receptor level*

The question arises in how far, in animal data acquisition and handling systems, the limit to sensitivity is set by internal noise, as is the case in many man-made sensitive detectors and amplifiers.

The primary limitation to sensitivity lies at receptor level. The performance of a receptor cell can be expressed in terms of a figure of merit on the basis of its responsivity which, in this case, is given by the degree of depolarization per unit of stimulus intensity, and the spectrum and amplitude distribution of signal fluctuations and of internal noise. In those receptors where input signal strength is continuously variable from zero upward (mechanoreceptors, including those in the acoustic and non-acoustic labyrinth, electroreceptors, thermoreceptors), sensitivity can be supposed to be limited by internal noise in the system. Both false-positive and false-negative receptor responses may occur. The question of whether the onnipresent thermal noise is, as such, the limiting factor as it would seem to be in the case of the ear or if other noise types are also involved will have to be considered for each particular case.

In those cases where the input signal is of a quantal nature as in the visual, olfactory and gustatory systems, the fluctuations in absolute threshold are primarily determined by the uncertainty as to the number of quanta (in its widest sense) contained in the stimulus, and the relative importance of internal noise is much less. The energy content of the unit (quantum) stimulus is such as to ensure excitation of the receptor; false-negative responses will not occur, the possibility of false-positives remains. It is to be noted that the classical threshold concept is not applicable either in the case of a non-quantal or in that of a quantal input; in the first-named case the limiting factor is internal noise, in the second, a 'threshold", should it exist, is always exceeded.[1])

'1.4.8. *Properties of the system as a whole*

Noise phenomena at receptor level are only one of the determinants of the performance of the system as a whole.

[1]) There is no correlation between the quantal or non-quantal nature of the adequate stimulus on one hand and the generation or non-generation, by the receptor, of a spike potential on the other. Whether or not an axon is present and, consequently, spikes are fired is a matter of the distance to be bridged.

The crucial question is that of whether, as a result of the application of an excitatory input to the receptors converging upon it, a first-order neuron is incited to fire; the first real hurdle lies not at receptor level but at the first synaptic junction, and besides receptor membrane noise, fluctuations in synaptic transmission as well as neuron membrane noise enter into the case.

1.4.8.1. Non-quantal inputs

In those types of receptors which do not deliver spike potentials the generator potential is a continuously rising function of input signal strength. The effect of the admixture of receptor membrane noise is that within a given range of input signal strengths, it is uncertain whether a signal of a given strength will occasion synaptic activity; in the case of large fluctuations, synaptic activity may be incited in the absence of an input. As a result, the neuron may fire "spontaneously" despite zero input on the receptors converging upon it.

Similarly, in a receptor delivering spikes, there is a range of input signal strengths where an input signal of a given intensity may or may not push initial depolarization to the critical level. In those receptor types where fluctuations are large, the receptors will fire continually in the absence of an input; the effect of an input signal is a change in firing pattern.

1.4.8.2. Quantal inputs

From the fact that the inpingement of one photon in the retina is not perceived, and that the near-simultaneous inpingement of a very few (two, according to BOUMAN, *l.c.*) on a small retinal area is, it follows that one photon excites a retinal receptor, but that the output signal delivered by an excited receptor is insufficient to provoke firing in the neurons connected with it.

The absorption of one quantum is a fortuitous happening; the near-simultaneous reception of a small number in a restricted area however may carry information. A similar reasoning applies, in the case of the olfactory system, to the perception of odoriferous substances. In both cases, use is made of the convergence principle to sift meaningful information from fortuitous occurrences.

1.4.8.3. Convergence and spatial summation; temporal summation

By virtue of the convergence of receptor output stages on first-order neurons the latter can, in the case of receptors which do not generate spikes, reach the critical depolarization level, and discharge, when some slight degree of depolarization, resulting from weak stimulation, occurs simultaneously in a number of the receptor elements converging upon it. Similarly in the case of receptors producing action potentials, the single spike produced by a brief stimulus, or, in the case of a weak stimulus of prolonged duration, the frequency of the pulse train delivered will, as a rule, be insufficient to excite the first-order neuron; here again, spatial summation is possible. In addition, temporal summation is, in the case of prolonged or repeated weak stimulation, possible both at receptor level and at that of the neuron. Both spatial and temporal summation can, to some degree, be considered as resulting in an increase in sensitivity which is, of course, bought in the first-named case at the price of a decrease in spatial resolution, and in the other at that of a decrease of resolution in time, in the sense of the introduction of a delay of unknown duration.

The decrease in spatial resolution is irrelevant in those cases where the signal carries no spatial cue (gustatory and olfactory senses), and neither of the two constitutes an appreciable setback in the periliminal range of stimulus intensities. The fact should be taken into consideration that the primary purpose of the whole system is to direct a requisite reflex response to particular stimuli and stimulus patterns. For a given response to occur, the exact location of the stimulus or stimuli within the reflexogenic area is immaterial. On the other hand, the time constants of decay of subliminal depolarization, setting a limit to integration times, are short compared to the total reflex time, which is mainly determined by conduction times and synaptic delays.

1.5. Plan of present investigation; choice of object

It is clear that it is only by performing some sort of correlation analysis that the neuronal computing system is able to extract the significant information from the jumble of signals arriving from the continuous inflow of input data in the presence of "noise" at receptor level, at that of the neurons, and at the synaptic

junctions, and of the "spontaneous" discharges ("neural noise") which may result from them. Before we can ever hope to analyse the way in which this is done, it is necessary to study the fluctuations named in detail; that is, to determine the noise power spectra involved.

This, however, presents experimental difficulties which are typical of physiological experimentation at cellular level.

The object of investigation is the living cell. It should stay alive during experimentation, that is, ambient conditions should not be far removed from natural conditions (temperature, composition of bathing fluid, oxygenation). This rules out many methods of investigation. In addition, the object is diminutive in size, with linear dimensions measured in thousandths of millimeters; within this small compass it is highly structured, labile, and sensitive to minute environmental influences.

The choice of the actual object to be investigated is, thus, largely dictated by utilitarian considerations such as accessibility, size, etc.

Ideally, of course, the receptor cell membrane, the dendritic membrane, and the initial axon segment would be best suited, but experimental difficulties have, so far, been insuperable.[1])

On the other hand, some characteristics of the resting nerve cell membrane apply to cells in general; all living cell membranes exhibit an inside-negative polarization which is, primarily, related to a difference between inside and outside potassium concentration; in all living cells, an active sodium extrusion mechanism operates. To some extent, the results obtained with the membrane of one type of cell can be considered as representative for any type.

Thus, the Hodgkin–Huxley equations [2]) in which the resting potential of the squid giant axon membrane is linked to inside and outside Na^+, K^+ and Cl-concentrations, and the electrical changes which constitute the action potential can be accounted for on the basis of the time and voltage dependent changes in permeability for sodium and the other ions, have been found to

---

[1]) Work is now in progress on noise measurement in muscle spindles and Pacinian corpuscle receptors; results will be published in due course.

[2]) The equations in question can be simplified to the Bonhoeffer–Van der Pol equation (FITZHUGH, 1961) which are a generalization of the well-known Van der Pol equation for electrical relaxation oscillations.

apply equally well to the Ranvier node of the medullated vertebrate nerve fibre, and to heart muscle fibre, allowing for minor variations in parameter values, which can be associated with differences in membrane thickness, number of ion-transport sites, etc. (HODGKIN and HUXLEY, 1952; DODGE, 1961; FRANKENHAEUSER and HUXLEY, 1964). In the present investigation the Ranvier node of the frog's spinal nerve fibre (isolated fibre from the sciatic nerve) was chosen; that is, the noise of the axon membrane was studied. As an object of investigation, the Ranvier node presents several advantages. Methods have been developed to isolate and mount a stretch of medullated fibre long enough to contain two or three nodes. The electrical properties of the node have been extensively investigated; the influence of changes in ionic composition of the bathing fluid and that of various drugs has been studied. Finally, the nature of the fluctuations in excitability and in latency, which are directly associated with fluctuations in resting membrane potential, is known thanks to the work of PECHER and of VERVEEN. Some quantitative data are collected in Table I.

TABLE I

Some dimensions and electric properties of frog myelinated axon

Data given by TASAKI (1955), TASAKI and FRANK (1955) for frog myelinated axons of 12–15 μ diameter (myelinated part) at 24–25° C.

Myelin sheath	
Segment length	2–2.5 mm
Thickness	2–3 μ
Resistance	290 $\pm$ 40 MΩ/mm
Capacitance	1.6 $\pm$ 0.2 pF/mm
Axoplasm resistance	15 MΩ/mm
Node of Ranvier	
Diameter	8 μ
Width	0.5–1 μ
Surface area	2–5 $\times 10^{-7}$ cm^2
Membrane resistance	41 $\pm$ 6 MΩ
Membrane capacitance	1.5 $\pm$ 0.6 pF

2. PRINCIPLE OF METHODS TO INVESTIGATE ELECTRICAL PROPERTIES OF NODAL MEMBRANE

2.1. Introduction

Fig. 2.1.–1 shows the electrical network equivalent to the myelinated axon. The internodal segments behave as coaxial cables with negligible series inductance and appreciable shunt conductance. The electrical properties of the nodes can be described in terms of membrane capacitance, C_m, membrane conductance g_m, and a standing potential difference E, across the membrane. In the resting state, E is about 60–70 mV inside-negative. In the following, the cable-like characteristics of the internodal segments will be left out of account: resistances r_a will respresent their longitudinal resistance (Fig. 2.1.–1c).

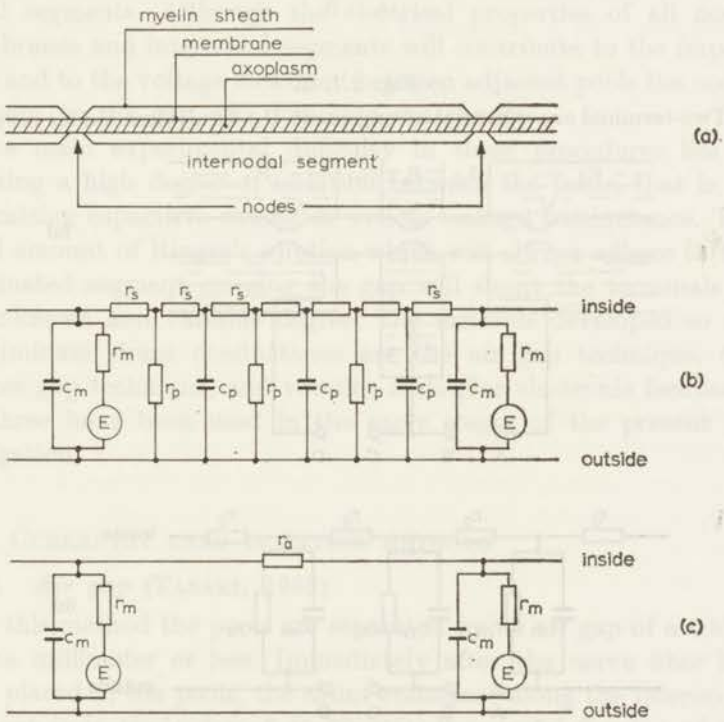

Fig. 2.1.–1.

(a) Axial cross-section of myelinated axon segment. (b) Equivalent electric network diagram. (c) Simplified electric network diagram.

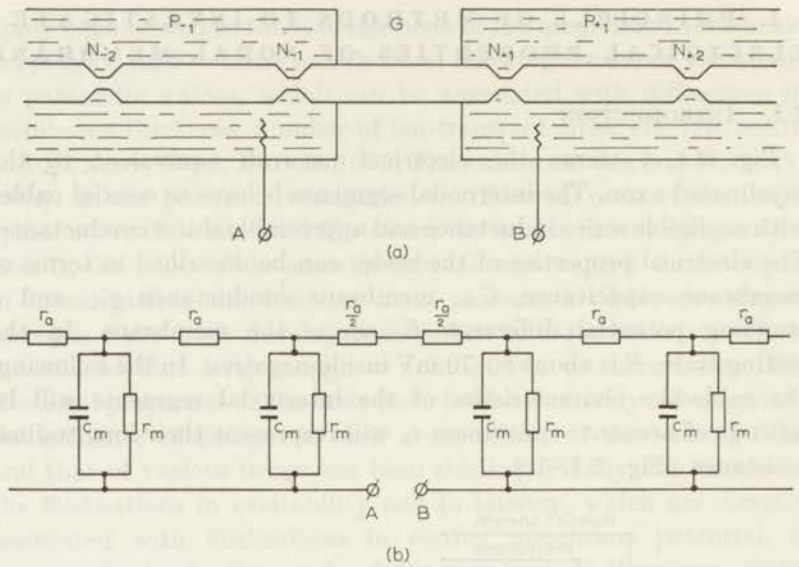

Fig. 2.1.–2.

(a) Two-terminal experimental arrangement. (b) Equivalent ladder network.

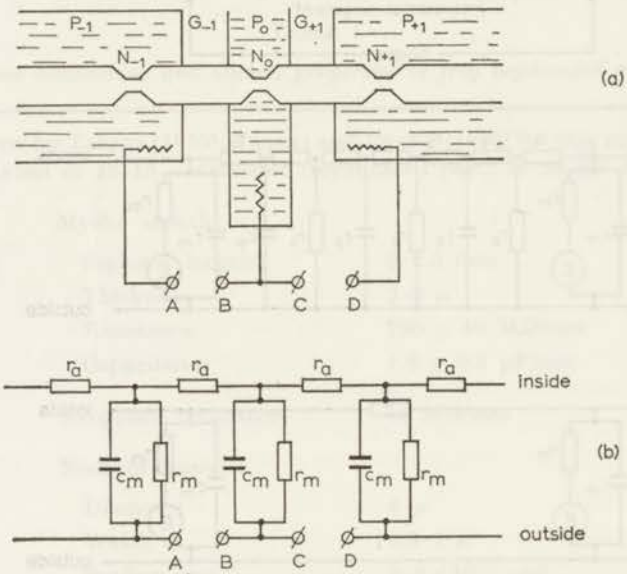

Fig. 2.1.–3.

(a) Three-terminal experimental arrangement. (b) Equivalent ladder network.

As the inside of the axon is not accessible for penetration by microelectrodes as a result of its extremely small size and its particular structure, the only way to investigate the electrical properties of the nodal membrane is through one or two neighbouring membranes and the internodal axoplasm. For this, the saline medium in which the nerve fibre bathes must be divided into two or three separate pools. Figs. 2.1.–2 and 2.1.–3 show schematically how this is realized. The arrangement pictured in Fig. 2.1.–2 (single gap technique) results in a two-terminal circuit element; that of Fig. 2.1.–3 (double gap technique) in a three-terminal one. In the two-terminal arrangement one internodal segment crosses the gap between two pools of Ringer's solution: in the other, the two gaps on either side of the pool in which the middle one of three adjacent nodes is bathed are crossed by the corresponding internodal segments. Although the electrical properties of all nodal membranes and internodal segments will contribute to the impedance and to the voltage measured between adjacent pools the nodes adjacent to the gap will dominate the results.

The main experimental difficulty in these procedures lies in realizing a high degree of isolation between the pools, that is, in minimizing capacitive shunts as well as leakage conductance. The small amount of Ringer's solution which will always adhere to the myelinated segment crossing the gap will shunt the terminals to an unknown and variable degree. The methods developed so far to eliminate shunt conductance are the air gap technique, the sucrose gap technique, and vaseline seals plus electronic feedback. All three have been used in the early stages of the present investigation.

2.2. Currently used isolation methods

2.2.1. *Air gap* (Tasaki, 1953)

In this method the pools are separated by an air gap of a width of one millimeter or less. Immediately after the nerve fiber has been placed in the pools, the shunt resistance along the internodal segment is in the order of 40–70 MΩ. By careful fanning of the internodal segment one arrives, after some 15 minutes, at a fairly stable situation where shunt leakage is in the order of one hundred to a few hundred MΩ. It is not possible to measure the degree

of shunting without assigning a given value to the amplitude of the action potential. In general, this stable situation does not last for more than one hour; the axoplasm begins to dry out, which finally results in deterioration of the fibre as a whole. The main advantage of this method is its simplicity. For long series of measurements and when good accuracy is desired it is less suitable.

2.2.2. *Sucrose gap* (STÄMPFLI, 1963)

In the sucrose gap technique, the saline adhering to the outside of the myelin sheath is washed away by a slow stream of isotonic sucrose solution. Vaseline seals separate the sucrose stream from the pools of Ringer's solution bathing the nodes. By this method, shunt resistance between pools can be increased to ten or a hundred times source resistance (MOORE, 1959). A stable situation can be maintained for a few hours at least, but the method is rather difficult technically. For measurements in the microvolts range, such as noise measurements, the sucrose solution must flow very evenly, and the flow circuit must be completely shielded to avoid mains hum pickup.

2.2.3. *Isolation by means of electronic feedback* (FRANKENHAEUSER, 1957)

In this method, longitudinal currents along the outer surface of the internodal segment are suppressed by an arrangement resembling the guard ring techniques used in electrostatic measurements. It is illustrated in Fig. 2.2.3.–1a [1]). Besides the two saline pools P_{-1} and P_0, bathing the corresponding nodes a third pool P_a, in the form of a narrow channel, wets the middle part of the internodal segment. Seals of petroleum jelly, S_1 and S_2 separate the pools. It has been reported (MOORE, 1959) that seals of this type have an ohmic resistance of 1–10 MΩ, which by itself, would, of course, be quite insufficient. A very high effective resistance between the outer pools can, however, be achieved by connecting a high-gain differential amplifier to the pools as shown in the figure.

This can be easily proved from the equivalent circuit of Fig.

[1]) The set-up pictured here differs from the original Frankenhaeuser arrangement in that in the latter P_{-1} is grounded instead of P_0 (cf. 2.4). Also, the treatment given below is different from that of FRANKENHAEUSER.

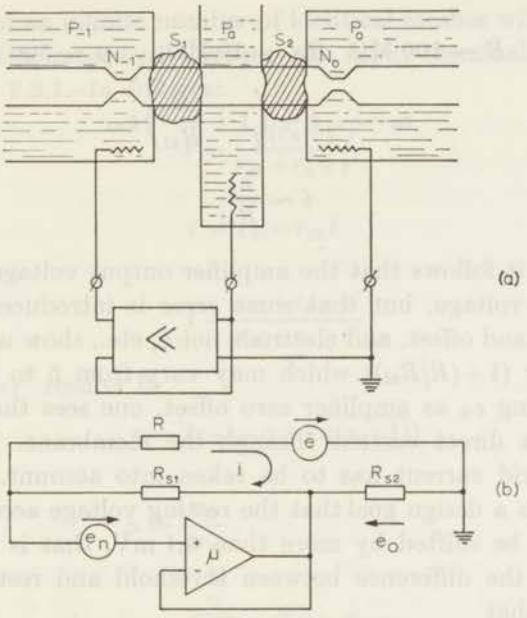

Fig. 2.2.3.–1.
(a) Two-terminal experimental arrangement with feedback isolation.
(b) Electric equivalent.

2.2.3.–1b. The reactive component of the source impedance (the nerve fiber preparation) will be left out of account, the fiber is therefore represented by a voltage source with internal resistance R. Also, stray capacities, amplifier phase shifts and frequency dependence of amplifier gain will be neglected. The seal resistance is represented by R_{s1}; the righthand seal is parallel to the amplifier output impedance and its resistance, if not excessively low, is of little consequence. Amplifier noise and drift are represented by a voltage source e_n in series with the live input terminal.
From Fig. 2.2.3.–1b follows

$$e_0 = \mu(e_n - iR_{s1})$$

$$i = \frac{e+e_0}{R+R_{s1}}.$$

As a consequence:

$$e_0 = -\frac{\mu R_{s1}}{R+(\mu+1)R_{s1}}\,e + \frac{\mu(R+R_{s1})}{R+(\mu+1)R_{s1}}\,e_n.$$

Now

$$R \sim 100\ \mathrm{M}\Omega,\ R_{s1} \sim 10\ \mathrm{M}\Omega \qquad \mu \sim 500$$

$$e_0 \sim -e + \left(1 + \frac{R}{R_{s1}}\right) e_n. \tag{2.1}$$

Further

$$i \sim \frac{e_n}{R_{s1}}. \tag{2.2}$$

From (2.1) it follows that the amplifier output voltage reproduces the source voltage, but that some error is introduced. Amplifier noise, drift and offset, and electrode noise, etc., show up multiplied by a factor $(1+(R/R_{s1}))$ which may vary from 5 to 2.

Considering e_n as amplifier zero offset, one sees that its consequence is a direct current through the membrane. In addition, amplifier grid current has to be taken into account.

Taking as a design goal that the resting voltage across the node should not be shifted by more than 0.1 mV, that is roughly one percent of the difference between threshold and resting voltage, it follows that

$$e_n \leqslant 10^{-4} \frac{R_s}{r_m}\ \mathrm{V} \tag{2.3}$$

while grid current i_g should satisfy the condition

$$i_g \leqslant 2.5 \times 10^{-12}\ \mathrm{A}. \tag{2.4}$$

The feedback isolation technique is attractive as far as ease of nerve fiber manipulation is concerned. It is, however, rather difficult from an instrumentation viewpoint. Also, an appreciable amount of noise is superimposed on the fluctuations of the preparation.

2.3. Determination of nodal membrane voltage fluctuations

2.3.1. *Source emf*

To arrive at an estimate of the noise emf between the electrodes, the shunting by nodal capacitance will be left out of account. The axon is supposed to be of infinite length. Fluctuation emf's of intensities $\overline{e_m^2}$ and $\overline{e_a^2}$ will be assumed to exist across the nodal membrane and in series with the internodal resistance respectively. It is evident that the addition of one more mesh to a ladder network

composed of an infinite number of identical meshes will not change the properties measured between the input terminals.
From Fig. 2.3.1.–1a follows:

$$r = \frac{r_m(r_a+r')}{r_m+r_a+r'}$$

and

$$e = e_m - r_m i$$

further

$$i = \frac{e_m+e_a-e'}{r_m+r_a+r'}.$$

Putting $r=r'$ results in

$$r = 2r_m(-\alpha+\sqrt{\alpha(\alpha+1)})$$

where

$$\alpha = \frac{r_a}{4r_m}.$$

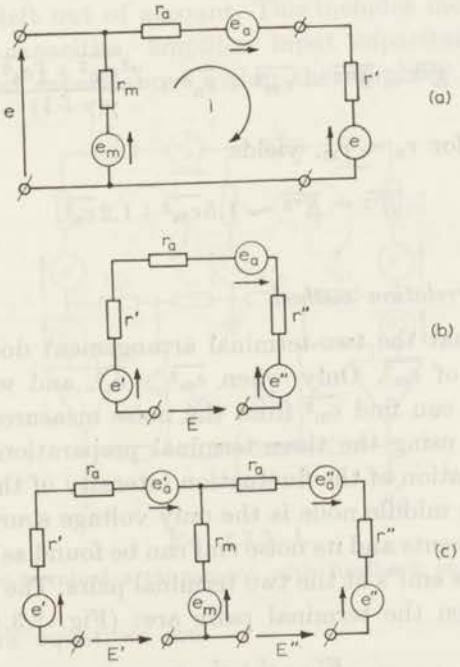

Fig. 2.3.1.–1.
(a), (b), (c) see text.

Substitution of the expression for i and r' into that for e, and putting $\overline{e^2}=\overline{(e')^2}$ results in

$$e^2 = \frac{\gamma^2\overline{e_m{}^2}+\frac{1}{4}\overline{e_a{}^2}}{\gamma(\gamma+1)}$$

in which

$$\gamma = \alpha+\sqrt{\alpha(\alpha+1)}.$$

For a two-terminal preparation the noise emf between the terminals (Fig. 2.3.1.–1b) is:

$$\overline{E^2} = 2\,\frac{\gamma^2\overline{e_m{}^2}+\frac{1}{4}\overline{e_a{}^2}}{\gamma(\gamma+1)}+\overline{e_a{}^2}. \tag{2.5}$$

For the case $r_a \sim r_m$ this yields:

$$\overline{E^2} \sim 0.9\overline{e_m{}^2}+1.2\overline{e_a{}^2}.$$

For the two terminal pairs of a three-terminal preparation (Fig. 2.3.1.–1c).

$$\overline{E'^2} = \overline{E''^2} = \overline{e_m{}^2}+\overline{e_a{}^2}+\frac{\gamma^2\overline{e_m{}^2}+\frac{1}{4}\overline{e_a{}^2}}{\gamma(\gamma+1)} \tag{2.6}$$

which, again for $r_a \sim r_m$, yields

$$\overline{E'^2} = \overline{E''^2} \sim 1.5\overline{e_m{}^2}+1.2\overline{e_a{}^2}.$$

2.3.2. *The correlation method*

It is clear that the two-terminal arrangement does not allow a determination of $\overline{e_m{}^2}$. Only when $\overline{e_m{}^2} \gg \overline{e_a{}^2}$, and when α can be estimated, one can find $\overline{e_m{}^2}$ from the noise measured between the electrodes. By using the three-terminal preparation, however, an exact determination of the fluctuation intensity of the middle node is possible. The middle node is the only voltage source common to both nerve segments and its noise emf can be found as the correlated part of the noise emf's at the two terminal pairs. The instantaneous voltages between the terminal pairs are: (Fig. 2.3.1.–1c)

$$E' = e'+e'_a-e_m$$

$$E'' = -e''-e''_a+e_m$$

from which follows:

$$\overline{E'\,E''} = \overline{e_m{}^2}. \tag{2.7}$$

Thus the value of $\overline{e_m{}^2}$ can be found by averaging, in time, the product of $E'(t)$ and $E''(t)$ as obtained by filtering through identical band-pass filters. This method, cross correlation at zero time shift, has been used in the main series experiments of the present investigation.

The obvious advantages of the correlation method are, however, obtained at the cost of increased complexity of measuring and data-processing equipment.

2.3.3. *The correlation method using feedback isolation*

In the majority of cases, the correlation method has been used together with a three-terminal version of Frankenhaeuser's feedback isolation method.

Fig. 2.3.3.–1 shows feedback isolation applied to both segments of a three-terminal preparation. In the following all capacitive effects will be left out of account. This includes membrane capacitance, stray capacities, amplifier input capacitance and band limiting internal capacitances within the amplifier.

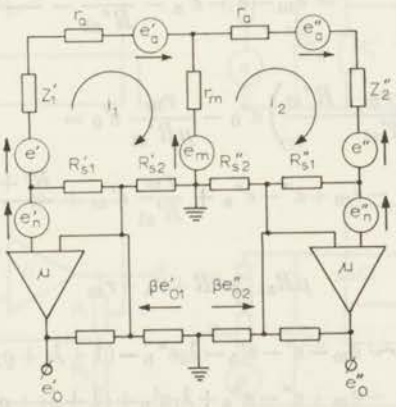

Fig. 2.3.3.–1.

Three-terminal arrangement with feedback isolation.

The network equations are

$$\beta e'_0 + e' + e'_a - e_m = (R' + r_a + r_m + R'_{s1})\, i_1 - r_m i_2$$
$$-\beta e''_0 - e'' + e''_a + e_m = -r_m i_1 + (R'' + r_a + r_m + R''_{s1})\, i_2.$$

The input voltages of the left-hand differential amplifier in Fig. 2.3.3.–1 are

$$e_1 = \beta e'_0 - R'_{s1} i_1 - e'_n$$
$$e_2 = \beta e'_0$$

while the output voltage is

$$e'_0 = -\mu(e_2 - e_1).$$

It follows that:

$$\frac{1}{\mu} e'_0 + e'_n = -R'_{s1} i_1$$

and for the other amplifier:

$$\frac{1}{\mu} e''_0 + e''_n = R''_{s1} i_2.$$

Substitution of i_1 and i_2 in the network equations and rearranging results in:

$$\left(\beta + \frac{R' + r_a + r_m + R'_{s1}}{\mu R'_{s1}}\right) e'_0 + \frac{r_m}{\mu R''_{s1}} e''_0 =$$
$$= e_m - e' - e'_a - \frac{r_m}{R''_{s1}} - \frac{R' + r_a + r_m + R'_{s1}}{R'_{s1}} e'_n$$

and

$$-\left(\beta + \frac{R'' + r_a + r_m + R''_{s1}}{\mu R''_{s1}}\right) e''_0 - \frac{r_m}{\mu R'_{s1}} e'_0 =$$
$$= -e_m + e'' - e''_a + \frac{r_m}{R'_{s1}} e'_m + \frac{R'' + r_a + r_m + R''_{s1}}{R''_{s1}} e''_n.$$

When

$$\mu R_{s1} \gg R + r_a + r_m$$

than

$$\beta e'_0 \sim e_m - e' - e'_a - \lambda_2 e''_n - (1 + \lambda_1 + \varrho_1) e'_n \qquad (2.8)$$

$$\beta e''_0 \sim -e_m + e'' - e''_a + \lambda_1 e'_n + (1 + \lambda_2 + \varrho_2) e''_n. \qquad (2.9)$$

Where

$$\lambda = \frac{r_m}{R_{s1}} \quad \text{and} \quad \varrho = \frac{r_a + R}{R_s}.$$

The correlated part of the amplifier output voltages is:

$$-\beta^2 \overline{e'_0 e''_0} = \overline{e^2_m} + \lambda_2(1 + \lambda_2 + \varrho_2)\,\overline{e''^2_n} + \lambda_1(1 + \lambda_1 + \varrho_1)\,\overline{e'^2_n}. \qquad (2.10)$$

For r_m, r and R_s approximately 40 MΩ and $R \sim 100$ MΩ:

$$\lambda_1 \sim \lambda_2 \sim 1$$

$$\varrho_1 \sim \varrho_2 \sim 3.5$$

so

$$-\beta^2 \overline{e'_0 e''_0} \sim \overline{e^2_m} + 5.5(\overline{e'^2_n} + \overline{e''^2_n}).$$

For identical amplifiers

$$\overline{e'^2_n} = \overline{e''^2_n} \equiv \overline{e^2_n},$$

so

$$-\beta^2 \overline{e'_0 e''_0} = \overline{e^2_m} + 11\overline{e^2_n}.$$

Obviously $\overline{e_m^2}$ should be measured over the whole spectral range of interest, further λ_1, λ_2, ϱ_1 and ϱ_2 must be determined in order to correct for amplifier noise. In the middle part of the frequency range (100 – 10 000 rad·sec^{-1}) the amplifier noise term is quite low. At frequencies below 100 rad·sec^{-1}, flicker noise, which has

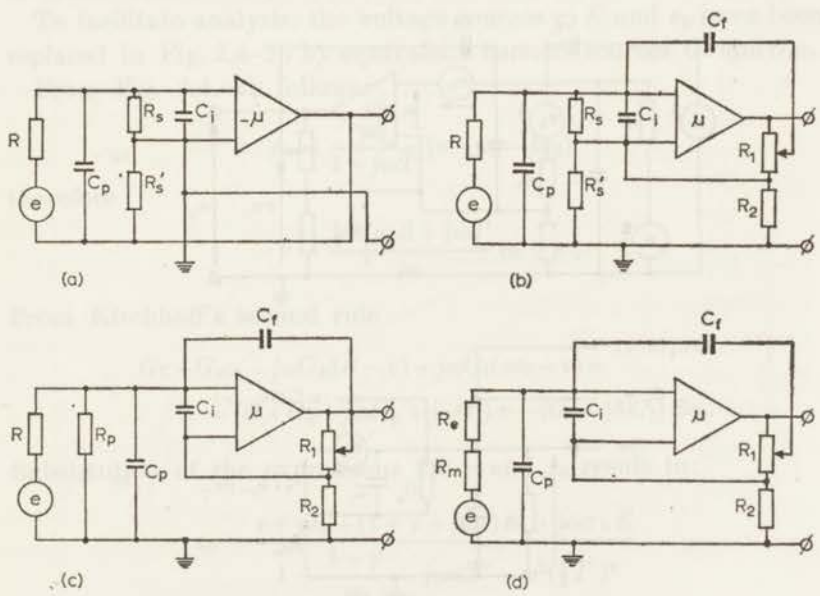

Fig. 2.4.–1.

Network equivalents of: (a) feedback isolation according to FRANKENHAEUSER, (b) feedback isolation as used in the present investigation, (c) circuit used for determining myelinated axon properties using air or sucrose gap techniques, (d) intracellular recording from neuron cell bodies.

a $1/f$ power spectrum, becomes increasingly important as the measuring frequency becomes lower. It is evident that amplifier noise must be kept as low as possible.

2.4. High frequency response, input capacitance neutralization

Figs. 2.4–1a–d show the electrical equivalent of a two-terminal sucrose or air gap arrangement (c), feedback isolation according to Frankenhaeuser (a), the version of feedback isolation as used in this investigation (b) and finally the situation in intracellular recording by means of electrolyte-filled micro-pipettes (d). It is clear that, if the shunt resistance across the gap can be made very high compared to the source resistance, there is no difference between the air and sucrose gap techniques on the one hand and the intracellular recording technique on the other. Of course in the latter, the source resistance is mainly the electrode resistance while in

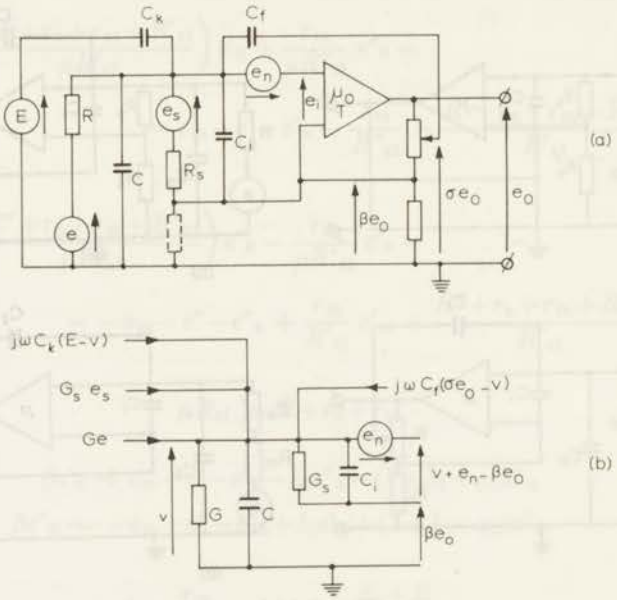

Fig. 2.4.–2.

(a) Detailed network equivalent of feedback isolation as used in the present investigation. (b) The same after substitution of voltage sources by equivalent current sources.

studies on myelinated axons, where fairly large electrodes can be used, the source resistance is practically identical with the resistance of the fiber preparation. Between the two versions of the feedback isolation method there are no differences. The network equations are identical. In the version used here the location of the grounded pool allows the double use of the method in order to arrive at a three-terminal arrangement. To evaluate feedback isolation more precisely the equivalent circuit of Fig. 2.4.–2a is used. The noise emf of the upper seal resistance is represented by a voltage source e_s.

The lower seal resistance and its noise emf are parallel to the output terminals of the amplifier and are consequently of no importance. Positive feedback from the amplified output voltage σe_0 through a small capacitance C_f is used to neutralize stray capacitance from the pool to the surrounding. A calibrating voltage E is connected through a small capacitor C_k to the live input terminal. Amplifier noise is represented by a voltage source E_n in series with the input.

To facilitate analysis, the voltage sources e, E and e_s have been replaced in Fig. 2.4–2b by equivalent current sources Ge and $G_s e_s$.

From Fig. 2.4.–2b follows:

$$e_0 = \frac{\mu_0}{1+j\omega T}\,(v + e_n - \beta e_0)$$

therefore

$$v = \frac{1+\mu_0\beta+j\omega T}{\mu_0}\,e_0 - e_n.$$

From Kirchhoff's second rule

$$Ge + G_s e_s + j\omega C_k(E-v) + j\omega C_f(\sigma e_0 - v) =$$
$$= (G + G_s + j\omega C_p + j\omega C_i)\,v - (G_s + j\omega C_i)\,\beta e_0.$$

Substitution of the expressions for v and e_0 result in:

$$e_0 = \frac{e+\gamma e_s + (1+\gamma+j\omega\tau)\,e_n + j\omega\tau_k E}{1 + \dfrac{1+\gamma}{\mu_0} + j\omega a T' - \omega^2(\frac{1}{2}T')^2}.$$

As $\dfrac{1+\gamma}{\mu_0} \ll 1$

$$e_0 = \frac{e+\gamma e_s + (1+\gamma+j\omega\tau)\,e_n + j\omega\tau_k E}{1 + j\omega a T' - \omega^2(\frac{1}{2}T')^2} \qquad (2.11)$$

where $$\gamma = \frac{R}{R_s}$$

and $$\tau_k = RC_k$$

$$\tau = R(C_p + C_i + C_k + C_f)$$

$$aT' = R\left(C_p + C_k + C_f - \frac{\sigma}{\beta}C_f\right) + \frac{\tau}{\mu} + (1+\gamma)\frac{T}{\mu}$$

$$T' = 2\sqrt{\tau\frac{T}{\mu}}$$

$$\mu = \mu_0\beta.$$

Except for the terms due to the presence of the seal resistance, expression (2.11) is the same as that derived by GULD (1962) for the case of intracellular recording by means of micropipette and capacitance-neutralized preamplifier. From his response curves (Fig. 2.4.–3) it can be seen that for $a \sim 0.7$, frequency response is constant till about $\omega T' \sim 1.5$.

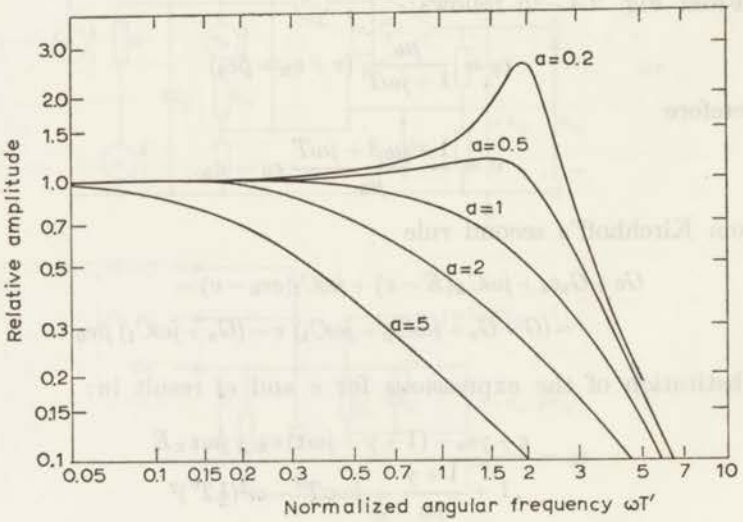

Fig. 2.4.–3.

Frequency responses of capacitance-neutralized electrometer amplifire for different settings of positive feedback parameter a. After GULD (1962), by courtesy of the author.

This means that

$$\omega_{max} \sim \frac{0.75}{\sqrt{\left(\tau \frac{T}{\mu}\right)}}. \tag{2.12}$$

However the source resistance presented by the nerve fiber is only more or less constant in the range from zero to $\omega = 1/\tau \sim 16000$ rad·sec^{-1} for $\tau = 60$ μsec. Still worse, the parallel capacitance of the source impedance changes from 0.42 pF at 3300 rad·sec^{-1} to 0.11 pF at 97000 rad·sec^{-1} (§ 2.5). As the effective input capacitance for optimal capacitance neutralization at $R_s = 100$ MΩ is in the order of 0.1 pF this means that with a nerve fiber optimal adjustment is limited to the range of angular frequencies 0–3300 rad·sec^{-1}. Beyond that the system must be readjusted for each of the frequencies in which noise measurements are to be made. The procedure is to connect a sine wave calibrating voltage of an amplitude inversely proportional to frequency to the coupling capacitors C_k and to adjust the positive feedback for constant a.c. output voltage over the whole range of measuring frequencies. In this way noise measurements up to 10–15 kc/s can be made. It must be realized however that a shunting effect of the membrane capacitance on the membrane noise emf is eliminated by this procedure, as there is no way to separate the parallel capacitance of the object investigated from the parallel capacitance of the amplifier.

In view of the foregoing it is doubtful whether FRANKENHAEUSER's claims (1957) concerning a 30 kc/s bandwidth for a circuit without capacitance neutralization can be justified. His own statement (FRANKENHAEUSER and HUXLEY, 1964) that the time resolution of his equipment was insufficient to show the influence of membrane capacitance leads to the same conclusion. A membrane time constant of, say, 60 μsec corresponds to 2.65 kc/s for 3 db amplitude decrease. This does not invalidate FRANKENHAEUSER's voltage clamp measurements in any way, however.

2.5. REQUIREMENTS AS TO AMPLIFIER INPUT IMPEDANCE; SOURCE IMPEDANCE

In order to state the requirements for amplifier input impedance and for electrical insulation between the pools, the impedance of

the nerve fiber preparation must be known first. Using the same assumptions as in § 2.3.1 but including membrane capacitance, it follows from Fig. 2.5.–1:

$$Z = \sqrt{\tfrac{1}{4}r_a^2 + r_a Z_m}$$

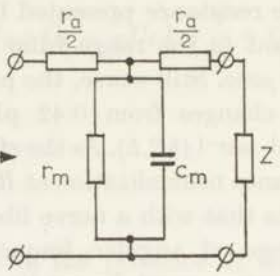

Fig. 2.5.–1.
Calculation of source impedance.

where

$$Z_m = \frac{r_m}{1 + j\omega\tau}$$

and

$$\tau = r_m c_m.$$

It follows that:

$$Z^2 = \frac{r_a^2(1+\omega^2\tau^2) + 4r_a r_m}{4(1+\omega^2\tau^2)} - j\,\frac{4r_a r_m \omega\tau}{1+\omega^2\tau^2}.$$

If we define

$$Z^2 = \varrho\,(\cos\gamma + j\sin\gamma)$$

then

$$Z = \varrho^{\frac{1}{2}}\,(\cos\tfrac{1}{2}\gamma + j\sin\tfrac{1}{2}\gamma),$$

the other root resulting in negative resistance values. Therefore

$$\varrho\cos\gamma = \frac{r_a^2(1+\omega^2\tau^2) + 4r_a r_m}{4(1+\omega^2\tau^2)}$$

and

$$\varrho\sin\gamma = -\frac{4\omega\tau r_a r_m}{1+\omega^2\tau^2}.$$

From these expressions ϱ, $\varrho^{\frac{1}{2}}$, $\cos \frac{1}{2}\gamma$ and $\sin \frac{1}{2}\gamma$ can be found and finally:

$$R = \varrho^{\frac{1}{2}} \cos \tfrac{1}{2}\gamma = r_m \left[2\alpha \left\{ \alpha + \frac{1}{1+\omega^2\tau^2} + \left(\alpha^2 + \frac{1+2\alpha}{1+\omega^2\tau^2} \right)^{\frac{1}{2}} \right\} \right]^{\frac{1}{2}}$$

$$X = -\frac{1}{\omega c_m} \frac{\omega^2\tau^2}{1+\omega^2\tau^2} 8\alpha \left[2\alpha \left\{ \alpha + \frac{1}{1+\omega^2\tau^2} + \left(\alpha^2 + \frac{1+2\alpha}{1+\omega^2\tau^2} \right)^{\frac{1}{2}} \right\} \right]^{-\frac{1}{2}}.$$

For each terminal pair of a three-terminal preparation:

$$R_s = R + \frac{r_a}{2} + \frac{r_m}{1+\omega^2\tau^2}$$

$$X_s = X - \frac{\omega\tau}{1+\omega^2\tau^2} r_m.$$

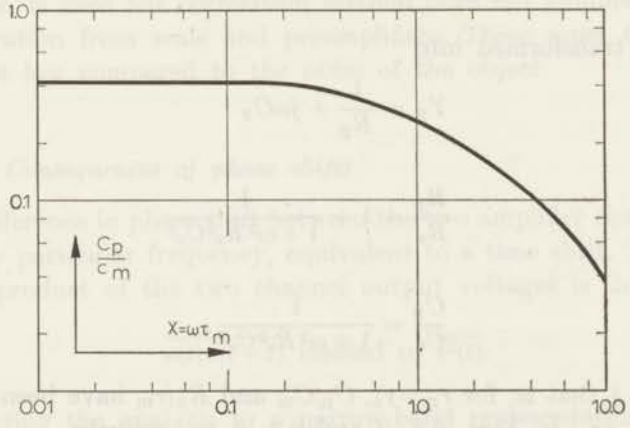

Fig. 2.5.–2.
Ratio between C_p and c_m as a function of $\omega\tau_m$.

$$\frac{R_s}{r_m} = 2\alpha + \frac{1}{1+x^2} + \left[2\alpha \left\{ \alpha + \frac{1}{1+x^2} + \left(\alpha^2 + \frac{1+2\alpha}{1+x^2} \right)^{\frac{1}{2}} \right\} \right]^{\frac{1}{2}} \qquad (2.13)$$

$$\frac{c_m}{C_s} = \frac{x^2}{1+x^2} \left[1 + 8\alpha \left[2\alpha \left\{ \alpha + \frac{1}{1+x^2} + \left(\alpha^2 + \frac{1+2\alpha}{1+x^2} \right)^{\frac{1}{2}} \right\} \right]^{-\frac{1}{2}} \right] \qquad (2.14)$$

with $x = \omega\tau$.

Now $$Z_s = R_s + \frac{1}{1+j\omega C_s}$$

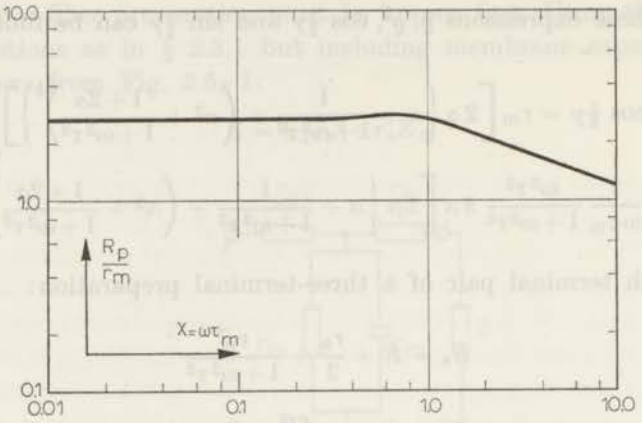

Fig. 2.5.–3.

Ratio between R_p and r_m as a function of $\omega\tau_m$.

can be transformed into

$$Y_p = \frac{1}{R_p} + j\omega C_p$$

where

$$\frac{R_p}{R_s} = 1 + \frac{1}{1+\omega^2 R_s^2 C_s^2}$$

and

$$\frac{C_p}{C_s} = \frac{1}{1+\omega^2 R_s^2 C_s^2}.$$

For $\alpha = \frac{1}{4}$ that is, for $r_m = r_a$, C_p/C_m and R_p/r_m have been plotted against $\omega\tau_m$ in Figs. 2.5.–2 and 2.5.–3 respectively.

2.6. Complications at high frequency

2.6.1. *Amplifier noise*

At frequencies above 500–1000 rad·sec^{-1} amplifier noise is mainly determined by shot effect in the cathode emission of the input stage vacuum tubes. Shot effect results in white noise of a rms intensity per cycle of bandwidth:

$$\overline{e_n^2} = 4kT\frac{\varepsilon}{g_m} \equiv 4kTR_n$$

where g_m is the transconductance of the tube, R_n is the equivalent

noise resistance and ε approximately 2.5 (VAN DER ZIEL, 1954).

From section 2.4 it follows that

$$\overline{e_0^2} \sim \overline{e^2} + \gamma^2 \overline{e_s^2} + \{(1+\gamma^2)+\omega^2\tau^2\}\,\overline{e_n^2}$$

as long as

$$\omega < \omega_{max} \equiv \frac{0.75}{\sqrt{\tau \frac{T}{\mu_0}}}.$$

This means that in the output voltage of the capacitance neutralized preamplifier shot noise shows up multiplied with a factor containing a term $\omega^2\tau^2$ which may vary in practice between 10 and 100 for $\omega \sim \omega_{max}$. It is further evident from (2.10) that, when feedback isolation is used the correlation method does not eliminate noise contribution from seals and preamplifiers. These must therefore be kept low compared to the noise of the object.

2.6.2. *Consequences of phase shifts*

A difference in phase shift between the two amplifier channels is, for any particular frequency, equivalent to a time shift. The averaged product of the two channel output voltages is then:

$$\overline{e(t)\,e(t+\tau)} \text{ instead of } \overline{e^2(t)}.$$

Restricting the analysis to a narrow-band representation of the output voltages $e_1(t)$ and $e_2(t)$:

$$e_1(t) = x_1(t)\cos\omega_0 t - y_1(t)\sin\omega_0 t$$

$$e_2(t) = x_2(t)\cos(\omega_0 t+\varphi) - y_2(t)\sin(\omega_0 t+\varphi)$$

where the variables x_1, x_2, y_1 and y_2 are slowly varying compared to $\cos\omega_0 t$ we can first integrate the product over one sine wave period $2\pi/\omega_0$:

$$\frac{\omega_0}{2\pi}\int_0^{2\pi/\omega_0} e_1(t)\,e_2(t)\,dt = (x_1x_2+y_1y_2)\,\tfrac{1}{2}\cos\varphi + (x_2y_1-x_1y_2)\,\tfrac{1}{2}\sin\varphi.$$

Averaging over a period much longer than $2\pi/\omega$ results in

$$\begin{aligned}\overline{e_1(t)\,e_2(t)} &= (\overline{x_1 x_2}+\overline{y_1 y_2})\,\tfrac{1}{2}\cos\varphi \\ &= (\overline{x^2}+\overline{y^2})\,\tfrac{1}{2}\cos\varphi \\ &= \overline{e^2}\cos\varphi\end{aligned}$$

because x and y are not correlated, and $\overline{x^2}=\overline{y^2}=\overline{e^2}$.

In general phase differences in the main amplifiers and band pass filters can be kept quite small.

A far more dangerous point are the capacitance-neutralized preamplifiers.

From

$$e_0 = \frac{e}{1+j\omega aT-\omega^2(\frac{1}{2}T')^2}$$

follows

$$e_0 = e\,\frac{(1-x^2)-2jax}{(1-x^2)^2+4a^2x^2}$$

with

$$x = \omega\,\frac{T'}{2}$$

so that

$$tg\,\varphi = \frac{2a}{x-\dfrac{1}{x}}.$$

It is evident that a and T' should be equal in both channels within the range of nearly flat frequency response mentioned. But from the expression given for a and T' it can be concluded that they depend on stray capacities, seal resistance, preparation resistance and so forth. One can check the magnitude of phase shifts by connecting the two preamplifiers through their coupling condensers C_k (which must be of equal capacitance) to the same audio generator. Relative phase shifts can then be measured over the frequency range of interest by one of several methods. It has been found that relative phase shift was below ten degrees up to 10 kc/s, which corresponds to an error of 1.5 %.

2.6.3. *Crosstalk*

Another source of error in the high frequency end of the measuring range is crosstalk through stray capacitance between the outer pools

and their electrodes, giving rise to a spurious correlated noise in the measuring channels. Its magnitude can be estimated by simulating the experiment without nerve fiber, injecting a.c. into one input circuit and comparing the a.c. output voltages of both systems. By adequate spacing of preamplifiers and electrodes, and designing the nerve chamber for low stray capacitance between the outer pools capacitive crosstalk could be reduced to 10 % at 10 kc/s.

A further reduction can be realised by means of cross-neutralizing techniques as in coaxial microelectrode work and by shielding. Shielding however tends to increase the input time constants.

2.7. Implementation

2.7.1. *Preparation, nerve chamber, seals*

The nerve chamber, which was designed for low stray capacities, was fashioned from a block of lucite (Perspex) [1]).

A construction drawing is shown in Fig. 2.7.1.–1. The five pools connect through radial channels to three parallel channels 0.5 mm wide and 1.0 mm deep, which are separated by 0.5 mm wide ridges [2]). A thin layer of silicone jelly was applied to the surface of the perspex block leaving free the inside walls of pools and channels. Before mounting the nerve fiber [3]), Ringer's solution was supplied to all pools and channels until finally a shallow bubble of liquid covered the block and interconnected all compartments.

Then, the freshly prepared nerve fiber was transferred quickly to the fluid and gently arranged into the correct position. Dots of

---

[1]) Perspex chambers have been used by several authors. The brand used in the present investigation, however, proved to contain a toxic compound causing a gradual reduction of action potential amplitude and an increase in noise level. These undesirable effects could be completely eliminated by several days' washing in water and at least two days' washing in ether. The multitude of surface cracks caused by this procedure disappears under hot air surface treatment. Several other materials have since been tested, the polycarbonate Makrolon (Bayer AG) was found to be excellent.

[2]) In the course of the investigation it was found desirable to decrease channel width and spacing to 0.2 mm, because the internodal length was often less than 1.75 mm. A chamber of this kind is now in use.

[3]) All preparations were dissected and mounted by Verveen, who also designed the improved nerve chamber referred to before. A description, by Verveen, of this chamber and of the preparation techniques developed in the course of this investigation will be published in these Acta.

silicone jelly were put on the ridges between the small channels, after which the excess fluid was drained off by suction. The seals although applied in a saline medium have resistances seldom below 100 to 50 MΩ because of the water-repellent properties of the

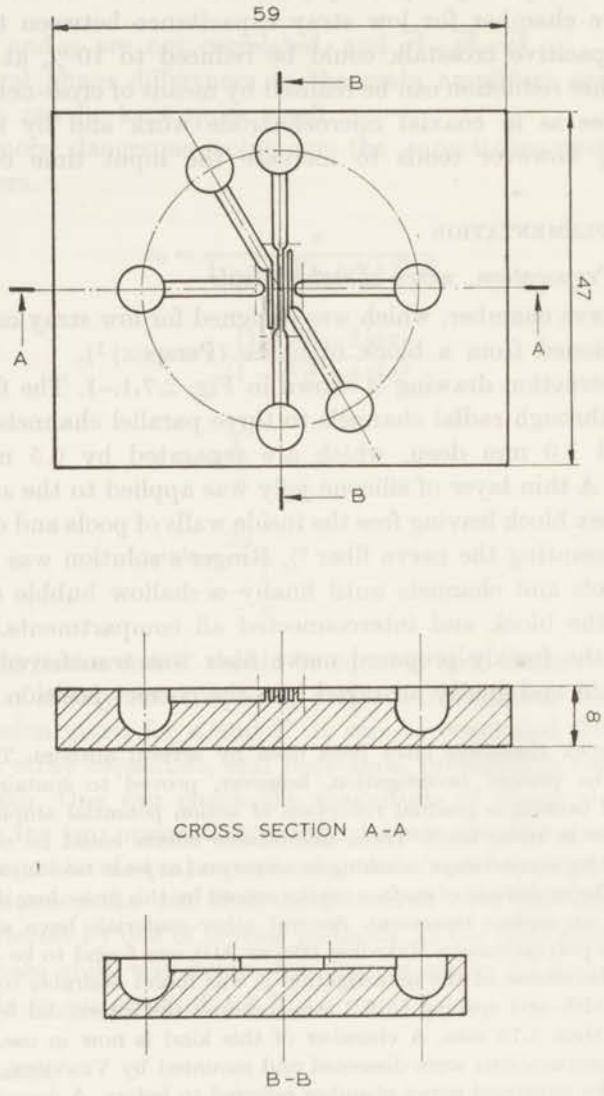

Fig. 2.7.1.–1.
Construction drawing of nerve chamber.

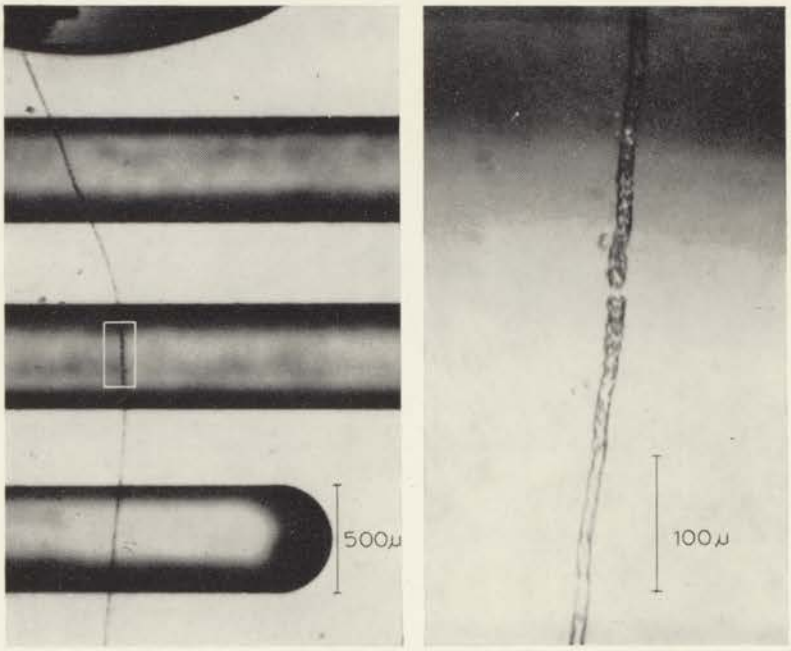

(a) (b)

Fig. 2.7.1.–2.

(a) Top view of chamber showing nerve fiber in place. (b) Enlarged view showing Ranvier node in central pool.

silicone compound. Fig. 2.7.1.–2 shows the nerve fiber in place. The nerve chamber, the two input stages of the preamplifiers and their associated circuitry were all contained in an aluminium shielding box, which fitted between lighting stage and objective of a dissecting microscope (Zeiss stereomicroscope no 1).

No provision for temperature control has been made. The experiments were done in a range of temperatures of 20 to 25 degrees centigrade. Changes in the composition of the solution around the middle node were made by removal by suction while at the same time refilling with the new bathing fluid (HUXLEY and STÄMPFLI, 1951a). This procedure took a few minutes.

2.7.2. *Electrodes*

Ideally, reversible electrodes, like silver-silver chloride or calomel, should be used. With feedback isolation however the requirements on relative offset between an electrode pair are severe. Although it has been reported (IVES and JANTZ, 1961) that offsets below 100 μV can be attained for sets of simultaneously prepared Ag–AgCl electrodes, it is rather difficult and moreover time consuming to attain that performance regularly. Therefore Ag–AgCl electrodes have been used only as auxiliary current carrying electrodes serving to depolarize or hyperpolarize the nodal membrane. Voltage fluctuations were led off through platinum-black coated platinum electrodes, prepared according to a classical prescription by KOHLRAUSCH (SCHWAN, 1963). Electrodes of this type are excellent for a.c. measurements. In a conducting solution they behave as a resistance in series with a capacitance, both of which are frequency-dependent. From SCHWAN's data it can be calculated that a platinum-platinum-black electrode of 10 mm^2 at an angular frequency of 1 rad$\cdot$sec^{-1} is characterized by 2.7 kΩ and 15 μF. This series impedance has a negligible influence when an electrometer preamplifier is used. The noise introduced by the electrode follows NYQUIST's formula down to low frequencies as has been shown by GESTELAND *et al.* (1959). It is therefore of no consequence.

It was necessary to use blocking capacitors in series with the electrodes because the electrodes produced a slowly varying, temperature dependent d.c. voltage of unknown origin. Although this arrangement was satisfactory, one source of information on the state of the nerve fiber, its resting potential, was lost.

2.7.3. *Amplifier design and construction*

2.7.3.1. Preamplifier requirements

The crucial parts of the apparatus used in this investigation are the two preamplifiers. Many of the requirements these have to satisfy are the same as for the wide-band electrometer amplifiers used in intracellular microelectrode work (MOORE and GEBHART; SCHOENFELD; GULD, all 1962). Further requirements have been formulated in the foregoing, most of them concern a low noise figure.

Summarizing:

A.1. Input current should not exceed 10^{-12} A; (§ 2.2.3.).

A.2. Input capacitance must be as low as possible in order to minimize C_T and, consequently, the term $\omega\tau$ in formula (2.11).
Input capacitance neutralization is an essential feature (§ 2.4).

A.3. Input resistance should preferably exceed $10^{10}\,\Omega$; if not, its magnitude must be accurately known.

B.1. The open-loop gain must exceed 5000. By means of feedback, net gain is stabilized to a factor ten, leaving a gain of 500 operative in feedback isolation. The gain vs. frequency curve is characterized by a dominant lag with a time constant T of approximately 10 μsec. Measurement of the overall input capacitance C_T, including stray capacitance of saline-filled pools and electrodes, gave a value of about 30 pF. According to formula (2.12) this would result, with a source resistance of 100 MΩ in $\omega_{max} = 97000$ rad·sec^{-1}, that is 15.4 kc/s.
Simulating the nerve fiber by a resistor of 100 MΩ $\pm$ 1 %, it was found that a flat frequency response was obtained from zero to 13 kc/s which is in satisfactory agreement with the value calculated.
Essentially the amplifier is a wide-band d.c. differential amplifier.

C.1. Amplifier noise must be kept as low as possible. In the audio frequency range, where white noise prevails, shot

effect noise must be low, necessitating a relatively high transconductance input tube. This conflicts with requirements 1.1 and 1.2 (§ 2.3.3).

C.2. Mains hum interference must be kept as low as possible. This includes power supply ripple, electrostatic and magnetic pickup.

C.3. Base-line drift, offset and flicker noise should be suppressed by stabilizing the amplifier by an auxiliary chopper-amplifier (§ 2.3.3).

C.4. Microphony must be minimal.

D.1. Any tendency to oscillation when a nerve fiber preparation is connected to the input terminals must be absent with a large margin of safety (formula 2.5).

2.7.3.2. Choice of active element at the preamplifier input

Most of the problems posed by this specification concern the amplifier input tube or active element. From many points of view, the insulated-gate field effect transistor seems to be highly promising. It can be expected that this device will replace the electrometer tube in the near future but at the time of writing it was not developed far enough to be an adequate substitute for the vacuum tube in this critical application.

The types tested so far (RCA developmental type TA 2330 and Siliconix 2N3113) had far too much noise in the sub-audio frequency region. A recently developed electrometer tube (Raytheon CK 587) of very low microphony, had too much shot effect noise in the a.f. region as a consequence of its low transconductance (70 micromho). Finally a suggestion given by GULD (1962) to adapt professional-quality vacuum tubes for this purpose, was followed. The high-mu subminiature "muvistor" tube RCA (Philips, Siemens) 7895 of coaxial construction was chosen.

About half of the twenty-four tubes tested had grid currents in the order of 10^{-11} A at the following settings:

$$V_a = 60\ \text{V} \qquad V_g = -1\ \text{V} \qquad V_f = 5\ \text{V}$$
$$I_a = 0.3\ \text{mA} \qquad g_m \sim 0.7\ \text{mA/V}.$$

The amount of grid current mentioned can be compensated to

within 10^{-12} A by connecting the grid through a $10^{10}\,\Omega$ leak resistance to a voltage source and voltage divider. The equivalent noise resistance of the amplifier was in the order of 20 kΩ above 1 kc/s. In the meantime tube types of the same construction have become available (RCA 8441 and developmental type RCA A 15299A) which are probably much better suited for this job. In general, the microphony of the coaxial tubes is exceptionally low, while flicker noise compares favorably with that in conventional miniature tubes such as the 12AX7 (CARINGELLA and EISENMAN, 1962).

The input stage of the preamplifier is a long-tail pair of two cascode arrangements (VALLEY and WALLMAN, 1948; KLEIN, 1955), followed by a balanced amplifier stage of two penthode tubes and, a cathode-follower output stage. The conventional precautions in low-level amplifier construction, such as the use of wire-wound resistors at critical places, of gold-plated contacts, and of high-grade ceramics or teflon as insulation materials, were observed. Anodes and filaments were energized from carefully regulated d.c. power supplies. These, in turn, were fed from 220 V stabilized a.c.

To ensure an adequate base-line stability, an output voltage offset not exceeding 100 μV is necessary and chopper stabilization, to suppress drift and flicker noise in the very low frequency range, was introduced. Although chopper stabilization of operational amplifiers with shunt feedback is quite common, application of this principle to follower circuits using series feedback is rather difficult. A suggestion (PHILBRICK, 1958) and a complete design for electrophysiological work (MOORE and GEBHART, 1962) have been published, but in both cases the signal amplitudes envisaged were at least in the millivolts range. The low-noise preamplifiers needed in this investigation pose some extra problems, because the additional circuitry required for connexion of the chopper amplifier input to the input terminals of the main amplifier must not deteriorate the main amplifier's noise figure or its frequency response.

2.7.3.3. Amplifier construction

The main features of the preamplifier are shown in Fig. 2.7.3.3.–1. The input voltage of the main amplifier is connected through a simple low-pass filter to a 50 c/s electromechanical chopper, the resulting a.c. voltage is amplified five hundred times, demodulated and supplied to the main amplifier through tube T.

The improvement in zero-point stability obtained by stabilization is demonstrated in Fig. 2.7.3.3.–2, where the output voltage of the main amplifier was recorded with the stabilizing amplifier disabled and functioning, respectively.

Drift, offset and especially very-low frequency fluctuations are reduced considerably (see also LANDSBERG, 1956).

It follows from formula (2.10) that this feature is essential to obtain reliable results on membrane voltage fluctuations in the sub-audio frequency range. Using active filters, which have a fairly high inherent noise level, an input signal of sufficient magnitude must be supplied. Further amplification was done by means of chopper-stabilized feedback amplifiers (Solartron AA900) with gain variable in 10 steps from 20 to 2000. Throughout, crest factors of five or more were observed. It has been shown (COHN, 1964) that for random noise, characterized by a Gaussian amplitude distribution, and using a square law detector, a crest factor of five

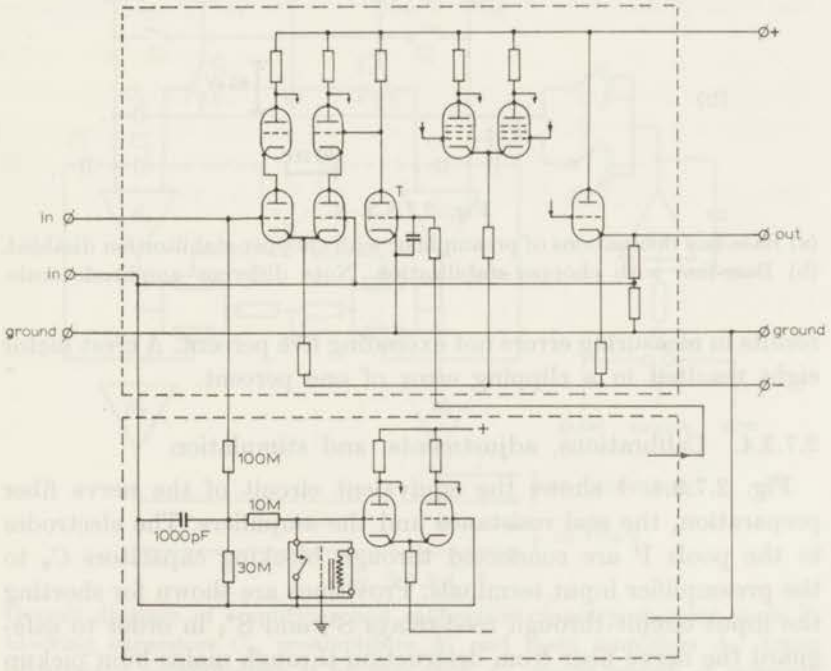

Fig. 2.7.3.3.–1.
Skeleton circuit diagram of chopper-stabilized electrometer preamplifier.

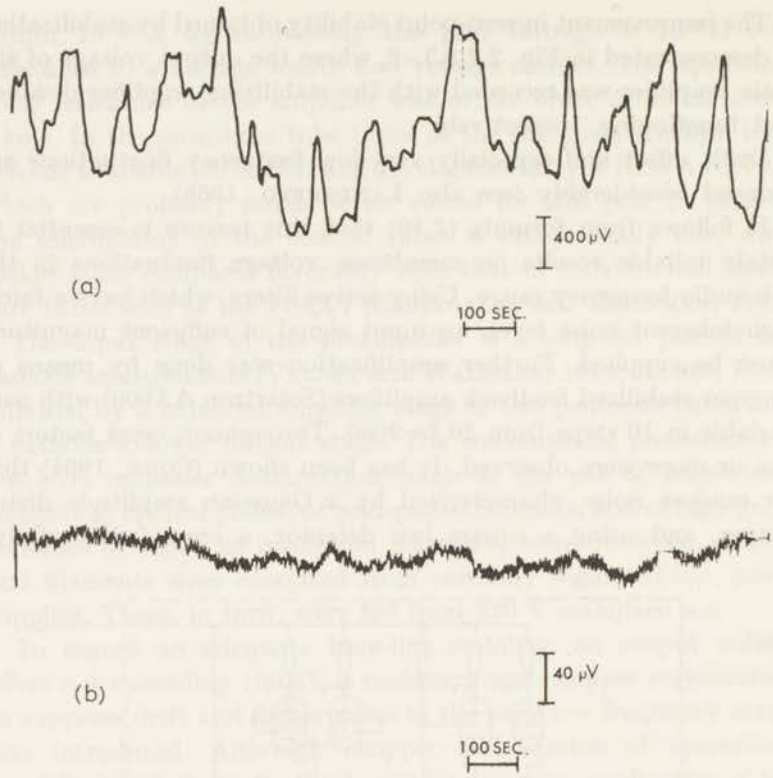

Fig. 2.7.3.3.–2.

(a) Base-line fluctuations of preamplifier with chopper-stabilization disabled.
(b) Base-line with chopper-stabilization. Note different amplitude scale.

results in measuring errors not exceeding five percent. A crest factor eight resulted in a clipping error of one percent.

2.7.3.4. Calibrations, adjustments, and stimulation

Fig. 2.7.3.4.–1 shows the equivalent circuit of the nerve fiber preparation, the seal resistance and the amplifiers. The electrodes in the pools P are connected through blocking capacitors C_s to the preamplifier input terminals. Provisions are shown for shorting the input circuit through reed-relays S'_1 and S''_1 in order to safeguard the nerve fiber from destruction through mains-hum pickup when the shielding box cover must be removed. By means of switches S_3 and S_4 and integrator A_3 a sinusoidal signal, a periodic

square wave or rectangular pulses of variable amplitude and duration can be injected into either input circuit or into both simultaneously.

By means of miniature three-way toggle switches the auxiliary pools P'_a and P''_a can be grounded, left floating, or incorporated in the feedback system. This allows a determination of the seal resistances R'_{s1} and R''_{s1}. The procedure is as follows. First, the input circuits are both grounded through ,100 MΩ seals the preparation not yet in place. A sine wave (generally 1 volt, 260 c/s)

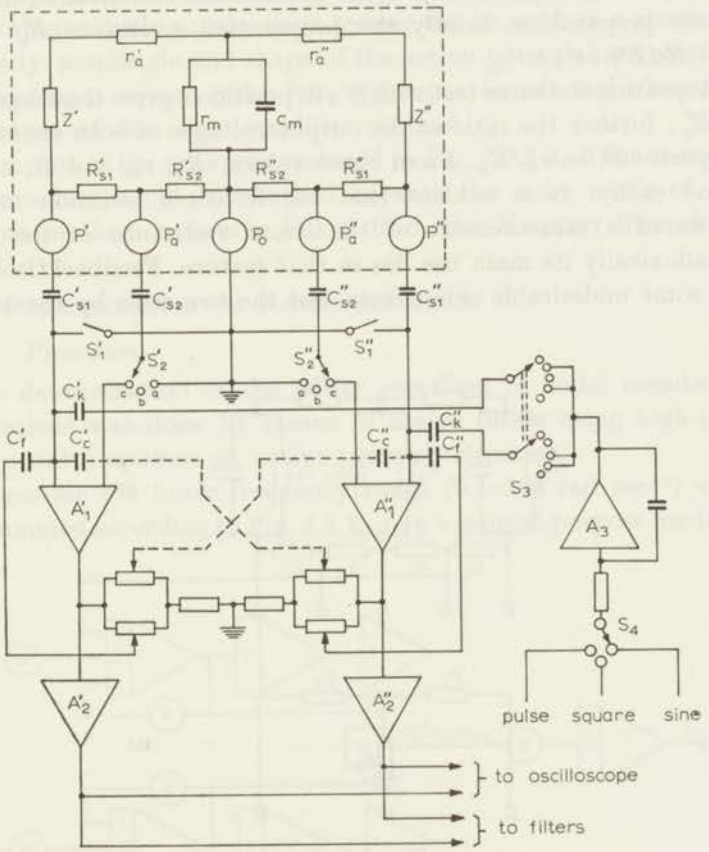

Fig. 2.7.3.4.–1.

Overall diagram of amplifying and calibration circuitry showing pools P, blocking capacitors C_s, preamplifiers A_1 and main amplifiers A_2. Input capacitance neutralization is by capacitors C_t, neutralization of crosstalk by capacitors C_c, injection of test current waveforms by C_k. The magnitudes of C_k, C_c and C_t are 0,5 pF.

is supplied to integrator A_3 and the output voltages of the two amplifiers are noted. The measuring frequency must be low enough to be free of capacitive shunting. When the situation is as in Fig. 2.7.3.4.–1, with switch S'_2 in position c, S''_2 in position a, and using a sine wave of the same frequency and amplitude one can compare the output voltage of channel I now obtained with that measured for a 100 MΩ resistance. From these values the resistance between input and earth can be found. It is composed of the seal resistance R_{s1} in parallel with one mesh in the electrical equivalent of the preparation, briefly the preparation resistance R'_p where $R'_p = Re(Z') + r'_a + r'_m$.

Repeating the same test with S''_2 in position c gives the magnitude of R''_p; further the ratio of the output voltages of both channels is proportional to r_m/R_p. From these values, R_p, r_m and R_s can be found easily. It is evident that the feedback isolation method allows of a measurement of the shunt resistance of the seals. Paradoxically its main use lies in that feature. Feedback isolation has some undesirable side effects, but the two seals by themselves

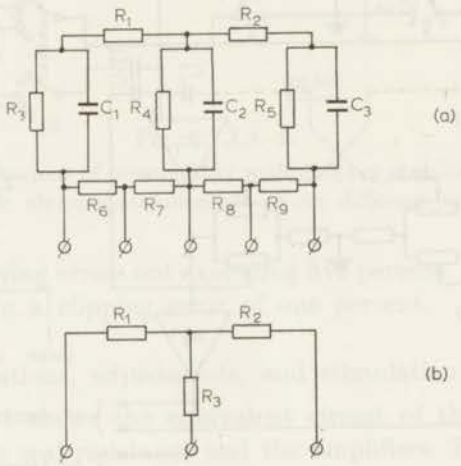

Fig. 2.7.3.4.–2.

Dummy circuits used for checking preamplifier stability and for verifying calibration

(a) $R_1 - R_5$: 40 MΩ
$R_6 - R_9$: 20, 60 or 100 MΩ
$C_1 - C_3$: 1 pF

(b) R_1, R_2 : 60 MΩ
R_3 : 0, 10, 40, 100 MΩ

represent a shunt resistance of more than 100 MΩ, which is as good as the air gap method, but is moreover constant and of known value.

In a fraction of the experiments to be described in the next chapter feedback was switched off during noise spectrum measurements, and correction for shunt resistance was made afterwards using the measured seal resistance values.

Frequency response is corrected by injecting a.c. and adjusting the voltage dividers at the preamplifier outputs until a constant output amplitude is obtained over the widest possible frequency band. Alternatively square-wave testing can be used as a shortout.

Finally, amplitude and shape of the action potential are checked by injecting a square pulse into one input circuit and observing the output of the other amplifier channel.

By means of the networks pictured in Fig. 2.7.3.4.–2 the measuring procedure could be checked because the noise emf's of the resistors in these networks follow from the NYQUIST formula.

2.8. DETERMINATION OF POWER SPECTRUM

2.8.1. *Procedure*

The determination of the power spectrum of nodal membrane fluctuations was done by means of active filters using high-gain operational amplifiers as active network elements.

Filters for the lower frequency range (0.1–100 rad·sec^{-1}) were programmed according to Fig. 2.8.1.–1 on a general-purpose medium

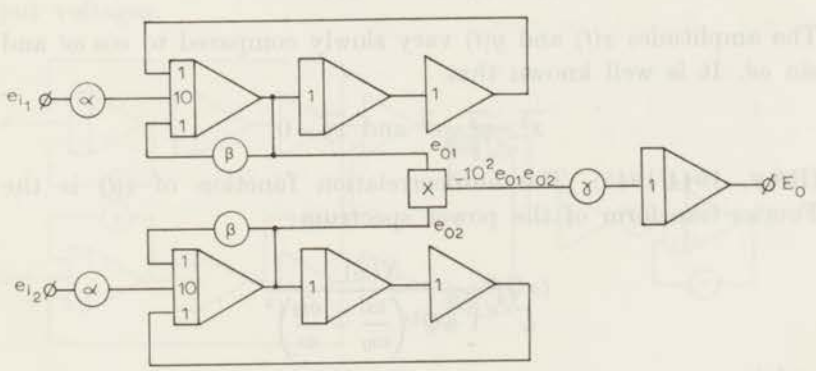

Fig. 2.8.1.–1.

Analog computer program showing band-pass filters, multiplier and integrator.

accuracy analog computer (Beckman-Berkeley EASE series 1000). (LOWENBERG and MCCULLOUGH, 1962; SUTCLIFFE, 1965.)

Three frequencies could be measured simultaneously.

An elementary analysis gives for the filter transfer function:

$$F(j\omega) = \frac{e_0}{e_1} = -\frac{\alpha}{\beta + j\left(\omega C - \frac{1}{\omega C}\right)}$$

where C is the integrator capacitance in μF of the two integrators and summing resistors at $\times 1$ inputs are 1 MΩ.
With $Q = 1/\beta$ and $\omega_0 = 1/C$ the above expression reads

$$F(j\omega) = -\alpha Q \frac{1}{1 + jQ\left(\frac{\omega}{\omega_0} - \frac{\omega_0}{\omega}\right)}. \tag{2.16}$$

Exactly the same expression is found for the impedance of a resonant circuit of passive elements L, C and R in parallel.

There $Q = R\sqrt{(C/L)}$. At frequencies below 100 c/s the use of inductors is impractical and active filters using only resistors and capacitors are fully equivalent and far more practical.

When e_i is a randomly fluctuating voltage (with a power spectrum $N(\omega)$ which varies only slowly within the filter passband) the output voltage is a narrow band noise voltage which can be represented by

$$e_0(t) = x(t) \cos \omega t - y(t) \sin \omega t.$$

The amplitudes $x(t)$ and $y(t)$ vary slowly compared to $\cos \omega t$ and $\sin \omega t$. It is well known that

$$\overline{x^2} = \overline{y^2} = \overline{e^2} \text{ and } \overline{xy} = 0$$

(RICE, 1944/1945). The autocorrelation function of $e(t)$ is the Fourier-transform of the power spectrum:

$$(\alpha Q)^2 \frac{N(\omega)}{1 + Q^2\left(\frac{\omega}{\omega_0} - \frac{\omega_0}{\omega}\right)^2}$$

and is

$$R(\tau) = \alpha^2 N f_0 \frac{\pi}{2} \exp(-\tau \cos \delta) \sin(\delta - \tau \sin \delta) \operatorname{cosec}(2\delta)$$

where

$$\cos(2\delta) = \frac{1-2Q^2}{Q^2} \quad \text{(Oberhettinger, 1957).}$$

For $\tau = 0$, $R(t)$ is the mean square of the filter output voltage:

$$R(0) = \overline{e_0{}^2(t)} = \alpha^2 N \frac{\omega_0 Q}{4}. \tag{2.17}$$

The circuit of Fig. 2.8.1.–1 performs the computation:

$$E_0 = \frac{1}{RC}\,\alpha^2\gamma \int_0^T e_{01}(t)\,e_{02}(t)\,\mathrm{d}t$$

where R, C, E_0 are output voltage, integrator capacitance and input resistance of the final integrator respectively.

$RC = 1$ sec, further e_{01} and e_{02} are the output voltages of the two filters.

Now

$$\begin{aligned} E_0 &= \alpha^2\gamma \int_0^T \{e_1(t) + e(t)\}\,\{e_2(t) + e(t)\}\,\mathrm{d}t \\ &= \alpha^2\gamma \int_0^T e^2(t)\,\mathrm{d}t + \varepsilon_1 \\ &= \alpha^2\gamma\,\overline{e^2(t)} + \varepsilon_1 + \varepsilon_2. \end{aligned}$$

Here $e(t)$ is the correlated part of e_{01} and e_{02}, $N(\omega)$ is the power spectral density of the corresponding correlated part of the filter input voltages.

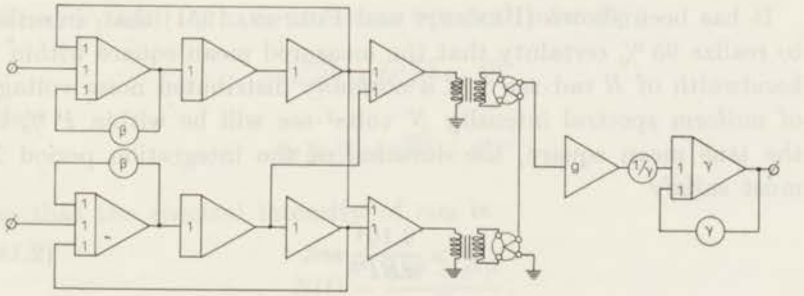

Fig. 2.8.1.–2.

Filters for frequencies from 100 rad·sec^{-1} upward showing quarter-square multipliez and low-pass filter. The integrator capacitors in the band-pass filter integrators are stepwise variable and of equal value.

For $T \to \infty$, ε_1 and ε_2 tend to zero.

Measurements at frequencies from 100 rad·sec^{-1} to 60000 rad·sec^{-1} have been made, using the circuit of Fig. 2.8.1.–2.

The same type of active filters was used with simple operational amplifiers as active elements. The integrator capacitors of the filter integrators could be switched to different values, giving a range of tuning frequencies. No multipliers were used. Sum and difference of the filter output voltages e_{01} and e_{02} were taken and supplied to matched, indirectly heated thermocouples.

As the output d.c. voltage of these devices is proportional to the square of the a.c. input voltage within a range extending from zero to a given upper limit, the difference between the output voltages is proportional to

$$(e_{01}+e_{02})^2-(e_{01}-e_{02})^2=4e_{01}e_{02}.$$

This scheme closely resembles the quarter-square multiplier used in analog computers. After amplification and low pass filtering we obtain an output voltage proportional to $e_{01}e_{02}$ when the time constant of the low pass filter is high enough. The thermocouples used (Philips TH91) attain their maximum output voltage at a heating current of 10 mA in about 10 sec. The active low-pass circuit can be switched to time constants of 1, 10, and 100 seconds.

2.8.2. *Required integration periods*

It has been shown (Bennett and Fulton, 1951) that, in order to realize 95 % certainty that the measured mean square within a bandwidth of B rad·sec^{-1} of a normally distributed noise voltage of uniform spectral intensity N volts^2·sec will be within P % of the true mean square, the duration of the integration period T must satisfy

$$T > \frac{8.10^4}{\pi B P^2} \text{ sec.} \tag{2.18}$$

This theorem sets the fundamental limit to the accuracy of noise measurements on living nerve elements at the lowest frequencies. A nerve fiber in very good condition does not remain constant

longer than three hours at most, taking the amplitude of the action potential, nodal resistance and the resting potential as criteria.

A ten percent accuracy at $\omega = 1$ rad·sec^{-1} and $Q = 10$ gives:

$$B = \frac{\omega_0}{4Q} = 0.025 \text{ rad} \cdot \text{sec}^{-1},$$

$$T = 10^4 \text{ sec}.$$

When a noise voltage is measured, at a certain frequency, by means of a correlation method it can be expected that the required integration time at equal bandwidth and desired accuracy will be longer in proportion to some function of the ratio between total noise and correlated component. According to a theorem given by VAN DER ZIEL (1954) the following relation holds for the time integral of a random variable $v(t)$ over an integration period T and the spectral intensity $N(f)$ of v:

$$\overline{X^2_T} = \frac{N}{2T} \qquad X_T = \frac{1}{T}\int_0^T v(t)\,dt.$$

Now consider two partly correlated noise voltages

$$e_1(t) = e'_1(t) + e(t)$$

$$e_2(t) = e'_2(t) + e(t)$$

for which

$$\overline{e_1(t)\,e_2(t)} = \overline{e^2(t)}.$$

When e'_1 and e'_2 have the same spectral intensity:

$$\overline{(e'_1)^2} = \overline{(e'_2)^2} = \overline{E^2}$$

then

$$(e_1 e_2)^2 = (\overline{E^2} + e^2)^2$$

so that the spectral intensity of $e_1 e_2$ is

$$N(f) = \frac{(\overline{E^2} + \overline{e^2})^2}{B}.$$

Therefore

$$\overline{X^2_T} = \frac{(\overline{E^2} + \overline{e^2})^2}{2BT}$$

when

$$X_T = \frac{1}{T} \int_0^T e_1(t)\, e_2(t)\, \mathrm{d}t.$$

The requirement

$$\overline{X^2}_T \ll (\overline{e^2})^2$$

results in

$$T \gg \frac{1}{2B}\left(1 + \frac{\overline{E^2}}{\overline{e^2}}\right)^2.$$

Combining this with Bennett's and Fulton's rule:

$$T \gg \frac{8.10^4}{\pi B P^2}\left(1 + \frac{\overline{E^2}}{\overline{e^2}}\right)^2.$$

2.8.3. *Comment*

The method of noise power spectrum determination just described was largely dictated by the means available and is not recommended as the ideal solution. First, the choice of three frequencies down from 100 rad·sec^{-1} which could be measured simultaneously on the analog computer, has been found too restrictive. In a number of cases the need was felt to measure five or six points below 100 rad·sec^{-1} or to evaluate the mean square noise intensity at integration periods differing in length or initial time. Measuring the higher frequency range successively proved to take too much time. At 100 rad·sec^{-1} for example, at least 500 seconds were necessary to arrive at an accuracy in the order of a few percent. Relatively fast changes in the power spectrum as occurring either spontaneously or after changing the solution bathing the node of Ranvier could not be followed. The conclusion is, that simultaneous measurements of rms noise voltage over as large a range of frequencies as is possible, is highly desirable. This means that as many computer circuits like that of Fig. 2.8.1.–1 must be constructed as one wants to have spot noise measurements. The low-pass filter circuits should have time constants inversely proportional to the filter tuning frequencies.

Their output voltages can then in a number of cases, together with the whole sub-audio frequency noise band, be recorded on FM tape for further analysis.

2.9. Determination of amplitude distribution

Measurements of power spectra give no information on the phase relationships between the frequency components of the analyzed waveform. That means that clues concerning temporal patterns must be found in a different way as, for example, by visual or auditory observation of the amplified noise voltage. Further, an analysis of a few well-chosen examples shows that determinations of amplitude distributions may discriminate between waveforms having identical power spectra.

In part of the experiments, amplitude distributions (cf. Fig. 2.9.–1) were determined from 1.5 μsec wide samples taken from the wide-band noise output of amplifier A'_2 or A''_2 in Fig. 2.7.3.4.–1. The sampling rate was approximately 1000 pps; the duration of the sampling period was at least one minute.

The channel width of the 128 channel pulse height analyzer was made equivalent to 100 μV at the preamplifier input terminal. At the low-frequency end, the noise band was limited by a high-pass element with a time constant of 10 sec. High frequency cutoff was governed by the preamplifier transfer function according to eq. (2.12). Numbers of counts per channel were expressed as percentage R, of the maximum; then the transformation

$$y = \pm c \sqrt{\log \frac{100}{R}}$$

was performed on these percentages (Onno, 1961). In the case of a Gaussian amplitude distribution y is linearly dependent on channel number.

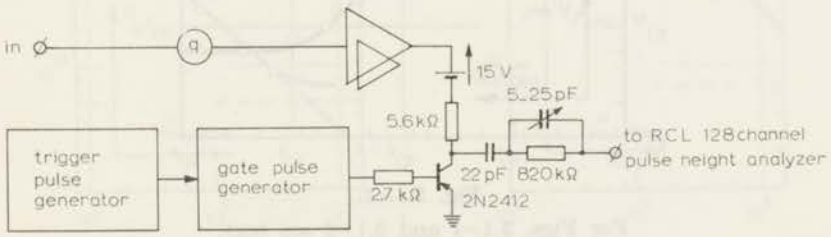

Fig. 2.9.–1.

Arrangement for sampling noise and determining amplitude distributions.

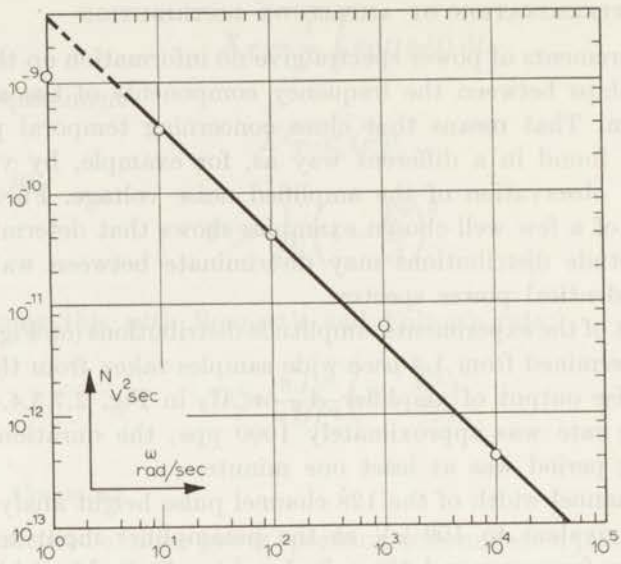

Fig. 3.1.–1.

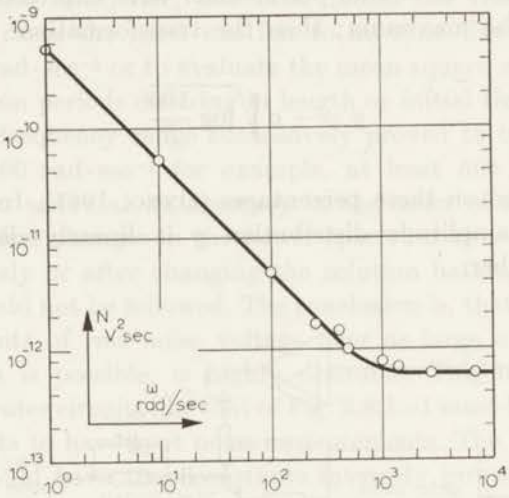

Fig. 3.1.–2.

For Figs. 3.1.–1 and 3.1.–2 see text.

3. RESULTS

3.1. Results from preliminary experiments; general aspect of power spectrum

In preliminary experiments, where either the airgap or the sucrose gap isolation method was used in a two-terminal arrangement, noise power spectra of seven preparations were measured (Verveen and Derksen, 1965).

Measurements were made at angular frequencies in the range between 1 and 10000 radians per second. In all cases a so-called $1/f$ spectrum was found such as also occurs in semiconductors carrying direct current, where it increases with increase of direct current, and in flicker noise; a log-log plot of noise power per cycle of bandwidth, N, against frequency gives a straight line with a slope of roughly minus one, as in Figs. 3.1.–1 and 3.1.–2. The quantity, ωN, which is a constant in the case of $1/f$ noise, was used as a measure for the intensity of the fluctuations.

The average value of ωN for the seven preparations was

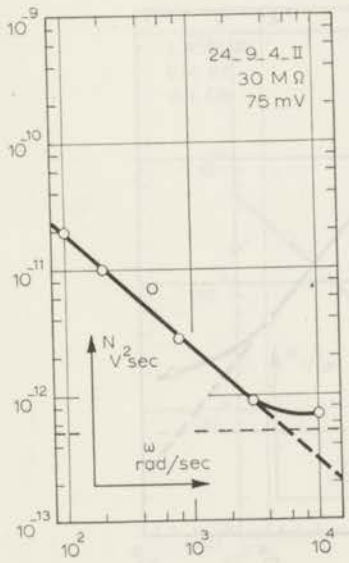

Fig. 3.2.1.–1.

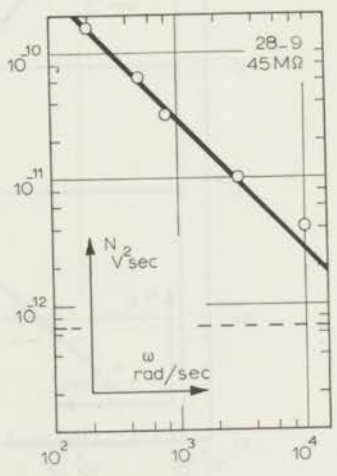

Fig. 3.2.1.–2.

For Figs. 3.2.1.–1 to 3.2.1.–10 see text.

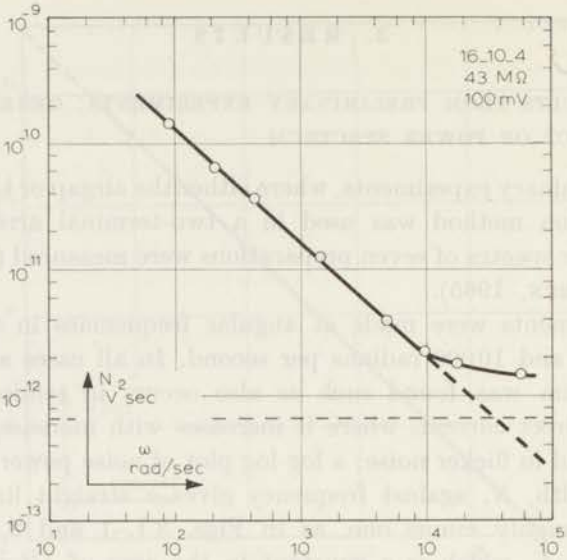

Fig. 3.2.1.–3.

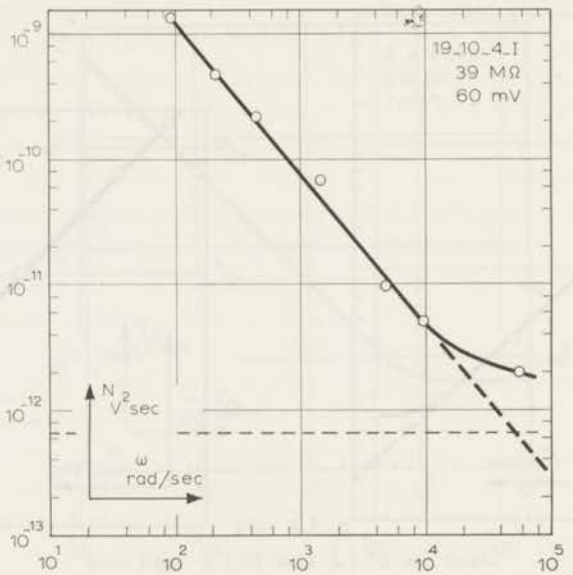

Fig. 3.2.1.–4.

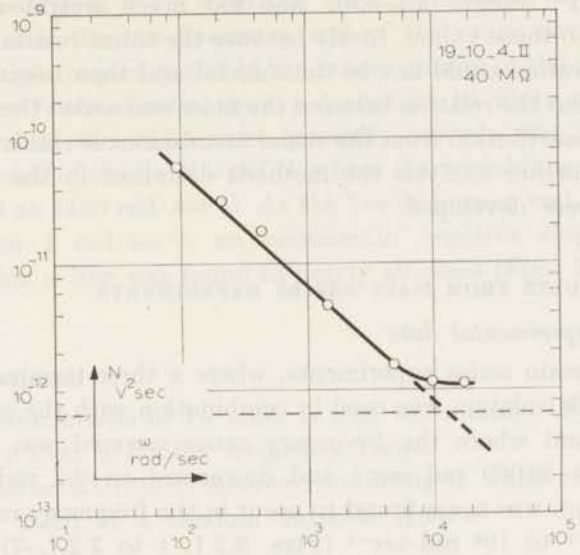

Fig. 3.2.1.–5.

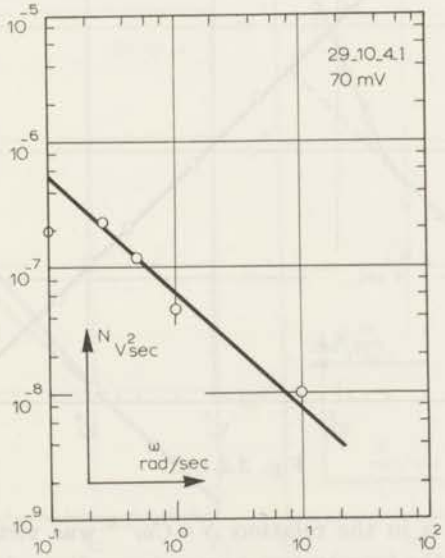

Fig. 3.2.1.–6.

$3.2 \times 10^{-9} V^2$ (range: 2.1–3.9). Not too much weight should be attached to those values, firstly because the shunt resistance across the preparation could not be determined and then because in this arrangement the relation between the noise emf across the terminals and the contribution from the nodal membranes is rather complex.

For a further analysis the methods described in the preceding chapter were developed.

3.2. Results from main series experiments

3.2.1. *Experimental data*

In the main series experiments, where a three-terminal version of feedback isolation was used in combination with the correlation method, and where the frequency range covered was extended upward to 56000 rad·sec^{-1} and downward to 0.2 rad·sec^{-1}, a $1/f$ spectrum was again found to occur in the frequency range from 1 rad·sec^{-1} to 10^4 rad·sec^{-1} (Figs. 3.2.1.–1 to 3.2.1.–7).

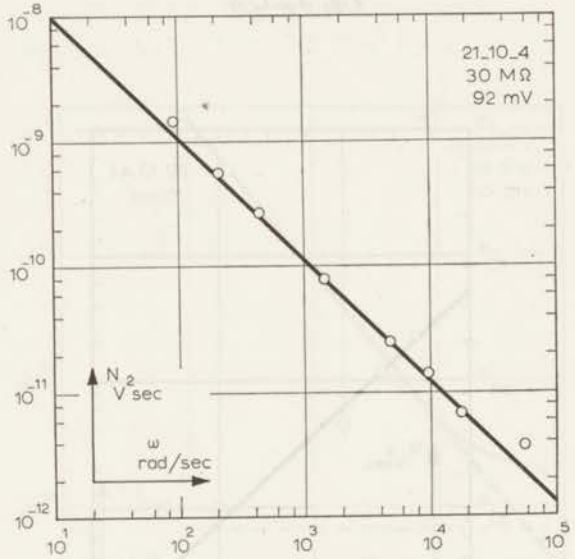

Fig. 3.2.1.–7.

The exponent α in the relation $N = C\omega^{-\alpha}$ was virtually equal to one in twelve of the twenty-two axon preparations, in the range 0.9 to 1 in seven and in the order of 0.7 in the remaining three.

Deviations from a $1/f$ spectrum were found both at the high-frequency and the low-frequency end of the range covered.

At the high-frequency end of the range, usually in the vicinity of 10^4 rad·sec^{-1}, the spectra show a transition to white noise. The power level of the white noise generally exceeds that calculated from Nyquist's formula $N = 4kTR$, where R is membrane resistance (measured at 1450 rad·sec^{-1}). At the low-frequency end, generally down from 1 rad·sec^{-1}, an increase in negative slope of the log N *vs* log ω line was found in nearly all cases (Figs. 3.2.1.–8 to 3.2.1.–10).

3.2.2. *Comment*

One characteristic of $1/f$ noise is that the relation, $N\omega = \text{const.}$, holds only over a limited frequency range.

The Wiener-Khintchin theorem, according to which the spectral intensity, $N(\omega)$ of a random variable $X(t)$:

$$N(\omega) = 4 \int_0^\infty \overline{X(t)\, X(t+\tau)} \cos \omega\tau \, d\tau \qquad (3.1)$$

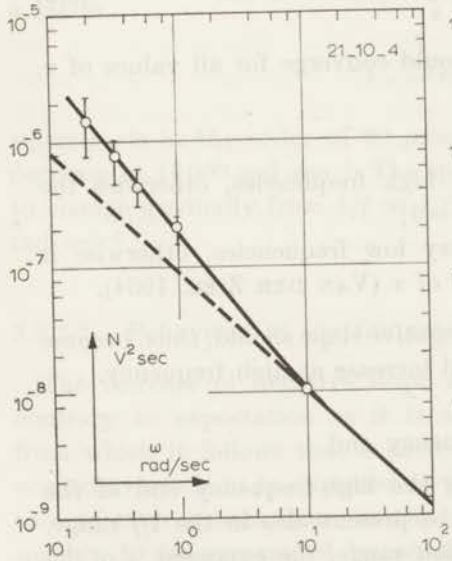

Fig. 3.2.1.–8.

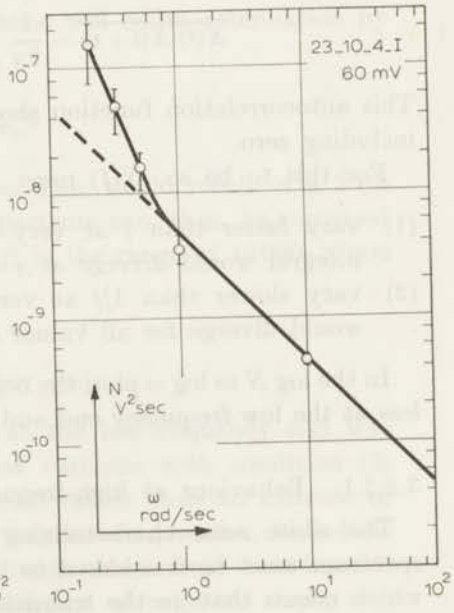

Fig. 3.2.1.–9.

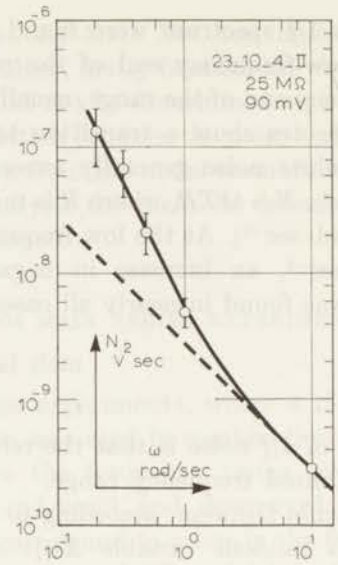

Fig. 3.2.1.–10.

may be reversed to

$$\overline{X(t)\,X(t+\tau)} = \frac{1}{2\pi}\int_0^\infty N(\omega)\cos\omega\tau\,\mathrm{d}\omega. \qquad (3.2)$$

This autocorrelation function should converge for all values of τ, including zero.

For this to be so, $N(f)$ must

(1) vary faster than f at very high frequencies, otherwise the integral would diverge at $\tau=0$;
(2) vary slower than $1/f$ at very low frequencies, otherwise it would diverge for all values of τ (VAN DER ZIEL, 1954).

In the log N *vs* log ω plot, the negative slope should, thus, become less at the low-frequency end and increase at high frequency.

3.2.2.1. Behaviour at high-frequency end

The white noise characterizing the high-frequency end of the spectrum must be considered to be present also in the $1/f$ range, which means that in the transition range, the exponent α of the contribution $N=C\omega^{-\alpha}$ is less than one.

It is not easy to judge the significance of the fact that the white noise level was found to be higher than the Nyquist level, which, for that matter, must be considered as representing the lower limit of the fluctuation intensity as has been shown, on the basis of thermodynamical arguments, by De Groot and Mazur (1962). Their reasoning is based on the generalized Nyquist theorem given by Callen and Welton (1951), which is valid for ionic systems.

Then the fact should be considered that minor maladjustments in capacitance neutralization can deflect the high-frequency part of the spectrum (either upward or downward). Also, at the high-frequency end, where membrane noise approaches its minimum, the contribution of seal noise and amplifier noise increases as does the influence of crosstalk. An increase in negative slope at the high-frequency end before the transition to white noise was never observed; the deviation from $1/f$ then occurs in a range of frequencies in excess of 10^4 rad·sec^{-1}.

The fact should, however, be taken into consideration that in the experiments the effect of membrane capacitance, which, in the present case, is the physical basis for the increase in negative slope at high-frequencies, is virtually eliminated.

The effect of membrane capacitance will be an attenuation by a factor

$$\frac{1}{1+\omega^2\tau_m{}^2}$$

where τ_m is in the order of 60 μsec. This would result in a 3 db decrease at 16000 rad·sec^{-1}. The spectrum can, thus, be supposed to change gradually from $1/f$ to $1/f^3$ in the range of 10000–20000 rad·sec^{-1}.

3.2.2.2. Behaviour at low-frequency end

The increase of negative slope at the low-frequency end was contrary to expectation as it is at variance with condition (2) from which it follows that a decrease rather than an increase of negative slope is to be expected at very low frequencies. An indication of such a behaviour, in the range down from 1 rad·sec^{-1}, quickly to be superseded by an increase of negative slope, was observed in a few cases only, Figs. 3.2.1.–6 and 3.2.2.2.–1. An

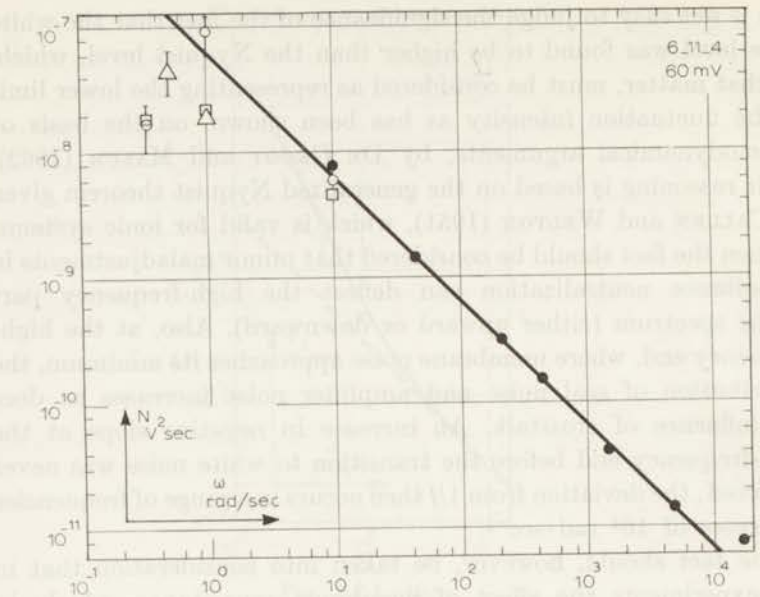

Fig. 3.2.2.2.–1.

Noise power spectrum showing decrease of negative slope down from 1 rad·sec^{-1}, as found in three runs.

insight as to the nature of the anomalous behaviour at low-frequency, which indicates the admixture of another type of noise with low-frequency preponderance, could be obtained from the time course of the integrator output voltage. Since the bandpass filters have equal relative bandwidths, $1/f$ noise results in equal rms intensity for different frequencies, and any difference in output between integrators corresponding to different tuning frequencies signifies a deviation from $1/f$ noise. In the majority of cases the integrator output voltages corresponding to the lowest frequencies – down from 1 rad·sec^{-1} – showed an erratic behaviour in that, instead of increasing steadily, but lagging behind the others, they showed transient, brief increases, with the result that their total output came to surpass that of the others. Further to investigate this phenomenon, the unfiltered amplifier output voltage was monitored during the lengthy (30–60 min) integration periods needed to achieve a reasonable degree of accuracy at frequencies of 1 rad·sec^{-1} and below. The integrator voltage jumps were found

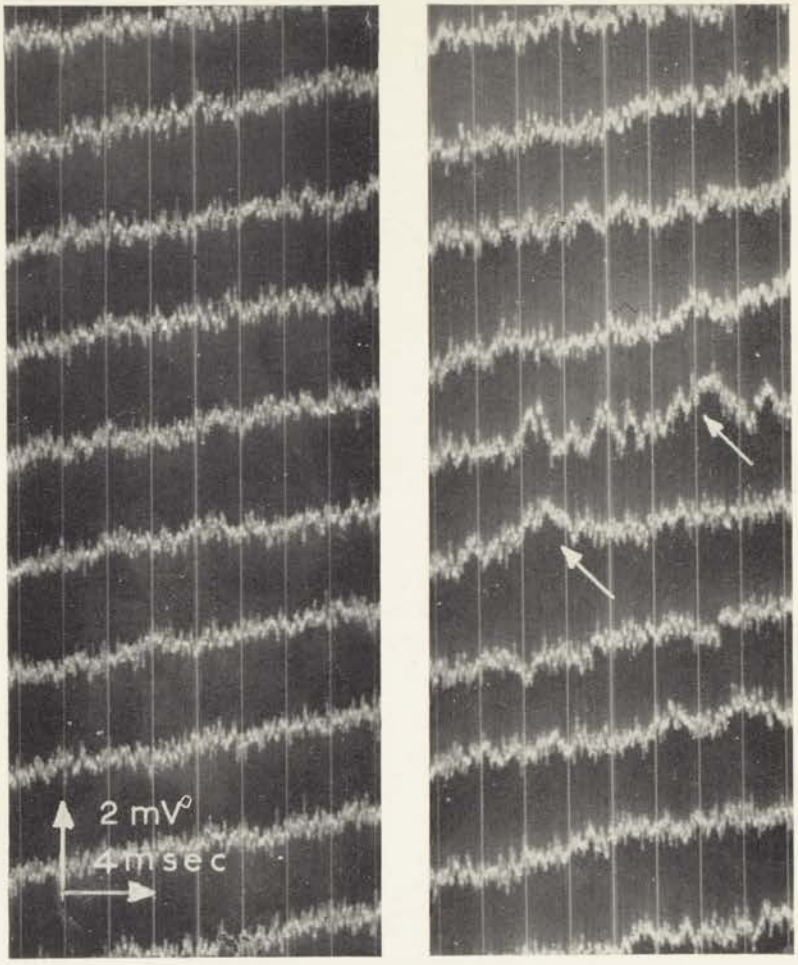

(a) (b)

Fig. 3.2.2.2.–2.

(a) Preamplifier output during quiet period. (b) Preamplifier output in the presence of burst activity.

to coincide with the appearance of triangular base line deflections, in the direction of depolarization, in both unfiltered output voltages simultaneously, the simultaneity indicating that they originate at the middle node. These deflections, which have an amplitude of 1–2 mV and a maximum duration in the order of one msec, occur in bursts of 10–100 at intervals of 5–100 msec; the bursts are

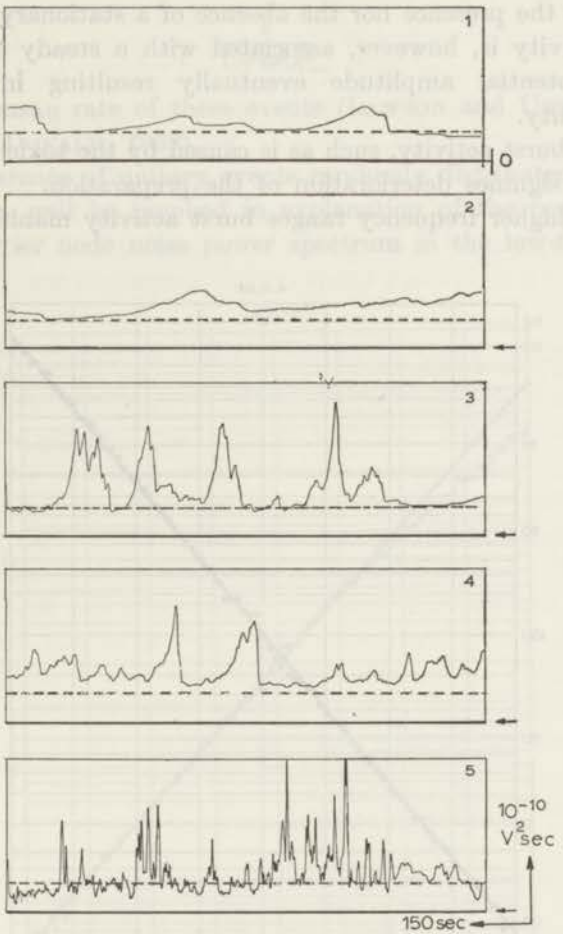

Fig. 3.2.2.2.–3.

Output of low-pass filter during noise measurement at 100 rad·sec^{-1}. Time constant in (1) and (2) is 100 sec, in (3) and (4) 10 sec and in (5) one second. Interrupted line gives intensity of $1/f$ noise component, peaks are caused by burst activity.

separated by quiet intervals of 1–10 min duration (Fig. 3.2.2.2.–2). In these quiet periods a few occasional deflections were nearly always present.

These phenomena are definitely less frequent in fibres dissected from nerves which have been stored in Ringer's solution at 0° C for twelve or more hours than in fibres obtained from freshly dissected nerve, so they do not signify deterioration during storage.

Neither the presence nor the absence of a stationary, moderate burst activity is, however, associated with a steady decrease in action potential amplitude eventually resulting in complete inexcitability.

Strong burst activity, such as is caused by the toxic substances in lucite, signifies deterioration of the preparation.

In the higher frequency ranges burst activity manifested itself

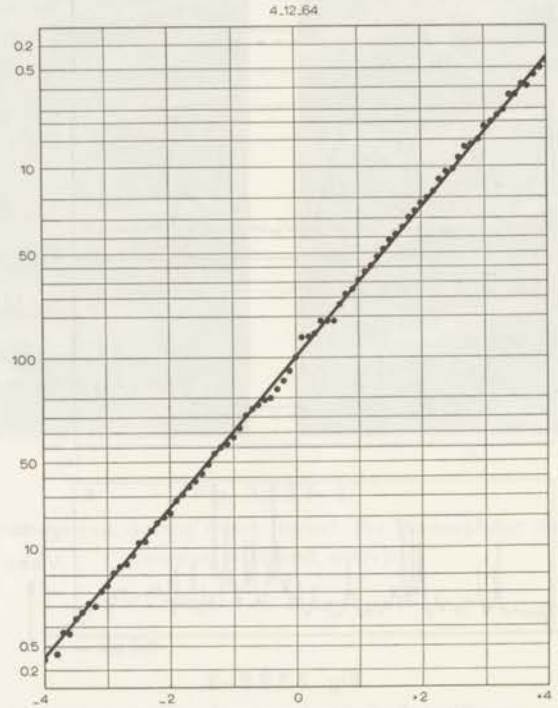

Fig. 3.2.2.2.–4.
Amplitude distribution of nodal membrane noise in the absence of burst activity.

as peaks in the low-pass filter output, Fig. 3.2.2.2.–3. That these peaks are indicative of a real disturbance could be concluded from a careful comparison with filtered white noise and filtered $1/f$ noise of a transistor.

A spectrum where the power per cycle of bandwidth increases sharply with decrease of ω can be occasioned by a train of randomly distributed unitary events where the power varies as

$$\frac{1}{1+\omega^2\lambda^2}$$

if λ is the mean rate of these events (LAWSON and UHLENBECK, 1950; MAC DONALD, 1962).

The occurrence of unitary events randomly distributed in time might, then, well be invoked in explanation of the peculiarities of the Ranvier node noise power spectrum in the low-frequency range.

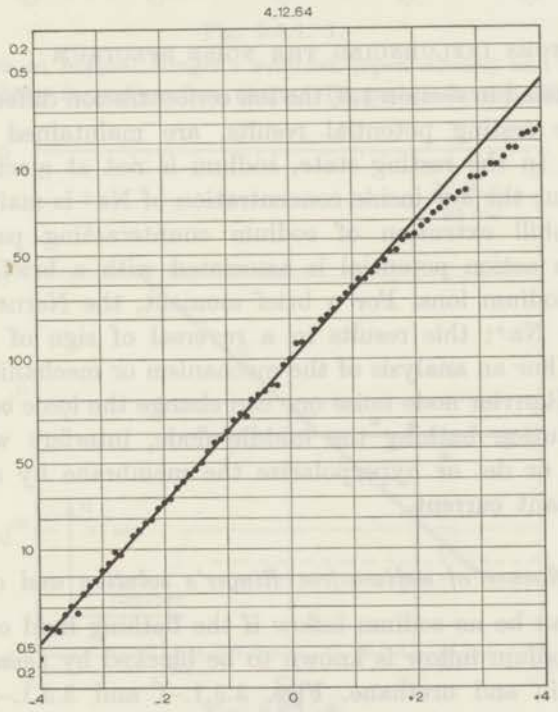

Fig. 3.2.2.2.–5.
Amplitude distribution sampled during a period of burst activity.

In a number of cases, amplitude distributions were determined in the manner described in section 2.9. Fig. 3.2.2.2.–4 shows the distribution when membrane noise was sampled during a quiet period. The distribution is Gaussian within the limits of experimental error. The amplitude distribution during a phase of burst activity is shown in Fig. 3.2.2.2.–5. From the quiet period behaviour it appears that the lower limit of the $1/f$ range lies somewhere in the vicinity of 1–0.1 rad·sec^{-1}. This is in good agreement with the upper limit (10000–20000 rad·sec^{-1}) computed in the preceding section. In the case of a $1/f$ spectrum, every frequency decade contributes an equal amount to the total rms noise voltage. The spectra of Figs. 3.2.1.–6 and 3.2.2.2.–1 have an intensity $\omega N \sim 10^{-8}V^2$, so the total r.m.s. voltage per decade approximately equals 60 μV. This limits the number of decades in which a $1/f$ relation is followed to four or five. For a lower limit between 0.1 and 1 rad·sec^{-1} this results in an upper limit somewhere near 10^4 rad·sec^{-1}.

3.3. Factors influencing the noise spectrum

As discussed in section 1.3, the ion concentration differences from which the resting potential results, are maintained by active transport. In the resting state, sodium is not at electrochemical equilibrium; the low inside concentration of Na^+ is maintained by active, uphill extrusion of sodium counteracting passive Na^+ inflow. An action potential is associated with a brief, explosive entry of sodium ions. For a brief moment, the Nernst equation applies to Na^+; this results in a reversal of sign of membrane potential. For an analysis of the mechanism or mechanisms underlying the Ranvier node noise one can change the ionic composition of the solution bathing the middle node, interfere with active transport, or de- or hyperpolarize the membrane by application of a constant current.

3.3.1. *Influence of sodium-free Ringer's solution and of urethane*

There can be no sodium inflow if the bathing fluid contains no sodium; sodium inflow is known to be blocked by agents such as tetrodotoxin and urethane. Figs. 3.3.1.–1 and 3.3.1.–2 refer to experiments where the fluid bathing the middle node was replaced by a sodium-free Ringer's solution, with choline as a sodium

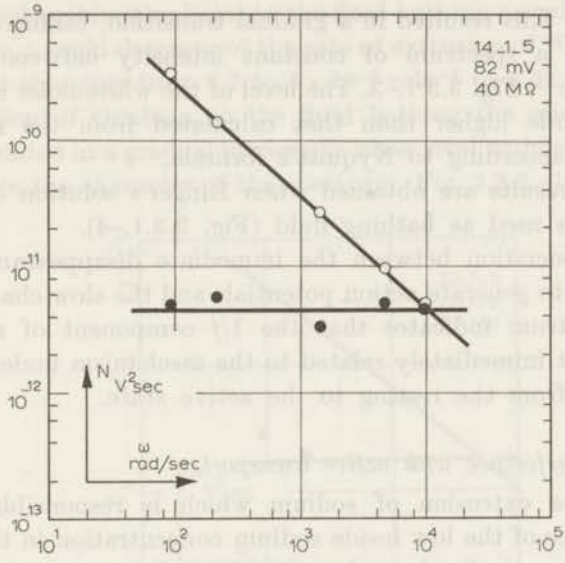

Fig. 3.3.1.–1.

Noise spectra in normal Ringer's solution (open circles) and after forty minutes bathing in sodium-free choline Ringer's solution (filled circles).

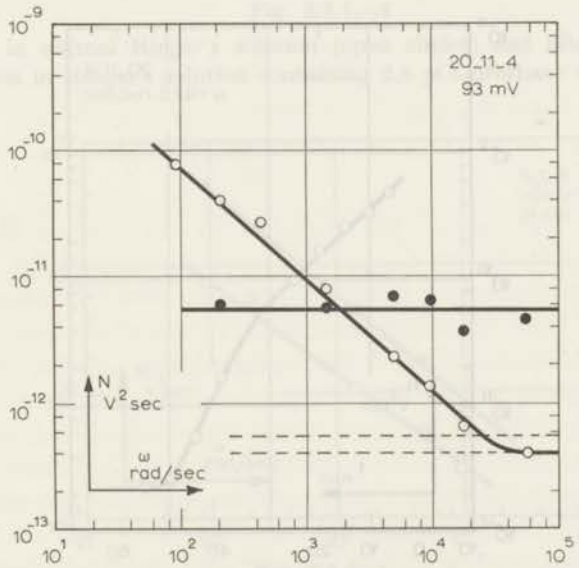

Fig. 3.3.1.–2.

Power spectra in normal Ringer's solution (open circles) and after fifty minutes' immersion in sodium-free choline Ringer's solution (filled circles).

substitute. This resulted in a gradual transition, taking about one hour, into a spectrum of constant intensity between 200 and 10^4 rad·sec^{-1}, Fig. 3.3.1.–3. The level of the white noise is an order of magnitude higher than that calculated from the membrane resistance according to Nyquist's formula.

Similar results are obtained when Ringer's solution containing urethane is used as bathing fluid (Fig. 3.3.1.–4).

The dissociation between the immediate disappearance of the possibility to generate action potentials and the slow change of the noise spectrum indicates that the $1/f$ component of membrane noise is not immediately related to the mechanism underlying the transition from the resting to the active state.

3.3.2. *Interference with active transport*

Since the extrusion of sodium which is responsible for the maintenance of the low inside sodium concentration in the resting fibre is energetically dependent on metabolism it can be arrested by poisoning with substances such as 2:4-dinitrophenol. It has further been shown (Caldwell and Keynes, 1959) that addition

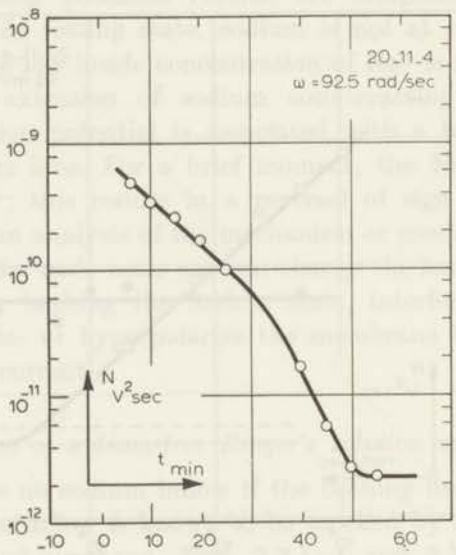

Fig. 3.3.1.–3.

Time course of decrease of noise intensity at 100 rad·sec^{-1} after change-over to sodium-free choline Ringer's solution.

of g-strophanthin (Ouabain) to the fluid bathing a squid giant axon results in a rapid decrease of the rate of extrusion of $^{22}Na^{+}$, the rate constant changing from 1.7 to 4×10^{-3} min^{-1} to 0.51×10^{-3} min^{-1}.

Addition of Ouabain to the fluid bathing the middle Ranvier node resulted in a gradual increase in noise level without appreciable change in the character of the spectrum, Fig. 3.3.2.–1. Here again,

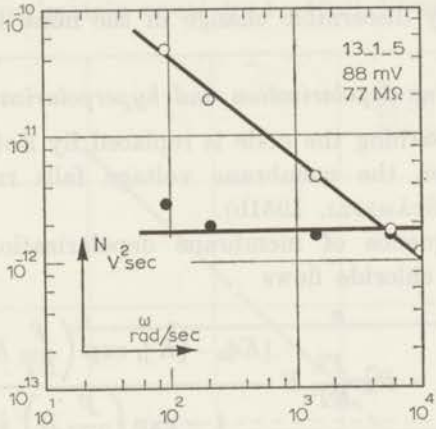

Fig. 3.3.1.–.4

Spectra in normal Ringer's solution (open circles) and after one hour's immersion in Ringer's solution containing 2,5 pCt urethane (filled circles).

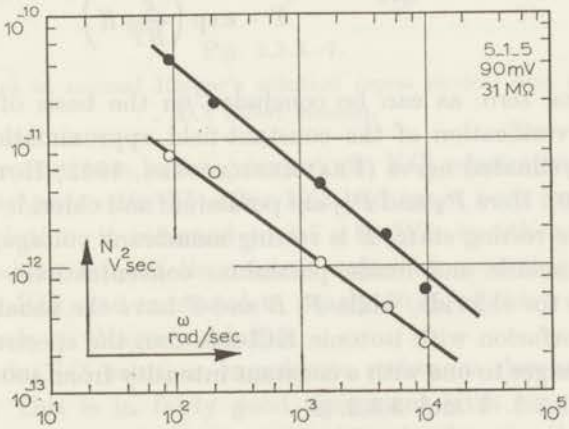

Fig. 3.3.2.–1.

Power spectra in normal Ringer's solution (open circles and in Ringer's solution containing 10^{-5} M/l Ouabain (filled circles).

a steady level was attained in about one hour, so blocking active transport has no direct effect on the noise spectrum.

Increase of the work load on the sodium extrusion mechanism was, in some experiments, brought about by stimulating the node at a rate of one hundred stimuli per second during five minutes, which results in an appreciable increase of inside Na^+ concentration (and a decrease of inside K^+ concentration). This procedure did not lead to any discernible change in the noise level.

3.3.3. *Membrane depolarization and hyperpolarization*

If the fluid bathing the node is replaced by isotonic potassium chloride solution the membrane voltage falls rapidly to zero, (Huxley and Stämpfli, 1951b).

As a consequence of membrane depolarization, the passive potassium and chloride flows

$$I_K = P_K \frac{F^2}{RT} E \frac{[K]_o - [K]_i \exp\left(\frac{F}{RT} E\right)}{1 - \exp\left(\frac{F}{RT} E\right)} \tag{3.3}$$

$$I_{Cl} = P_{Cl} \frac{F^2}{RT} E \frac{[Cl]_i - [Cl]_o \exp\left(\frac{F}{RT} E\right)}{1 - \exp\left(\frac{F}{RT} E\right)} \tag{3.4}$$

will become zero, as can be concluded on the basis of Frankenhaeuser's verification of the constant-field approximation for the case of myelinated nerve (Frankenhaeuser, 1962; Hodgkin and Katz, 1949). Here P_k and P_{Cl} are potassium and chloride permeabilities in the resting state, E is resting membrane voltage, $[K]_o$ and $[K]_i$ are outside and inside potassium concentrations, $[Cl]_o$ and $[Cl]_i$ those for chloride, while F, R and T have the usual meaning.

Upon perfusion with isotonic KCl-solution, the spectrum immediately changes to one with a constant intensity from 400 rad·sec^{-1} up, Figs. 3.3.3.–1 and 3.3.3.–2.

Measurements at 220 and at 100 rad·sec^{-1} might suggest that, down from 50 rad·sec^{-1} the $1/f$ character is maintained, Fig. 3.3.3.–2.

After a change-over back to Ringer's solution the $1/f$ noise was

immediately restored over a range extending upward to 5×10^3 rad·sec^{-1}, but at a lower power level. If low-frequency burst activity is left out of consideration, virtually all the spectra measured can be described by

$$N = \frac{C_1}{\omega} + C_2 \tag{3.5}$$

where C_2 is approximately equal to 4×10^{-11} V^{2}sec.

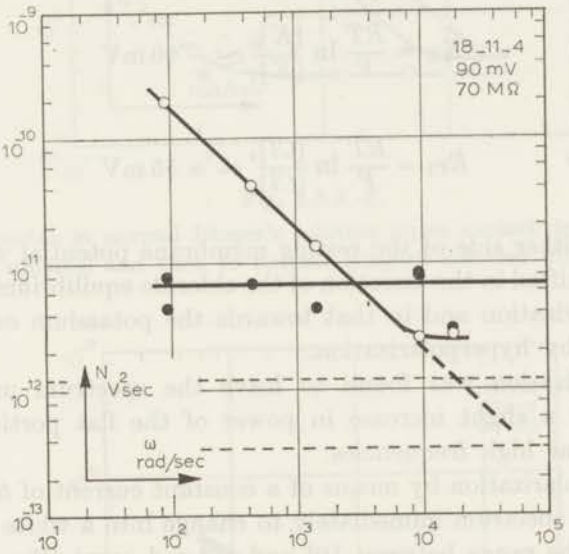

Fig. 3.3.3.–1.
Power spectra in normal Ringer's solution (open circles) and in isotonic KCl (filled circles).

In the present case bathing in isotonic KCl-solution reduced C_1 from 4×10^{-7} to 4×10^{-9}V^2; after KCl had again been replaced by Ringer's solution, it returned to 2.7×10^{-7}V^2; in other words, it was reduced to 1 % of its original value by replacing Ringer's solution by KCl, and increased to nearly 70 % of this value upon transfer back to Ringer's solution.

In isotonic KCl solution, membrane resistance decreased by a factor 3.5. This is in fairly good agreement with the results of FRANKENHAEUSER and WALTMAN (1959) who found a decrease in membrane resistance by a factor 4.4. to 4 from determinations of electrotonic attenuation along whole nerve.

Besides reducing the passive K^+ and Cl^- flows to zero, bathing in isotonic KCl-solution of course excludes sodium inflow. This factor, however, was found not to be directly related with the character of the noise spectrum (cf. § 3.3.1 and § 3.3.2), which, then, can be considered as signifying fluctuations in potassium and/or chloride currents through the resting membrane.

As follows from (3.3) and (3.4), passive potassium and chloride currents are also reduced to zero at the equilibrium potentials.

$$E_K = \frac{RT}{F} \ln \frac{[K]_o}{[K]_i} \sim -90\,\text{mV}$$

and

$$E_{Cl} = \frac{RT}{F} \ln \frac{[Cl]_i}{[Cl]_o} \sim -55\,\text{mV}$$

lying on either side of the resting membrane potential which can, thus, be shifted in the direction of the chloride equilibrium potential by depolarization and in that towards the potassium equilibrium potential by hyperpolarization.

Depolarization was found to leave the spectrum unchanged, except for a slight increase in power of the flat portion of the spectrum at high frequencies.

Hyperpolarization by means of a constant current of 5×10^{-10} A causes the spectrum immediately to change into a white spectrum covering the range between 10^2 and 10^4 rad·sec^{-1} (Fig. 3.3.3.–3).

The membrane potential shift caused by the hyperpolarizing current will be about 20 mV, approximately the shift required to attain the potassium equilibrium potential of -90 mV. It can, then, tentatively be concluded that $1/f$ noise is associated with passive potassium outflow, either as such or possibly through interaction with passive potassium inflow (HODGKIN and KEYNES, 1955). A dependence on currents of chloride and other anions is highly improbable, since anion outward current increases by hyperpolarization, while, at least in physical devices, the intensity of $1/f$ noise always increases with increase of direct current strength. What remains to be done is to plot a series of spectra for a range of hyperpolarizing currents. From the spectra pictured in Fig. 3.3.3.–4 it is apparent that the spectrum shifts upwards when the membrane is depolarized, and downwards when it is hyperpolarized. At still

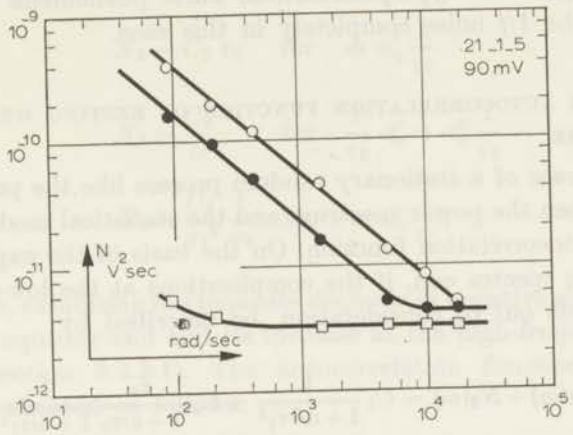

Fig. 3.3.3.–2.

Power spectra in normal Ringer's solution (open circles), in isotonic KCl (open squares) and back to normal Ringer's solution (filled circles).

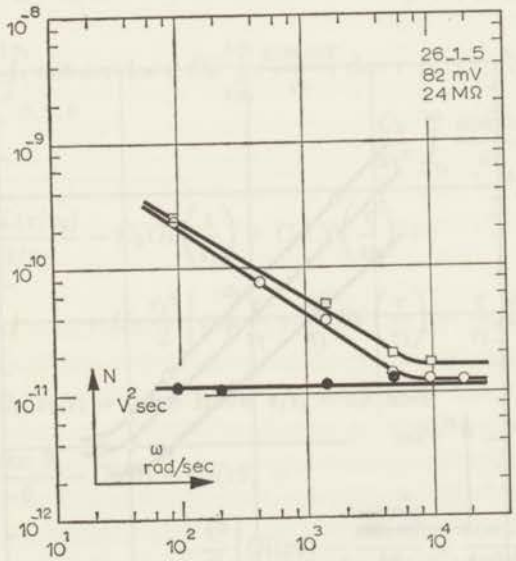

Fig. 3.3.3.–3.

Normal power spectrum (open circles), depolarization by 5×10^{-10} A (open squares), hyperpolarization by -5×10^{-10} A (filled circles).

higher degrees of hyperpolarization, burst phenomena started to obscure the $1/f$ noise completely in this case.

3.4. The autocorrelation function of resting membrane noise

In the case of a stationary random process like the present, the link between the power spectrum and the statistical model is given by the autocorrelation function. On the basis of the experimental results the spectra can, if the complications at the low-frequency end are left out of consideration, be described by

$$N(\omega) = N_1(\omega) + N_2(\omega) = C_1 \frac{1}{1+\omega^2\tau_1^2} + C_2 \frac{\tau_2}{1+\omega\tau_2} \frac{1}{1+\omega\tau_1^2}. \qquad (3.6)$$

They consist of two components, viz.

(1) a white noise spectrum N_1 of rms intensity C_1 per cycle of bandwidth; the membrane time constant is τ_1,

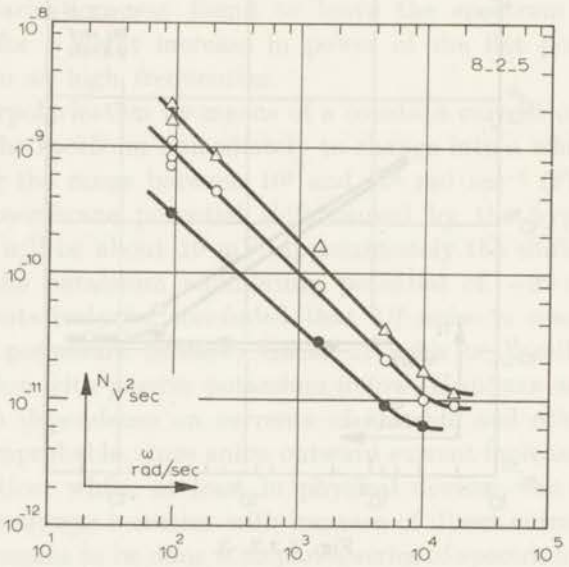

Fig. 3.3.3.–4.
Normal power spectrum (open circles), 10 mV depolarization (open triangles), 10 mV hyperpolarization (filled circles).

(2) a $1/f$ spectrum N_2 obeying

$$N_2 = C_2\,\tau_2 \quad \text{for} \quad \omega \ll \frac{1}{\tau_2}$$

$$N_2 = \frac{C_2}{\omega} \quad \text{for} \quad \frac{1}{\tau_2} \ll \omega \ll \frac{1}{\tau_1}$$

$$N_2 = \frac{C_2}{\tau_1^2}\,\frac{1}{\omega_3} \quad \text{for} \quad \omega \ll \frac{1}{\tau_1},$$

that is, exhibiting the requisite decrease in negative slope at the low-frequency end and its increase at the high-frequency end (cf. section 3.2.2.1). The autocorrelation function can be approximated as follows:

$$R(\tau) = \int_0^\infty N(\omega)\cos\omega\tau\,\mathrm{d}\omega = C_2\tau_2\int_0^\infty \frac{1}{1+\omega\tau_2}\,\frac{1}{1+\omega^2\tau_1^2}\cos\omega\tau\,\mathrm{d}\omega + C_1\int_0^\infty \frac{1}{1+\omega^2\tau_1^2}\cos\omega\tau\,\mathrm{d}\omega$$

$$\sim C_2\tau_2\int_0^{1/\tau_2}\cos\omega\tau\,\mathrm{d}\omega + C_2\int_{1/\tau_2}^{1/\tau_1}\frac{\cos\omega\tau}{\omega}\,\mathrm{d}\omega + \frac{C_2}{\tau_1^2}\int_{1/\tau_1}^{\infty}\frac{\cos\omega\tau}{\omega_3}\,\mathrm{d}\omega + \frac{C_1}{\tau_1}\frac{\pi}{2}$$

$$= C_2\,\frac{\sin(\tau/\tau_2)}{\tau/\tau_2} - C_2 Ci\left(\frac{\tau}{\tau_1}\right) + C_2 Ci\left(\frac{\tau}{\tau_2}\right) + C_2\,\frac{\tau_1^2}{2}\left\{\cos\frac{\tau}{\tau_1} + \frac{\tau^2}{\tau_1}\,Ci\left(\frac{\tau}{\tau_1}\right) - \frac{\tau}{\tau_1}\sin\frac{\tau}{\tau_1}\right\} + \frac{C_1}{\tau_1}\frac{\pi}{2}$$

with $\tau/\tau_2 = \theta$, $\tau_2/\tau_1 = z$ we have $\tau/\tau_1 = z\theta$ and

$$R(\tau) \sim C_1\left[\frac{\sin\theta}{\theta} - Ci(\theta) + Ci(z\theta) + \frac{\tau^2}{2}\left\{Ci(z\theta) - \frac{\sin z\theta}{z\theta} + \frac{\cos z\theta}{(z\theta)^2}\right\}\right] + \frac{C_1}{\tau_1}\frac{\pi}{2}.$$

The spectrum $N_2(\omega)$ and the corresponding normalized autocorrelation function have been plotted in Fig. 3.4.–1 a and b for $\tau_2 = 1$ and $\tau_1 = 10^{-4}$ sec.

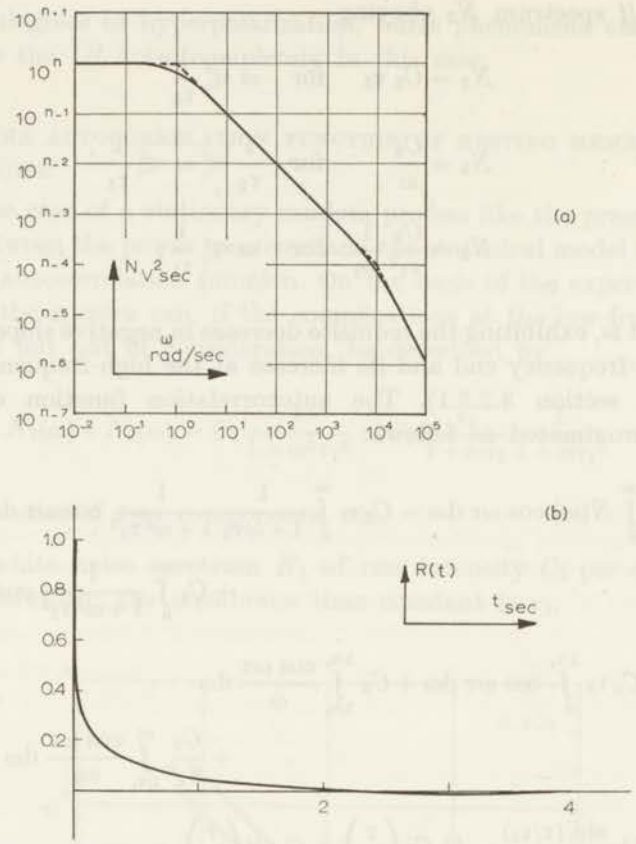

Fig. 3.4.–1, a, b, see text.

Any statistical model to be considered must lead to the above autocorrelation function and account for the existence of the long correlation times following from the fact that the range of the $1/f$ component extends to very low frequencies. As to the relation between membrane voltage noise and fluctuations of excitability, it is of special interest to note that the (first) X-intercept of the autocorrelation function lies at $\tau \sim 2$ sec, which is in excellent agreement with the minimum permissible duration of stimulus intervals in VERVEEN's experiments on excitability fluctuations, where the condition is that the fibre must be recovered from the effect of one stimulus pulse, whether it has resulted in the generation of a spike or not, before the next is applied.

4. COMMENT

It remains, first, to try and get some insight into the mechanism underlying the generation of $1/f$ noise in the nerve membrane, and then to consider the consequences of the presence of this noise for neuronal data processing.

4.1. Applicability of existing theories on the origin of $1/f$ noise

The term, $1/f$ noise, is used to denote current or voltage fluctuations exhibiting a spectral intensity obeying the relation $N(f) = c \cdot f^{\alpha}$ with $\alpha \sim -1$ over several frequency decades. Fluctuations of this type have been found in the electron emission of oxide-coated cathodes (flicker effect), in carbon resistors and carbon microphones, some metal film resistors, and contacts (excess noise), in bulk semiconductor material and semiconductor devices (diodes, unipolar and bipolar transistors, tunnel diodes), and in thermistors. In all cases, the carrying of direct current by the sample is a prerequisite for $1/f$ noise to be generated. In the present case, external currents were mostly absent but, as has been pointed out in section 1.3, the resting membrane is not in thermodynamic equilibrium and several species of ions are transported across it.

So far, there is not one unified theory on the origin of $1/f$ noise and as a matter of fact it is hardly to be expected that such a theory will ever be evolved in view of the great variety of cases where this kind of noise spectrum has been found. The theories developed as a rule apply at best to one special case and cannot be extended to cover the others (Sautter, 1960; Van der Ziel, 1959) although most of them have in common the notion of fluctuation in carrier density.

It is certain that in the present case despite the striking similarity in behaviour – even extending to the transient V–I tunnel diode characteristic – the physical substrate underlying the generation of $1/f$ noise is fundamentally different from that in the materials and devices named. This means that some of the existing theories can be ruled out because the mechanism invoked cannot be operative, and have no statistical equivalent, in the present case.

It also means that difficulties – mostly of a quantitative nature – which argue against a given theory in the case of semiconductors,

need not hinder its application to a membrane model presuming a mechanism statistically equivalent to that invoked by the theory in question.

Various combinations of time-dependent processes may result in the generation of $1/f$ noise. Among them are (a) superposition of elementary noise sources whose relaxation times follow a hyperbolic distribution over a wide range, (b) a switched random process, or, alternatively, one random process modulating another, (c) one single random process in conjunction with non-linear coupling. In the following, theories will be grouped according as to which processes are invoked.

4.1.1. *Superposition of sources with hyperbolically distributed relaxation times*

It is self-evident that $1/f$ noise must result, if the noise is produced by a great number of elementary sources whose relaxation times have a hyperbolic distribution. The question is, however, if there is any reason for an assumption of the kind. Such an assumption is at the basis of one of the best-known theories of noise in semiconductor material, which was developed by McWhorther (1957). In this theory, the generation of flicker noise is supposed to be due to the presence, at the surface of the sample, of anomalies, so-called surface traps, which can temporarily bind carriers and thus change the number of free carriers, first by actual trapping and then because a change in surface trap occupancy alters the generation of minority carriers at the fast recombination centers near the surface. Because of the limited effective range of the traps, trapping in individual surface elements with areas in the order of this range can be considered as independent and a time constant τ of the trapping process may be assigned to each individual element. Assuming that the density (number per unit area) of the holes is negligible compared to that of electrons, the time constant is given by

$$\tau \sim \frac{N_0}{n_{s0}\, p_{t0}\, c_n}$$

where N_0 is electron density, n_{s_0} the equilibrium electron density in the absence of a field, p_{t0} the density of unoccupied traps, and c_n the probability, per unit time, that an electron is captured by

an empty trap. Assuming that trapping times are exponentially distributed according to

$$g(\tau)\,\mathrm{d}\tau = \exp\left(-\frac{\tau}{\tau_0}\right)\mathrm{d}\left(\frac{\tau}{\tau_0}\right)$$

where τ_0 is the average trapping time, that is, assuming the autocorrelation coefficient to be given by $c(\tau)=\exp(-\tau/\tau_0)$, then if the fluctuation in the number of trapped carriers in a surface area ΔS, be ΔN, the spectral intensity $S_{\Delta N}(f)$ is given, according to the Wiener-Khintchin theorem by

$$S_{\Delta N}(f) = 4\overline{\Delta N^2}\,\frac{\tau_0}{1+\omega^2\tau_0^2}$$

and, since $\Delta N^2 = N_0 \Delta S$

$$S_{\Delta N}(f) = 4 N_0 \Delta S\,\frac{\tau_0}{1+\omega^2\tau_0^2}\,.$$

For summation over individual independent ΔS to result in $1/f$ noise it is necessary that the distribution of trapping times over individual sections follows the function

$$g(\tau_0)\,\mathrm{d}\tau_0 = \frac{g_0\,\mathrm{d}\tau_0}{\tau_0} \quad \text{for} \quad \tau_1 < \tau_0 < \tau_2 \tag{4.1}$$

$g(\tau_0)\,\mathrm{d}\tau_0 = 0$ for $\tau_0 < \tau_1$ and for $\tau_0 > \tau_2$ where g_0 has to be chosen so that

$$\int_0^\infty g(\tau_0)\,\mathrm{d}\tau_0 = 1,$$

from which

$$g_0 = \frac{1}{\ln\dfrac{\tau_2}{\tau_1}}\,.$$

That, in semiconductor material, such a distribution actually occurs, follows from the measurements, made by McWHORTHER, of the frequency dependence of the conductivity modulation of the sample upon application of an ac field.

The most likely process leading to a distribution as in eq. 4.1 is a tunneling process where c_n is determined by tunneling through a potential barrier of variable width.

In semiconductor noise theory, McWHORTHER'S concept offers a

reasonable explanation of the slight temperature dependence of semiconductor $1/f$ noise. It is to be noted that this linear theory is applicable only if the surface potential fluctuations associated with the trapping and release of carriers are small compared to KT/e.

It seems difficult to apply McWHORTHER's theory to the present case, that is, to assign a substrate to its statistical equivalent. More particularly, it is hardly possible to imagine a process, in nerve membrane, leading to the most unusual hyperbolic distribution of time constants. Its main advantage, the explanation of the slightness of temperature dependence of the spectrum, need not apply to the present case; systematic investigation of the influence of temperature – which can, at best, in the case of frog nerve, cover a range of some 20 degrees centigrade – have not been made, but there is good reason to expect a marked temperature dependence.

4.1.2. *Switched random processes; one random process modulating another*

A randomly switched random process can be considered as a special case of one random process modulating another. Mechanisms of this kind are assumed to operate in various semiconductor and contact noise theories. MACFARLANE (1950) proposed a theory of contact noise, in which the noise is attributed to the random modulation of the Schottky barrier potential at emitting patches by random fluctuations in the concentration of mobile adsorbed ions. The surface of a semiconducting crystal is supposed to be partially covered by a film of adsorbed atoms which have, by capture of electrons from the crystal, changed into negative ions, which are supposed to move at random over the crystal surface. The diffusion of ions in and out of a patch results in fluctuations in ion concentration, and thus of the height of the Schottky potential barrier set up as a result of atom adsorption; these fluctuations, in their turn, give rise to fluctuations in electron emission. The resulting noise spectrum depends on the shape of the patch; $1/f$ noise extending over a limiting frequency range is produced. Geometrically there is some resemblance to the present object, because of the fact that the cross-section of the axon is circular. The assumption of free diffusion certainly does not apply, however; there is no equivalent of a membrane in this theory.

An approach presenting interesting features was made by BELL (1958). He considers the rate at which carriers leave the conduction band as being due to a queueing situation rather than to a relaxation mechanism, and, by doing so, is able to give an explanation of the fact that the $1/f$ spectrum of semiconductor material, if it should follow from his theory that such a spectrum would be generated, would extend to very low frequencies despite the fact that the lifetimes of injected carriers are in the microsecond range. The trouble is, however, that he cannot go beyond stating that a $1/f$ spectrum is compatible with his theory. The problem of queueing had already been studied for the case of telephone exchanges, and a general formula for the expected delay in the case of a random service queue with a mean calling rate which is less than the mean service rate had been given by POLLACZEK (1946). In random queueing theory, as developed for the case of telephone exchanges, queue members are supposed to arrive independently and at random, with a probability uniform in time; the available service outlets are indistinguishable from each other; when a member of the queue finds a vacant outlet it occupies it for a given holding time; holding times are exponentially distributed. In applying this theory to semiconductor noise, BELL considers the queue to be constituted by the charge carriers in the conduction band, which join it at random as a result of random excitation from the base levels. Vacant base levels or recombination centers serve as service outlets; duration of base level occupation is again assumed to follow an exponential distribution. The rather formidable formula derived by POLLACZEK for the expectation of a delay $> t$:

$$A(t) = -\pi(2b\theta)^{\frac{1}{2}}[1+\pi^{\frac{1}{2}}b \exp(-b^2)\{1+\Phi(b)\}]^{-1} \cdot \cdot H_1^{(1)}\{2j(2b\theta)^{\frac{1}{2}}\} \cdot \{1+O(s^{-\frac{1}{2}})\} \qquad (4.2)$$

where Φ is the Gaussian integral, $H_1^{(1)}$ a Hankel function, S the number of available outlets, η the average calling rate per outlet,

$$b = (1-\eta)(S)^{\frac{1}{2}} \text{ and } \theta = t(\tfrac{1}{2}S)^{\frac{1}{2}}$$

can, for the case of semiconductors, where $S \to \infty$, $\eta \to 1$ and assuming $(1-\eta)S$ to remain a finite quantity Z, be simplified to

$$A(t) \sim -\pi(Zt)^{\frac{1}{2}}H_1^{(1)}\{2j(Zt)^{\frac{1}{2}}\} \qquad (4.3)$$

which is still bad enough.

BELL, while making the obvious statement that, if one regards $A(t)$ as the expectation that a charge carrier which entered the conduction band at $t=0$ will still be there at time t, the auto-correlation function of the conductivity pulse constituted by that carrier will be

$$R(\tau)=\int A(t)A(t+\tau)\,\mathrm{d}\tau \tag{4.4}$$

and that, in principle, the corresponding power spectrum can be obtained by evaluating $R(\tau)$ as a function of τ and then taking the cosine Fourier transform of this function, adds that he sees no way of carrying out these operations on the original Pollaczek formula or even in the simplified form. It has been shown, however (ROUKENS, to be published), that (4.2) can be transformed into a first order Bessel function of the second kind, lending itself to numerical computation. Computations have been carried out by ROUKENS with the aid of an IBM 7094 Computer.

It was found that the corresponding power spectrum is indeed flat at the low-frequency end, but that it then changes into a $1/f^2$ spectrum extending over at least seven decades. It can be concluded that, though in the case of membrane noise, a substrate for a queueing situation can easily be imagined, the model proposed by BELL cannot serve to explain the $1/f$ character of axon membrane voltage fluctuations.

4.1.3. *One random process plus non-linear coupling*

MORRISON (1956) proposed a theory in which he shows that $1/f$ noise may be generated by the combination of one simple random process with non-linear coupling. His argument can be summarized as follows: Let ΔN be the number of trapped carriers in excess of equilibrium, and let the resulting change in barrier height, ΔV, be proportional to ΔN. Then

$$\frac{\mathrm{d}\,\Delta N}{\mathrm{d}t}=B\left[\exp\left(-\frac{e\Delta V}{kT}\right)-1\right]=B[\exp\left(-\beta\Delta N\right)-1] \tag{4.5}$$

where $\beta=(e/kT)(\mathrm{d}V/\mathrm{d}N)$, and B is the equilibrium rate at which charge carriers cross the barrier.

From eq. 4.5 follows

$$\Delta N(t) = \frac{1}{\beta} \ln [1 - A\exp(-\beta Bt)].$$

A being the integration constant.

Assuming ΔN to follow a unimodal symmetrical distribution, this expression can be used to calculate the autocorrelation function and, from that, the power spectrum, which obeys in this case a $1/f$ relation within a certain frequency range.

4.2. Possible physical substrates for the generation of noise in nerve membrane

4.2.1. *Generation of* $1/f$ *noise*

From the experimental data summarized in chapter 3 it can be concluded that the $1/f$ component of axon membrane noise is associated with passive potassium transport through the membrane. A variety of statistical models might account for the generation of $1/f$ noise in axon membrane potential, many of them, however, can be discarded since they cannot be translated into a physical model compatible with known facts about the properties of the axon membrane, while others can be made to fit only by the introduction of *ad hoc* assumptions which cannot be verified. The established facts about the molecular dynamics of the axon membrane are, unfortunately, small in number. About the only thing which can be stated with any degree of certainty is that the membrane possesses functional pores, or transportation sites, of a minimum length of 30 times the diameter of the solvated K^+ ion, and of a diameter about equal to that of the ion. It can also be stated that, though the behaviour of the ensemble of pores may be likened to simple unidirectional diffusion the behaviour of individual pores should be considered in the interpretation of the membrane noise generated.

The behaviour of the potassium ion within the pores is certainly far removed from that in free diffusion, which would, for that matter, result in a white noise spectrum. It has been argued earlier (cf. § 4.1.1) that it seems difficult to find a statistical equivalent of McWhorther's theory which would be applicable in the present

case. Consequently one is left with the choice between a randomly switched random process or one random process modulating another, and one random process combined with non-linear coupling.

The first random process to be considered, and which is operative in any case, is the entry of individual potassium ions in the pore entrances. To enter a pore, a potassium ion will at a given moment have to be in the near vicinity of an unoccupied pore entrance, and have a sufficiently large velocity component coincident with the produced pore axis. A random fluctuation in time of the number of available pores, if these are supposed to be of equal diameter, could serve as the second random process. This would be equivalent to a random fluctuation of functional pore widths in the case of a fixed pore number. Alternatively, a fixed number of pores of fixed diameter together with a queueing situation such as proposed by BELL might be considered, even though Pollaczek's concept, where a mean calling rate less than the mean service rate is an essential feature, has been shown not to apply to the present case.

As to the question of electrochemical equilibrium, this must, of course, be maintained in the bulk phases, but need not be rigidly obeyed in areas of molecular dimensions. Pores unoccupied by potassium may allow of either the inward movement of other cations or the outward movement of anions able to cross the membrane.

As far as the question presently investigated is concerned, the most important aspect of the mechanisms discussed is that they can easily account for long correlation times.

Several avenues of further investigation present themselves. First of all, further information will almost certainly be obtained by studying axon membrane noise at different temperatures. Then the overall permeability of the membrane is known to be markedly decreased by (outside) calcium even in minute amounts. Whether this influence of calcium is brought about by diminution of the number of pores or by a decrease of their functional diameter is, for the time being, immaterial. The influence, on the noise spectra, of a bathing fluid either free from calcium, or containing more than the normal concentration of calcium, will have to be studied to arrive at a further analysis of the physical basis of the axon membrane noise. In myelinated frog nerve, it is impossible to change the

composition of the fluid enclosed by the axon membrane; that is, to replace potassium partly or wholly by kations such as rubidium or caesium. This is possible, however, in the case of the squid giant axon, and experiments of the kind can be supposed to be able to contribute to further elucidation of the processes involved in the generation, by the axon membrane, of $1/f$ noise. Experiments along the lines suggested are in preparation.

4.2.2. *Origin of the white component of the axon membrane noise*

It has been stated earlier that the level of the white noise found in the frequency range from about 10^4 rad·sec^{-1} upward exceeds the Nyquist noise level $4KTR$, where R is the membrane resistance measured at 1450 rad·sec^{-1}. Insuperable technical difficulties preclude measurement of membrane resistance in the frequency range upwards from about 10^4 rad·sec^{-1}, where the $1/f$ noise dips below the white noise level. It is not unreasonable to suppose that, considering the dimensions of the system involved, the real, dissipative component of membrane impedance will be frequency-dependent in the sense of an increase at high frequencies. For the time being, it does, in consequence, not seem to be necessary to invoke another noise source than thermal noise to interpret the difference between the $4KTR$ level, which is a minimum level anyway, and the actual white noise level in the range from 10^4 rad·sec^{-1} upward.

Here again, though the useful range is limited to about 20–25 degrees Cent., measurements at different temperatures can be supposed to supply more information on this point.

4.3. Consequences of membrane noise and neural noise for neuronal data processing

The consequences of fluctuations in receptor membrane voltage, dendritic membrane voltage, axon membrane voltage, and synaptic coupling have been discussed, in a general way, in section 1.

They have been the subject of investigations by several authors who have tried to construct noisy models to account for experimentally found spike interval distributions (Hagiwara, 1954; Viernstein and Grossman, 1961; Ten Hoopen, Den Hertog

and REUVER, 1963; WEISS, 1964; GOLDBERG, ADRIAN and SMITH, 1964), for the distribution of time intervals between miniature end-plate potentials (FATT and KATZ, 1952), etc.

Thus FATT and KATZ, who studied spontaneous subthreshold activity at the myoneural junction of resting muscle fibres discussed the possibility that, in a sufficiently minute structure, the noise voltages across the axon membrane may occasionally exceed the critical depolarization level. They assume the noise voltage to be due to thermal agitation of ions within the membrane only. Model studies were, among others, made by GOLDBERG *et al.* (1964), and by WEISS (1964); GOLDBERG, ADRIAN and SMITH, who studied the response of neurons of the superior olivary complex of the cat to acoustic stimuli of long duration, introduce a random component $N(t)$ modulating either the excitatory input or the firing threshold. They arbitrarily assume $N(t)$ to be a Gaussian noise passed through an ideal low-pass filter. WEISS, who gives a model for firing patterns of auditory nerve fibres, introduced a Gaussian white noise, basing himself on VERVEEN's findings.

Now that the membrane noise has been shown not to be white, the models in question need to be revised.

Recently, SMITH and SMITH (1965) have shown that the distribution of interspike intervals in continually active cortical neurones in the isolated forebrain of the cat can be described in terms of a high-frequency Poissonian activity gated at random instants. Not only does the autocorrelation function of the random pulse train in question closely resemble that of Fig. 3.4.1.–b, but it has the same time scale. This strongly suggests that the $1/f$ noise in nerve membrane is indeed closely associated with the time patterns of "spontaneously" generated spikes.

Besides the avenues of further investigation suggested in section 4.2 the possibility of a further analysis with the aid of modern computational devices should be considered.

Even the original Hodgkin-Huxley equations are of such a complexity that numerical computation with the aid of a large and powerful digital computing system takes much time. It is practically out of the question that, with the complications due to the fluctuations in membrane voltage thrown in, a digital system could cope with the problem now presented. A single neuron exhibiting membrane voltage fluctuation with a noise

spectrum of the type found in the present experiments, could be simulated on a fairly large general purpose analog computer (BEKEY and PAXON, 1957).

The behaviour of networks of noisy neurons with synaptic couplings of fluctuating strength, however, can be studied only with the aid of a special purpose computer with neuron analogs as operative elements. Several neuron analogs simulating more or less closely the electrical properties of the neurons have, in the last few years, been developed (HARMON, 1959; KÜPFMÜLLER and JENIK, 1961; DERKSEN, 1961; LEWIS, 1964).

In the physiological laboratory in Leyden a neuron analog computer (LUNAC, for Leyden University Neuron Analog Computer) has been set up. Its elements are the neuron analogs described earlier (DERKSEN, 1961). Provision has been made for variations in coupling strength and for the introduction of uncorrelated noise sources. With the aid of this system, the behaviour of small groups of neural elements (of the order of a few hundred) showing $1/f$ fluctuations in resting membrane potential can be studied. Results will be published in due course.

SUMMARY

The vertebrate nervous system is described in terms of a computing system. The data acquisition system consists of transducers (receptors) transforming input signals into electric signals serving as input data for the computing system, which is of a hybrid, digital-analog character. The elements of which it consists, the neurons, are pulse generators delivering uniform output pulses serving as input signals for other neurons. They are arranged in a series—parallel network characterized by a combination of convergent interconnexions. Computing is parallel and asynchronous. The neuron can serve as a kind of summing amplifier; it can act as an *or*-gate, an *and*-gate, a *nand*-gate or an inverter.

Neurons and receptor cells are enveloped by a lipoid-protein membrane exhibiting selective permeability towards certain ions and electrolytes. In the resting state, inside potassium concentration is about 20 times that in the outside fluid; transmembrane voltage is dominated by the inside-outside potassium concentration ratio. Low inside sodium is maintained by active extrusion. At a critical level of partial depolarization of the neuron membrane there is a transient increase of sodium conductance resulting in an inrush of sodium and in a reversal of polarity which is self-propagating (action wave); the membrane behaves as a monostable device exhibiting a transient tunnel diode characteristic.

At the output stage (terminal arborization of the axon; presynaptic terminal) the arrival of the action wave gives rise to the liberation of a unit amount of transmitter substance which, in the case of an excitatory coupling (excitatory synapse) incites partial depolarization of the input stage (dendritic tree) of the next element in line.

In the transducers (receptors) application of the requisite stimulus gives rise to local depolarization (generator potential) which, in those cases where the receptor possesses an axon, may result in the generation of a propagated action potential; in those receptors which have no axon, it leads directly to graded synaptic activity.

The system is probabilistic rather than deterministic because:

1) the generator potential incited by a stimulus of given strength exhibits fluctuations;
2) the excitability threshold of the neural membrane exhibits fluctuations associated with fluctuations in resting membrane potential;
3) at the synapse the arrival of an impulse may fail to evoke a unit post-synaptic potential; on the other hand, transmitter substance may be liberated in the absence of a presynaptic impulse;
4) in neurons exhibiting marked fluctuations in resting membrane potential, the critical depolarization level may sometimes be reached in the absence of an input stimulus, so they will occasionally fire "spontaneously" (neural noise).

The consequences of these phenomena for neural data processing are discussed.

A method has been developed to determine the spectrum of membrane voltage fluctuations of a single Ranvier node of the sciatic nerve of the frog. A three-terminal version of Frankenhaeuser's feedback isolation method was used to eliminate shunt leakage along the internodal segments. In this way two sources of noise voltage were obtained, with the noise voltage across the central node as the common component, which was extracted by means of cross-correlation.

A nerve chamber and techniques for mounting the axon, and for obtaining a high degree of electrical isolation between nodes were developed to meet the requirements of the measuring method. Low-noise, wide-band, chopper-stabilized electrometer amplifiers were developed. Noise spectra were measured by means of active filters realized on a general-purpose analog computer. Amplitude distributions were determined with the aid of a sampling circuit and a 128-channel pulse height analyzer.

In standard Ringer's solution the noise spectral density was found to be inversely proportional to frequency in the range $1–10^4$ rad·sec^{-1}. This type of spectrum is known to occur in current-carrying carbon resistors and semiconductor devices. At frequencies in excess of 10^4 rad·sec^{-1} the spectral intensity is constant and in the order of the Nyquist noise level for a metallic conductor having a resistance equal to that of the membrane at the fre-

quencies considered. The amplitude distribution of the fluctuations is gaussian.

The $1/f$ spectrum was not immediately influenced by blocking active sodium extrusion, by substituting choline for sodium or by blocking sodium inflow through addition of urethane to the bathing fluid. This rules out a direct connexion between sodium transport and $1/f$ noise. When the nerve is transferred to an isotonic KCl solution, however, the spectrum immediately changes into a flat spectrum of a much lower level. The same result can be obtained by hyperpolarization of the membrane to such a degree that transmembrane potential approximates the potassium equilibrium potential. These observations lead to the conclusion that the intensity of the $1/f$ spectrum is determined by the magnitude of the potassium flow through the membrane.

Superimposed on the noise of the type just described there are randomly occurring, roughly triangular, depolarizing deflections. As a result of this, the spectrum changes occasionally into a $1/f^2$ spectrum in the 0.1–10 rad $\cdot$ sec^{-1} range.

This phenomenon often precluded measurements of the $1/f$ spectrum in that frequency range. In relatively undisturbed periods indications have been found for the expected transition from a $1/f$ spectrum into a flat one at the lower end of the frequency range covered.

Several theories on $1/f$ noise in current-carrying carbon resistors, thin metal films and semiconductor devices as well as in the electron emission of vacuum tube oxyde cathodes have been proposed. A scrutiny of these theories reveals that, in general, either a hyperbolic distribution of relaxation times, an interaction between two independent random processes or one random process combined with non-linear coupling are invoked. At the present it is not possible to say what kind of mechanism gives rise to $1/f$ noise in the resting axon membrane voltage. Interaction between passive inflow and outflow of potassium ions due to knock-on transport and the influence of migrating calcium ions on these fluxes are the most promising starting points for further investigation.

REFERENCES

ADOLPH, A. R., J. Gen. Physiol. **48**; 297 (1964).

BEKEY, G. A. and B. PAXON, 2nd National Simulation Conference, Houston, Texas, April 1957.

BELL, D. A., Proc. Phys. Soc. **72**; 27 (1958).

BENNETT, R. R. and A. A. FULTON, J. Appl. Physiol. **22**; 1187 (1951).

BLACKMAN, J. G., B. L. GINSBORG and C. RAY, J. Physiol. **167**; 389 (1963).

BLAIR, E. A. and J. ERLANGER, Amer. J. Physiol. **106**; 524 (1933).

BOUMAN, M. A., History and Present Status of Quantum Theory in Vision. *In:* W. Rosenblith, ed., Sensory Communication (The M.I.T. Press and John Wiley and Sons, New York, 1961).

BULLOCK, T. H. and F. P. J. DIECKE, J. Physiol. **134**; 47 (1956).

CALDWELL. P. C. and R. D. KEYNES, J. Physiol. **148**; 8P (1959).
CALLEN, H. B. and T. A. WELTON, Phys. Rev. **83**; 34 (1951).
CARINGELLA, P. C. and W. L. EISENMAN, Rev. Sc. Instr. **33**; 645 (1962).
COHN, C.E., Rev. Sc. Instr. **35**; 701 (1964).
DERKSEN, H. E., Acta Physiol. Pharmacol. Neerlandica **10**; 164 (1961).
DODGE JR., F. A., Ionic Pe meability Changes Underlying Nerve Excitation. *In:* A. M. Shanes, ed., Biophysics of Physiological and Pharmacological Actions, 119. Publication no. 69 of the American Association for the Advancement of Science, Washington DC, 1961.
FATT, P. and B. KATZ, J. Physiol. **117**; 109 (1952).
FINKELSTEIN, A., Biophysical J. **4**; 421 (1964).
FITZHUGH, R., Biophysical J. **1**; 445 (1961).
FRANKENHAEUSER, B., J. Physiol. **135**; 550 (1957).
——— and B. WALTMAN, J. Physiol. **148**; 677 (1959).
———, J. Physiol. **160**; 40 (1962a).
———, J. Physiol. **160**; 46 (1962b).
———, J. Physiol. **160**; 54 (1962c).
——— and A. F. HUXLEY, J. Physiol. **171**; 302 (1964).
GEMERT, A. G. M. VAN, Acta Physiol. Pharmacol. Neerl. **4**; 274 (1955).
GESTELAND, R. C., B. HOWLAND, J. Y. LETTVIN and W. H. PITTS, Proc. I.R.E. **47**; 1856 (1959).
GOLDBERG, J. M., H. O. ADRIAN and F. D. SMITH, J. Neurophysiol. **27**; 706 (1964).
GROOT, S. R. DE and P. MAZUR, Non-equilibrium Thermodynamics (North-Holland Publishing Company, Amsterdam, 1962).
GULD, C., Proc. I.R.E. **50**; 1912 (1962).
HAGIWARA, S., Jap. J. Physiol. **4**; 234 (1954).
HARMON, L. D., Science **129**; 962 (1959).
HODGKIN, A. L. and B. KATZ, J. Physiol. **108**; 37 (1949).
——— and A. F. HUXLEY, J. Physiol. **117**; 500 (1952).
——— and R. D. KEYNES, J. Physiol. **128**; 61 (1955).
HOOPEN, M. TEN, A. DEN HARTOG and H. A. REUVER, Kybernetik **2**; 1 (1963).
HUXLEY, A. F. and R. STÄMPFLI, J. Physiol. **112**; 476 (1951a).
——— and ———, J. Physiol. **112**; 446 (1951b).
ILINSKII, O. B. and V. B. FIKS, Dokl. Akad. Nauk USSR **152/1**; 218 (1963).
IVES, D. J. G. and G. J. JANZ, eds., Reference Electrodes, Theory and Practice (Academic Press, New York, 1961).
KATZ, B. and R. MILEDI, J. Physiol. **168**; 389 (1963).
KLEIN, G., Philips Res. Rep. **10**; 241 (1955).
KUNO, M., J. Physiol. **175**; 81 (1964).
KÜPFMÜLLER, K. and F. JENIK, Kybernetik **1**; 1 (1961).
LANDSBERG, S., Philips Research Reports **11**; 161 (1956).
LAWSON, J. L. and G. E. UHLENBECK, eds., Threshold Signals (Mc Graw-Hill Book Comp., New York, 1950).
LEWIS, E. R., An Electronic Model of the Neuron based on the Dynamics of Potassium and Sodium Ion Fluxes. *In:* R. F. Reiss, ed., Neural Theory and Modeling (Stanford University Press, Stanford, Calif., 1964).

LOEWENSTEIN, W. R., Ann. N.Y. Ac. Sciences **94**; 510 (1961).
LOWENBERG, E. C. and C. E. MCCULLOUGH, Electroenceph. clin. Neurophysiol. **15**; 706 (1962).
MAC DONALD, D. K. C., Noise and Fluctuations (John Wiley and Sons Inc., New York, 1962).
MAC FARLANE, G. G., Proc. Phys. Soc. **B 63**; 807 (1950).
MACHIN, K. E., Symposium no. 16 of the Society for Experimental Biology (Cambridge University Press); 227 (1962).
MARTIN, A. R. and G. PILAR, J. Physiol. **175**; 1 (1964).
MCWHORTHER, A. L. *In:* Semiconductor Surface Physics (University of Pennsylvania Press, 1957).
MOORE, J. W., Proc. I.R.E. **47**; 1869 (1959).
——— and J. H. GEBHART, Proc. I.R.E. **50**; 1928 (1962).
MORRISON, S. R., Phys. Rev. **104**; 619 (1956).
OBERHETTINGER, F., Tabellen zur Fourier Transformation (Springer Verlag, Berlin, 1957).
ONNO, P., Rev. Sc. Instr. **32**; 1253 (1961).
PECHER, C., Arch. int. Physiol. **49**; 129 (1939).
PHILBRICK, Researches, Inc., Rep. 18/10M/and/763: Notes on operational amplifiers, (1958).
PIRENNE, M. H. and F. H. C. MARRIOTT, The Quantum Theory of Light and the Psycho-Physiology of Vision. *In:* S. Koch ed., Psychology, A Study of a Science (McGraw-Hill Book Company, Inc., New York, 1959).
POLLACZEK, F., C.R. Acad. Sci., Paris, **222**; 353 (1946).
RICE, S. O., Bell Syst. Tech. J. **23**; 282 and **24**, 46 (1944/45).
SAUTTER, D., Noise in Semiconductors. *In:* Progress in Semiconductors **4**; 125 (Heywood Comp., London, 1960).
SCHOENFELD, R. L., Proc. I.R.E. **50**; 1942 (1962).
SCHWAN, H. P., Determination of Biological Impedances. *In:* W. L. Nastuk, ed., Physical Techniques in Biological Research, vol. VI part B (Academic Press, New York, 1963).
SMITH, D. R. and G. K. SMITH, Biophys. J. **5**; 47 (1965).
STÄMPFLI, R., Helv. Physiol. Acta **21**; 189 (1963).
STEIN, R. B., Biophys. J. **5**; 173 (1965).
SUTCLIFFE, H., Proc. Inst. El. Eng. **112**; 301 (1965).
TASAKI, I., Nervous Transmission (Charles C. Thomas, Springfield, Illinois, 1953).
——— and K. FRANK, Am. J. Physiol. **182**; 572 (1955).
———, Am. J. Physiol. **181**; 639 (1955).
VALLEY, G. E. and H. WALLMAN, eds., Vacuum Tube Amplifiers (Mc Graw-Hill Book Company, New York, 1948).
VERVEEN, A. A., Thesis, Amsterdam (1961).
———, Acta Morphologica Neerlando–Scandinavica **5**; 79 (1962).
——— and H. E. DERKSEN, Kybernetik **2**; 152 (1965).
VIERNSTEIN, L. J. and R. G. GROSSMAN, Neural Discharge Patterns. *In:* C. Cherry, ed., Fourth London Symposium on Information Theory (Butterworths, London, 1961).

VRIES, HL. DE, Progress in Biophysics and Biophysical Chemistry 6; 207 (Pergamon Press, London, 1956).

——— and M. STUIVER, The Absolute Sensitivity of the Human Sense of Smell. *In:* W. Rosenblith, ed., Sensory Communication (The M.I.T. Press and John Wiley and Sons, New York, 1961).

WEISS, T. F., Technical Report 418, R.L.E., M.I.T. (1964).

WYNJA, W., Master's Thesis, Department of Electrical Engineering, Technical University, Delft (1964).

ZIEL, A. VAN DER, Noise (Prentice-Hall, Inc., 1954).

———, Fluctuation Phenomena in Semi-Conductors (Butterworth, London, 1959).

Op verzoek van de Faculteit der Wiskunde en Natuurwetenschappen volgen hier enige persoonlijke gegevens:

In 1944 behaalde ik het einddiploma HBS-B te Leiden. Van 1945 tot 1952 studeerde ik natuurkunde aan de Rijksuniversiteit te Leiden. Ik legde in 1949 het candidaatsexamen a af en in 1952 het doctoraalexamen natuurkunde met hoofdrichting experimentele natuurkunde en bijvak technische natuurkunde.

Van 1952 tot 1955 werkte ik onder leiding van prof. Dr. C. J. GORTER als assistent op het Kamerlingh Onnes Laboratorium te Leiden. Mijn werk betrof in hoofdzaak de instrumentatie van het onderzoek naar paramagnetische relaxatie.

In 1955 trad ik in dienst van het Koninklijke Shell Laboratorium te Amsterdam waar ik werd belast met het ontwerp van practica, demonstratieproeven en cursussen voor middelbaar natuurkundig personeel en regeltechnici.

Vanaf oktober 1958 ben ik verbonden aan het Fysiologisch Laboratorium te Leiden, aanvankelijk als wetenschappelijk ambtenaar eerste klas en sedert 1962 als wetenschappelijk hoofdambtenaar. Mijn werk was ten eerste het inrichten van een electronische afdeling en het ontwerp van meetopstellingen voor fysiologisch onderzoek en vervolgens wetenschappelijk onderzoek over fysiologische regelsystemen en over informatieverwerking in het zenuwstelsel. Analoog-rekentechnieken en de simulatie van zenuwcellen door electronische modellen waren daarbij belangrijke hulpmiddelen. Het in dit proefschrift beschreven onderzoek werd begonnen in november 1963 en werd afgesloten in februari 1965.

Het onderzoek werd verricht in nauwe samenwerking met de fysioloog Dr. A. A. Verveen. Nog afgezien van zijn vele andere bijdragen tot dit onderzoek dient te worden vermeld dat alle onderzochte zenuwvezels door hem werden geprepareerd en gemonteerd. De electronische apparatuur werd mede ontwikkeld door F. van der Mark en H. R. Roman en werd gebouwd en afgeregeld door A. P. van Kempen en W. C. Deegenaars. Niet onbelangrijke bijdragen van mechanische aard werden onder leiding van R. P. de Graaf geleverd door W. Opgelder. Mej. G. R. M. Muller verzorgde een aantal versies van het manuscript, de tekeningen werden door P. de Boer vervaardigd. L. Jonkers programmeerde de numerieke verwerking van de amplitudedistributies. Ir. J. Roukens van IBM-Nederland besteedde een zeer groot aantal uren van zijn vrije tijd aan de analyse en het programmeerwerk betreffende het in het vierde hoofdstuk van dit proefschrift besproken wachttijdenprobleem.

STELLINGEN

I

Ontwikkelingswerk aan hybride computers is, ook afgezien van de vraag of deze systemen van voordeel zijn als computer voor algemene doeleinden, van niet gering belang.

II

Het woord vergelijking in wis- of natuurkundige teksten dient te worden vervangen door gelijkstelling.

III

De door DE VRIES gegeven evaluatie van de door hem gebruikte wisselstroombrug met synchrone detector voor meting van paramagnetische relaxatie ten opzichte van de eveneens door hem toegepaste, door VAN DEN BROEK geintroduceerde stapfunctiemethode is niet steekhoudend.

VRIES, A. J. DE, dissertatie R.U. Leiden, 1965, pp. 70–72.

IV

De argumentatie van VAN GERVEN *et al.* betreffende de door hen gevonden paramagnetische resonantie in Cu_2Cl_2 in een longitudinaal magneetveld is weinig overtuigend.

VAN GERVEN, L., A. VAN ITTERBEEK, P. GROBET en J. VAN DAM, Proc. XII Colloque Ampère. North-Holland Publishing Company, Amsterdam (1964).

V

De voorstellen van LITTLE over supergeleiding bij kamertemperatuur in bepaalde moleculaire structuren zijn niet realiseerbaar.

LITTLE, W. A., Phys. Rev. 134, A 1416–A 1424 (1962).

VI

Het biedt voordeel om bolometer-detectoren voor warmtestraling op te nemen in een RC-oscillator.

VII

De aflevering van een fotomultiplicatorbuis dient vergezeld te gaan van een ijkcertificaat waarop de gevoeligheidsverdeling over het kathodeoppervlak wordt aangegeven.

VIII

De door Endeman ingevoerde aanname (longitudinale polarizeerbaarheid langs de halogeen-zuurstof binding kleiner dan de transversale) ter verklaring van de bevinding dat natriumchloraat en natriumbromaat van overeenkomstige absolute configuratie een tegengestelde optische draaiing vertonen, is prematuur gezien het feit dat de metingen slechts bij een golflengte zijn uitgevoerd.

ENDEMAN, H. J., dissertatie R.U. Utrecht, 1956.

IX

Het is onjuist de biofysica te zien als een zelfstandige tak van wetenschap.

X

Gezien de zeer belangrijke potentiele toepassingen in de biologie dient de practisch-technische mogelijkheid van opwekking van coherente röntgenstraling grondig te worden nagegaan.

SCHAWLOW, A. L., Course 31, Proc. Int. School of Physics "Enrico Fermi". Academic Press, New York (1964).

XI

Een onderzoek naar de invloed van ultrasone trillingen van bekende intensiteit en over een zo groot mogelijk frequentiegebied op de electrisch meetbare eigenschappen van de zenuwmembraan is van fundamenteel belang.

XII

Bij het nagaan van de invloed van buigingsverschijnselen op het oplossend vermogen van het visuele systeem dienen zowel de onwillekeurige oogbewegingen als de frequentieresponsie van de zintuig- en zenuwcellen in de beschouwing te worden betrokken.

XIII

Bij de opzet van neurofysiologisch onderzoek en bij de discussie van de resultaten worden ethologische gegevens nog steeds onvoldoende in overweging genomen.

XIV

Aan het gebruik in de biologie van aan de regel- en communicatietechniek ontleende terminologie en denkwijzen zijn een aantal bezwaren verbonden die tot dusver onvoldoende naar voren zijn gebracht.

YOUNG, J. Z., The life of mammals, ch. I; Clarendon Press, Oxford (1957).

GLOSSARY

Acoustic labyrinth — see cochlea.

Action potential — nerve impulse: self-propagating transient wave of inside positivity, i.e. reversal of membrane polarity.

Adequate stimulus — stimulus mode to which a receptor cell is particularly sensitive.

Afferent — leading toward the central nervous system, i.e. from receptors.

Axon — long process of a nerve cell along which action potentials can travel away from the cell body to its terminal ramifications which enter into synaptic connexion with the dendritic tree of other neurons or with effector cells or fibers. Nerve fiber.

Axon membrane — membrane surrounding the axon and separating the axoplasm from the extracellular fluid. In the resting state the membrane is polarized, inside negative.

Axoplasm — viscid fluid inside the axon.

Cell — morphotic and functional unit of the body, usually of microscopic dimensions.

Cochlea — that part of the inner ear subserving perception of sound.

Conduction time — transmission time of action potential along a nerve fiber.

Cortical neurons — nerve cells, the cell bodies of which lie in the cerebral cortex.

Dendrites — short, fine, arborized neuronal processes serving as input stage of a neuron.

Effector — cell which, upon excitation, normally by nerve impulses, exerts mechanical or chemical action on external or internal environment, i.e. muscle fiber or gland cell.

Efferent — conducting away from the central nervous system, i.e. to effectors.

Electroreceptors — receptors, found in some tropical fishes, particularly sensitive to electric currents.

Enzyme — specific biocatalyst, consisting usually of a protein and an active non-protein prosthetic group.

Excitability — the reciprocal of the strength of a stimulus, as measured in an appropriate unit, which is just sufficient to incite a response.

Excitatory — leading to increased excitability or even to the generation of a nerve impulse.

Extracellular fluid — fluid matrix in which the cells are embedded.

Generator potential — sustained partial depolarization of receptor membrane without reversal of polarity resulting from absorption of stimulus energy.

Inhibitory — leading to diminished excitability.

Interstitial — see extracellular.

Mechanoreceptor — receptor for which the adequate stimulus is mechanical deformation.

Medullated — see myelinated.

Membrane potential — potential difference between outside and inside (inside negative) of a cell.

Mesentery — peritoneal fold by which the intestine is attached to the posterior wall of the abdominal cavity.

Microsmatic — possessing a poorly developed sense of smell.

Muscle spindle — mechanoreceptor embedded in skeletal muscle signalling degree of muscle stretch.

Myelinated — possessing a myelin sheath.

Myoneural junction — see neuromuscular junction.

Nerve — bundle of nerve fibers.

Nerve fiber — see axon.

Neuromuscular junction — a junction, or synapse, between efferent axon of motoneuron and muscle fiber.

Neuron — morphotic and functional unit of nervous tisue.

Non-acoustic labyrinth — those portions of the inner ear which subserve detection of gravitational pull and linear acceleration (utricle) and of angular acceleration (semicircular canals).

Ouabain — see g-strophantin.

Pacinian corpuscle — ellipsoidal body subserving response to pressure, a mechanoreceptor consisting of an axon-like process embedded in a number of concentric lamellae; stimulation is brought about by deformation or shearing stress.

Ranvier nodes — short complete interruptions of the myelin sheath, exposing the bare axon and occurring at regular intervals along myelinated nerve fibers.

Receptor — sensory cell transducing an environmental influence into a change in its membrane potential, the generator potential.

Reflex response — response mediated via the central nervous system by which the organism reacts to changes in its inner and outer environment.

Reflexogenic area — area from which a specific reflex response can be elicited.

Refractory period — period of non-excitability (absolute) following an action potential, followed by one of decreased excitability (relative).

Sciatic nerve — a nerve trunk in the frog's lower leg.

Sensory system — system consisting of an array of receptors which transduce environmental stimuli of the same kind and feeding into information-processing neuronal networks.

Spike — action potential, nerve impulse.

Squid giant axon — large diameter (0,5–1 mm) unmyelinated axon in the fin nerve of the squid.

Superior olivary complex — synaptic station in the central auditory pathway.

Synapse — junction between receptor and neuron, between neurons or between neuron and effector cell.

Synaptic delay — period between arrival of presynaptic action potential and electrically measurable postsynaptic effect.

Tetrodotoxin — poison of blowfish.

Threshold potential — value of membrane potential at which an action potential is just initiated by an intracellular depolarizing current.

Threshold stimulus — magnitude of stimulus (e.g. electric current) that depolarizes an excitable membrane to its threshold potential.

Urethane — ethyl carbamate, $NH_2CO \cdot OC_2H_5$; a narcotic.